AN EXPERIMENTAL INVESTIGATION OF THE T-BAR FED SLOT ANTENNA ON PLANAR AND CYLINDRICAL SURFACES

Michael R. Crews

Ohio State University
Columbus, Ohio

March 1975

174041

AN EXPERIMENTAL INVESTIGATION OF THE T-BAR FED SLOT ANTENNA ON PLANAR AND CYLINDRICAL SURFACES

Michael R. Crews

The Ohio State University

ElectroScience Laboratory

Department of Electrical Engineering
Columbus, Ohio 43212

TECHNICAL REPORT 4111-1

Contract N00140-75-C-6116

March 1975

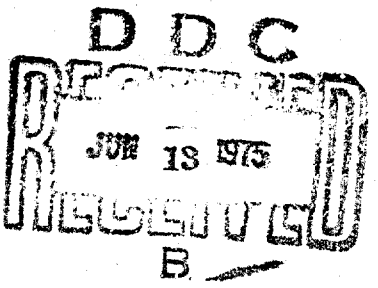

Naval Regional Procurement Office
Philadelphia Newport Division
Building No. 132-T
Newport, Rhode Island 02840

NOTICES

When Government drawings, specifications, or other data are used for any purpose other than in connection with a definitely related Government procurement operation, the United States Government thereby incurs no responsibility nor any obligation whatsoever, and the fact that the Government may have formulated, furnished, or in any way supplied the said drawings, specifications, or other data, is not to be regarded by implication or otherwise as in any manner licensing the holder or any other person or corporation, or conveying any rights or permission to manufacture, use, or sell any patented invention that may in any way be related thereto.

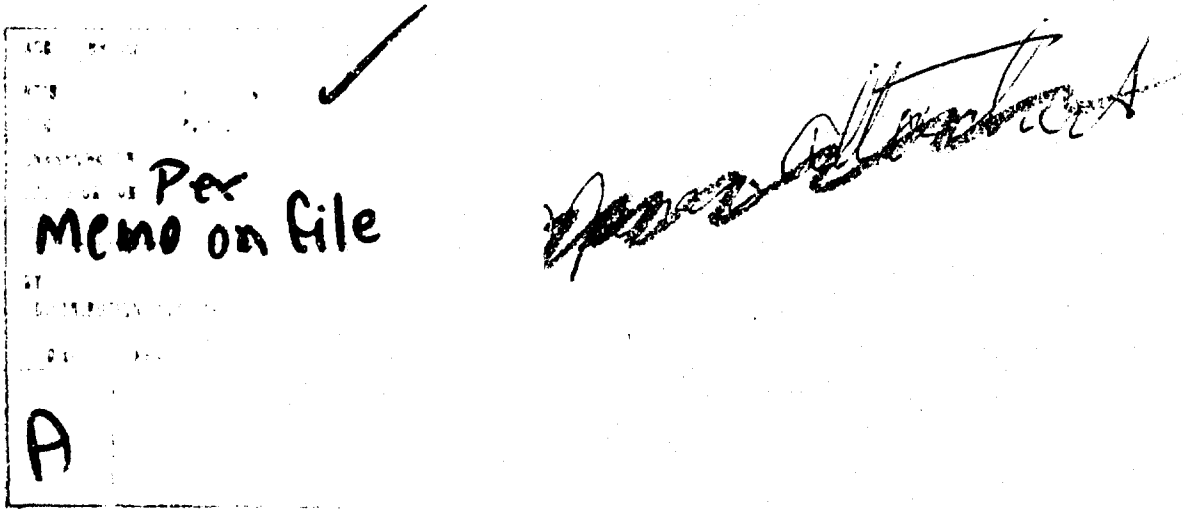

UNCLASSIFIED

SECURITY CLASSIFICATION OF THIS PAGE (When Data Entered)

REPORT DOCUMENTATION PAGE

READ INSTRUCTIONS BEFORE COMPLETING FORM

1 REPORT NUMBER	2 GOVT ACCESSION NO. / 3 RECIPIENT'S CATALOG NUMBER
4 TITLE (and Subtitle): AN EXPERIMENTAL INVESTIGATION OF THE T-BAR FED SLOT ANTENNA ON PLANAR AND CYLINDRICAL SURFACES	5 TYPE OF REPORT & PERIOD COVERED: Technical Report
	6 PERFORMING ORG. REPORT NUMBER
7 AUTHOR(s): Michael R. Crews	8 CONTRACT OR GRANT NUMBER(s): Contract N00140-75-C-6116
9 PERFORMING ORGANIZATION NAME AND ADDRESS: The Ohio State University ElectroScience Laboratory, Department of Electrical Engineering, Columbus, Ohio 43212	10 PROGRAM ELEMENT, PROJECT, TASK AREA & WORK UNIT NUMBERS: Project N66604-5-000045
11 CONTROLLING OFFICE NAME AND ADDRESS: Naval Regional Procurement Office, Philadelphia Newport Division, Building No. 132-T Newport, Rhode Island 02840	12 REPORT DATE: March 1975
	13 NUMBER OF PAGES: 79
14 MONITORING AGENCY NAME & ADDRESS (if different from Controlling Office)	15 SECURITY CLASS. (of this report): Unclassified
	15a DECLASSIFICATION/DOWNGRADING SCHEDULE

16 DISTRIBUTION STATEMENT (of this Report)

17 DISTRIBUTION STATEMENT (of the abstract entered in Block 20, if different from Report)

18 SUPPLEMENTARY NOTES

19 KEY WORDS (Continue on reverse side if necessary and identify by block number)

Aperture antenna
Insertion loss measurement
Circumferential slot antenna
Transverse slot antenna
Slot antenna
T-bar antenna

20 ABSTRACT (Continue on reverse side if necessary and identify by block number)

This report describes the results of an intensive experimental effort directed toward the electrical improvement and size reduction of slot antennas. In particular, the T-bar fed cavity backed slot antenna mounted on both a planar surface and also transversely mounted on a circular cylinder are investigated over the four to one frequency bandwidth of 500 to 2000 MHz.

DD FORM 1 JAN 73 1473 EDITION OF 1 NOV 65 IS OBSOLETE

UNCLASSIFIED PRICES SUBJECT TO CHANGE

SECURITY CLASSIFICATION OF THIS PAGE (When Data Entered)

20.

The results of the experimental investigation of the T-bar fed slot antenna mounted on a planar ground plane show two important improvements in T-bar fed slot antennas. The first improvement is that the bandwidth of the T-bar slot antenna can be increased by a factor of two over the conventional T-bar slot antenna design. The second improvement is that the depth of the antenna may be significantly reduced from that required of previous designs. The improved T-bar fed slot antenna offers a viable solution to some unusual receiving design requirements.

Results also show that the planar T-bar antenna can be successfully adapted to a cylindrical surface. Furthermore, considering the size of the T-bar fed slot compared to the cylindrical surface on which it was mounted, the T-bar fed slot antenna shows promise of being adaptable to a wide range of surface geometries while retaining most of the characteristics of a planar model.

ACKNOWLEDGMENT

The author's advisor, Professor Gary A. Thiele, deserves a special note of appreciation for his guidance during the planning and execution of this research program as well as for his critical review during the preparation of this thesis. Professor Carlton H. Walter, a member of the author's reading committee, has provided many helpful suggestions and comments which have been incorporated throughout this thesis.

Appreciation is extended to Ross Caldecott for his assistance in utilizing the computer routines available at the ElectroScience Laboratory for data analysis. Peter Bohley's assistance in the experimental investigation of the planar T-bar fed slot antenna and introduction to the experimental equipment and measurement procedures is greatly appreciated. Summers A. Redick's assistance in recording the data using the IBM informer computer is also appreciated.

The work reported in this thesis was supported in part by Contract N00140-75-C-6116 between Naval Regional Procurement Office, Newport, Rhode Island, and The Ohio State University Research Foundation.

The material contained in this report is also used as a thesis submitted to the Department of Electrical Engineering, The Ohio State University as partial fulfillment for the degree Master of Science.

CONTENTS

CHAPTER I

INTRODUCTION

This report describes the results of an intensive experimental effort directed toward the electrical improvement and size reduction of slot antennas. The desired slot antenna should possess a wide bandwidth (4:1) in terms of reasonable VSWR (Voltage Standing Wave Ratio) and efficiency, exhibit certain pattern properties such as having the pattern maximum normal to the center of the slot, and be flush mountable circumferentially on a circular cylinder. Specifically, the final design should be transversely mounted on a seven inch diameter cylinder, require a cavity depth no more than 1.5 inches, and possess the characteristics described above over the 4:1 frequency range of 500 to 2000 MHz.

From information obtained in Jasik [1], the T-bar fed cavity backed slot antenna,* which exhibits considerable bandwidth (2:1) and high efficiency, was chosen for experimental analysis. Figure 1-1 shows the T-bar slot antenna which is described by Jasik.

In an experimental parametric study of the T-bar slot antenna conducted at the Ohio State University ElectroScience Laboratory, E. H. Newman [2] concluded that a T-bar of thin rectangular cross section exhibits essentially the same input impedance as T-bars of circular cross section and that the T-bar geometry is an important factor in determining bandwidth. Therefore, due to the relative ease of fabrication, the T-bar slot antennas constructed for experimental investigations each contained thin rectangular cross section T-bars which will be referred to as planar T-bars. The final design of the T-bar slot antenna utilizing a planar T-bar is shown in Fig. 1-2. As described by Jasik, the aperture length is $\lambda/2$ at the lowest frequency of the desired bandwidth and the aperture width is 1/3 that value. In this investigation the cavity depth and T-bar depth were left variable by providing a moveable coax connector and a sliding shorting plate. Table 1-1 contains a list of symbols used to describe the geometry of the T-bar slot antennas.

It was assumed at the beginning of this investigation that once the significant design parameters were established for the conventional T-bar slot antenna mounted in a ground plane as shown in Fig. 1-2, then adaptation of the slot antenna to a cylindrical surface would follow.

---

*For brevity the T-bar fed cavity backed slot antenna shall be referred to as the T-bar slot antenna, or simply T-bar antenna.

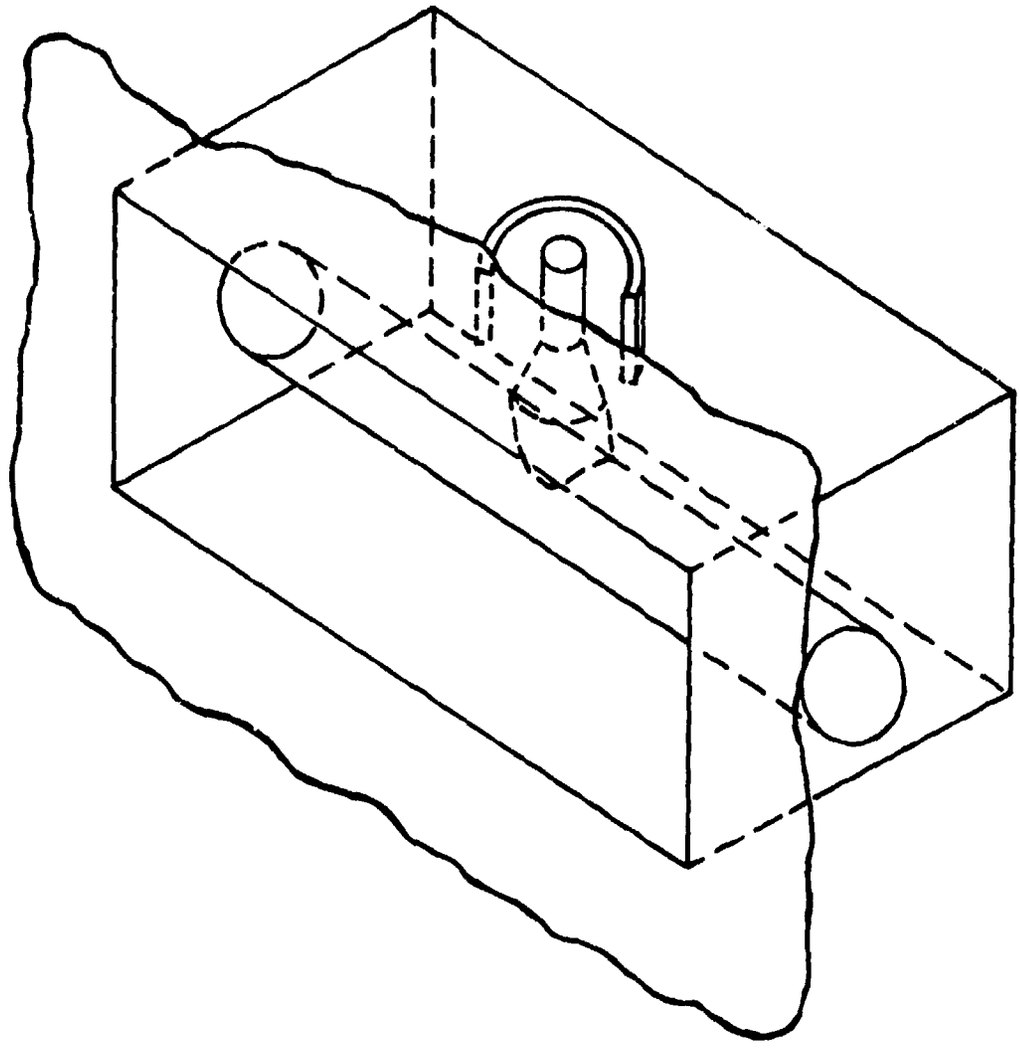

Fig. 1-1. A cavity-backed T-bar fed slot antenna mounted on a flat ground plane as described by Jasik.

TABLE 1-1

Symbol	Descriptions and Units of Measuarement Used
a	aperture length (12.0 inches)
b	aperture width (4.0 inches)
CD	cavity depth of antenna (inches)
L	length of slot within the T-bar, 7.5 cm unless noted otherwise (centimeters)
X	position of the slot within the T-bar relative to the bottom of the slot, 4.0 cm unless noted otherwise (centimeters)
Y	distance from the aperture plane to T-bar probe, 0.75 unless noted otherwise (inch)
T-bar D	the T-bar whose dimensions are described on page 13. If X or L is not specified T-bar D was used.

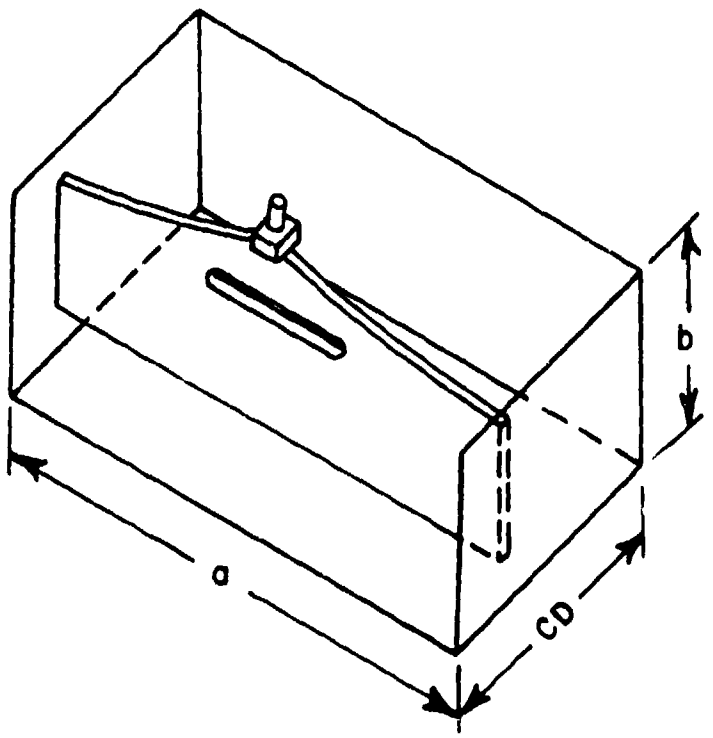

Fig. 1-2. a) A cavity-backed T-bar fed slot antenna with top removed for viewing purposes. Note the use of a planar T-bar.

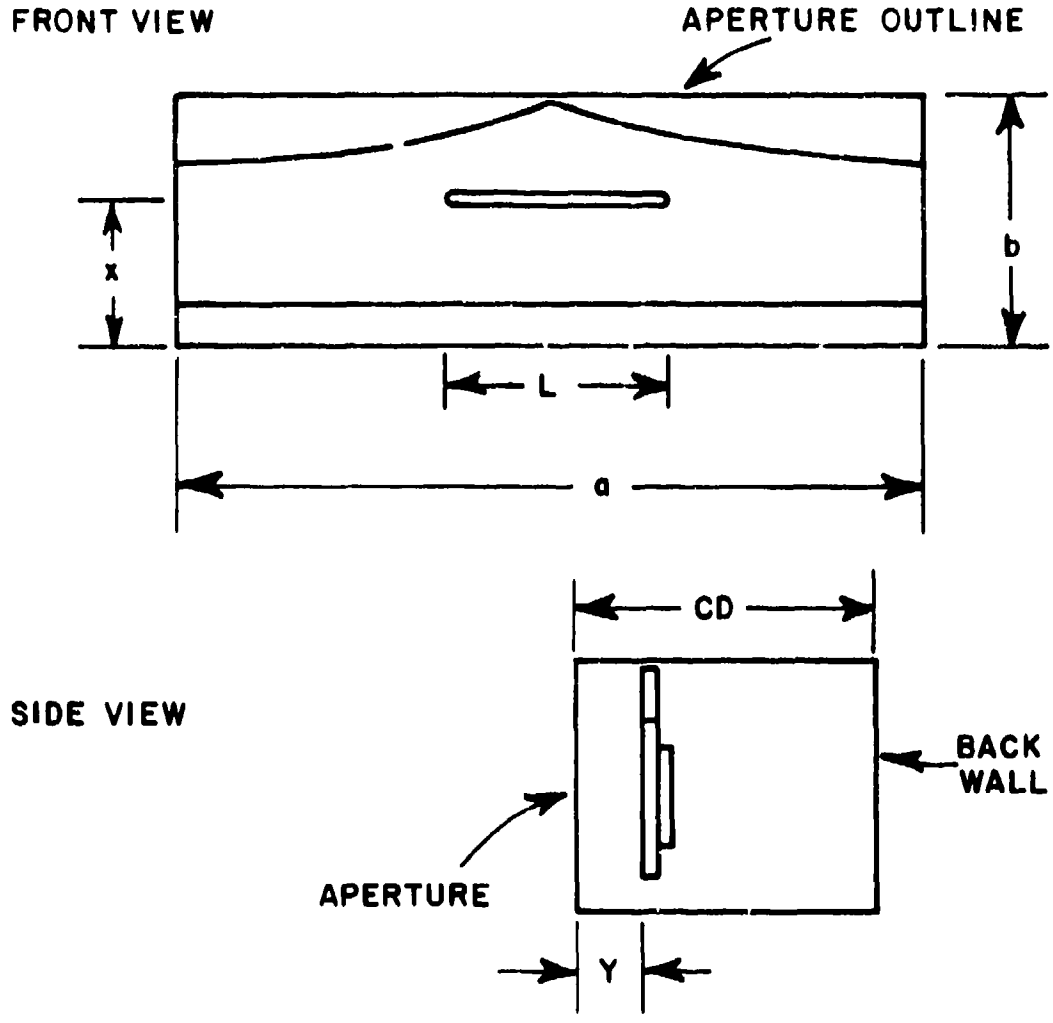

Fig. 1-2. b) Front and side view of the cavity-backed T-bar fed slot antenna.

To distinguish between the two applications of the T-bar slot antenna discussed in this report, the following terminology shall be adhered to: (1) the T-bar slot antenna mounted in a ground plane as shown in Fig. 1-2 shall be termed the planar T-bar slot antenna, and (2) the T-bar slot antenna mounted transversely on a cylindrical surface as shown in Fig. 1-3 shall be termed the cylindrical T-bar slot antenna. Whenever the feed probe of the slot antenna of either case is discussed, the term T-bar shall be used and it is assumed that the T-bars are of a thin rectangular cross section.

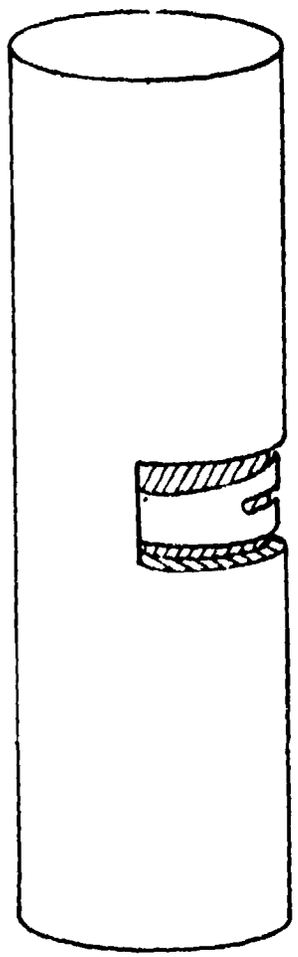

Fig. 1-3. A cavity-backed T-bar fed slot antenna mounted transversely on a circular cylinder.

Chapter II of this report describes the investigation procedures and results of the planar T-bar slot antenna. The final design exhibited reasonable performance over the 4:1 frequency range and provided insight into the characteristics of this antenna. In Chapter III, the design of a T-bar fed slot transversely mounted on a cylinder is described along with the results of an experimental investigation. Considering the size of the slot mounted on the cylinder, the design procedures obtained from the planar T-bar antenna investigation proved quite successful. Chapter IV describes an attempt to probe the apertures of the two T-bar antennas to gain more information pertaining to the coax to cavity transition accomplished by the T-bar. Finally, Chapter V contains a summary of the conclusions derived from this study.

CHAPTER II

EXPERIMENTAL INVESTIGATION OF PLANAR T-BAR SLOT ANTENNAS

A. Introduction

This chapter describes the experimental development of the T-bar fed slot antenna mounted in a flat (or planar) ground plane. The T-bar feeds used all have a thin rectangular cross section and are, for brevity, simply referred to as T-bars.

In a previous study of T-bar fed slot antennas, E. H. Newman[2] has concluded that T-bars of thin rectangular cross section exhibit essentially the same input impedance as T-bars of circular cross section and that the T-bar geometry is one of the important parameters of bandwidth performance. Considering these conclusions, the first antenna parameter to optimize over the desired four to one bandwidth would be the T-bar geometry. Newman, in his study, considered bandwidth as that frequency range where the VSWR of the antenna remains below 2.0. However, other important performance parameters such as efficiency, gain, and radiation patterns (not necessarily independent of each other) may also be expressed in terms of bandwidth. Investigating each of the performance parameters over a four to one frequency range, with the optimum T-bar as the final goal, would be a lengthy process if one considers all possible combinations of the T-bar slot antenna variables such as cavity depth, T-bar depth, cavity tuning, and dielectric loading. Therefore, an experimental system which would sample each of the performance parameters simultaneously as the antenna parameters were varied and would quickly describe the interrelationship of the antenna parameters was needed. The antenna swept frequency insertion loss measurement provided such information. A block diagram of this experimental procedure is shown in Fig. 2-1. Measuring the forward or reverse transmission coefficient (S_{12} or S_{21}) at the scattering parameters device, the ratio of power received to power transmitted is obtained as given by Frii's transmission formula stated below from Reference 3.

$$\frac{W_r}{W_t} = \frac{A_{er} A_{em}}{\lambda^2 r^2} = \frac{G_r G_t \lambda^2}{16\pi^2 r^2}$$

W_r and W_t are the power received and transmitted, respectively. The gains G_r and G_t are defined with respect to the receiving and transmitting antennas. Frii's transmission formula is expressed in terms of wavelength, antenna separation, and gain. If the insertion loss characteristics are known for two reference antennas, then a comparison of this data to the insertion loss measurements recorded when one reference antenna is replaced with a test antenna reveals a relative

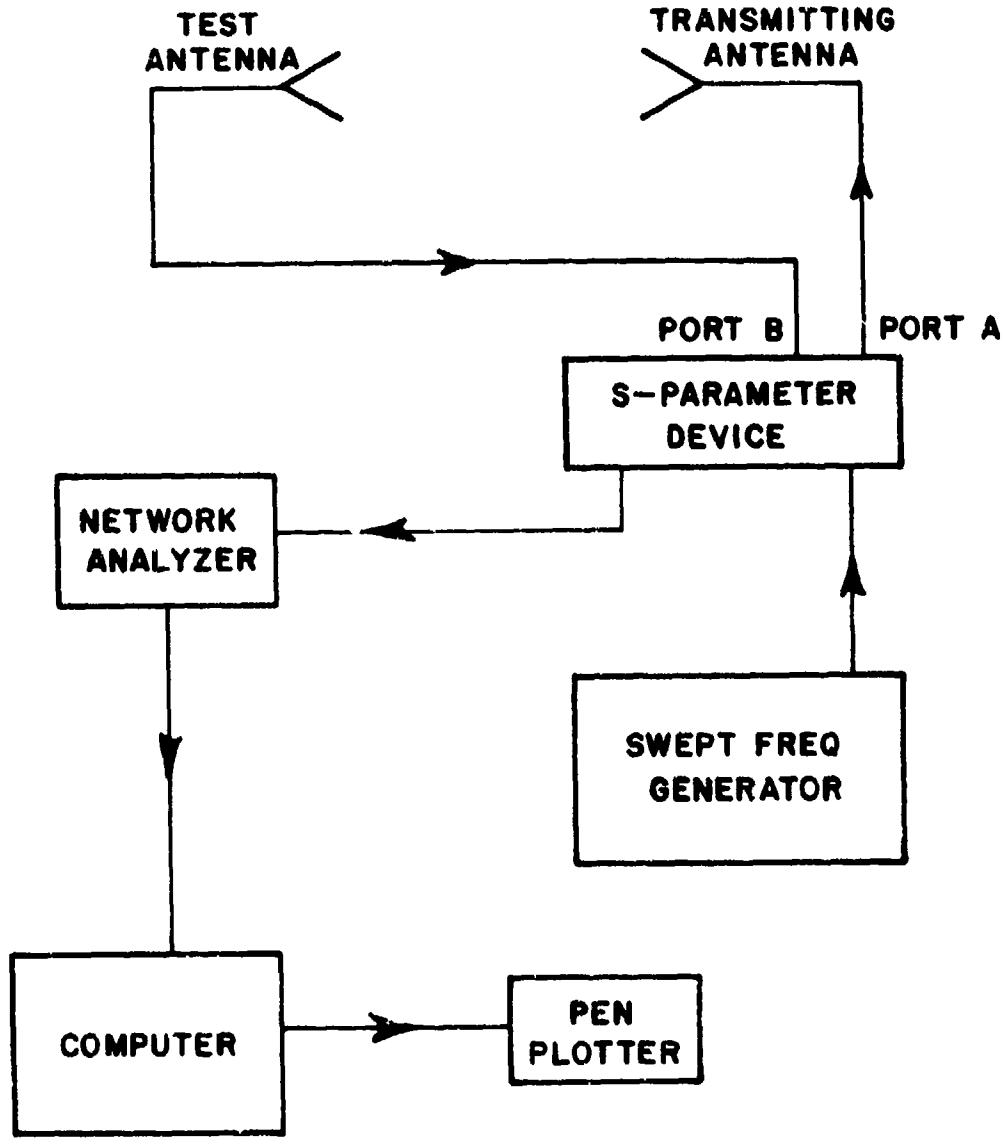

Fig. 2-1. A block diagram of the experimental procedure used to measure the insertion loss between two antennas.

gain for the test antenna in a given direction. This relative gain is related to efficiency, directivity, antenna-transmission line mismatch, and the radiation pattern in a narrow region broadside to the antenna. Therefore, the insertion loss measurement over a swept frequency range provides a method to quickly check each of the important performance parameters previously mentioned while investigating different combinations of antenna variables. To complement the insertion loss measurements, the S-parameter device will also measure the return loss at the antenna port which gives the VSWR of the antenna. Using the insertion loss and VSWR measurement system, the T-bar geometry was varied in a successful attempt to optimize the T-bar slot antenna as described below.

B. T-Bar Optimization

One method to expand the bandwidth of a waveguide is the application of a single or double ridge. The ridge expands the bandwidth of a waveguide by decreasing the lower cutoff frequency and increasing the cutoff frequency of the higher order modes.[4] The T-bar slot antenna (whose cavity exhibits some waveguide characteristics) was altered as shown in Fig. 2-2 and a ridge of dimensions 4.88 x 5.08 cm, corresponding to a bandwidth of 2.74 for a waveguide of similar dimensions was installed.[5] Experimental investigation of the ridged T-bar slot antenna showed an improvement in insertion loss performance over the nonridged case. During further attempts to improve the performance of the ridged T-bar slot antenna with different T-bar geometries and ridge sizes, the best results were obtained when (1) the ridge was removed, (2) the notch in the T-bar terminated leaving a rectangular slot in the T-bar, and (3) the peaked feed point of the T-bar replaced with a gradual slope as shown in Fig. 2-3.

This investigation also showed an eight to twelve dB drop in insertion loss which occurred at approximately 1500 MHz thus limiting the bandwidth performance. Investigating another waveguide matching technique, tuning stubs of various sizes were positioned about in the cavity while measuring the insertion loss. The spike at 1500 MHz can be effectively reduced using this procedure without any loss elsewhere in the bandwidth if the stubs are located on the bottom of the cavity, in the vicinity of the T-bar and therefore shorter than the distance between the T-bar and cavity bottom. The best performance was achieved when the tuning stubs were located $\pm$ 10 cm from the center of the aperture which corresponds to a spacing of one wavelength at the troublesome frequency of 1500 MHz. For the remainder of the planar T-bar antenna investigations tuning stubs were positioned as described above unless noted differently.

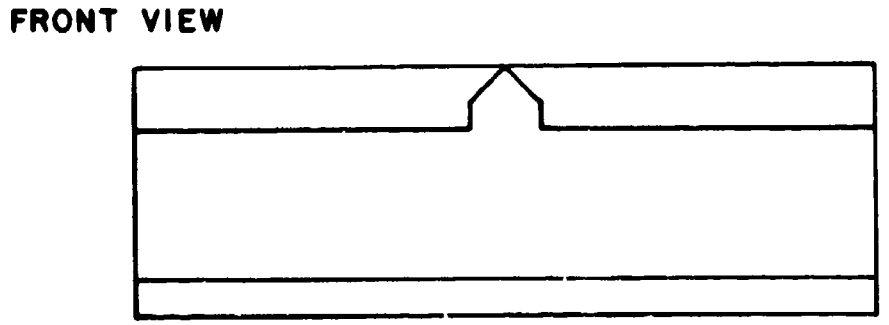

Fig. 2-2. a) Front view of the original planar T-bar slot antenna.

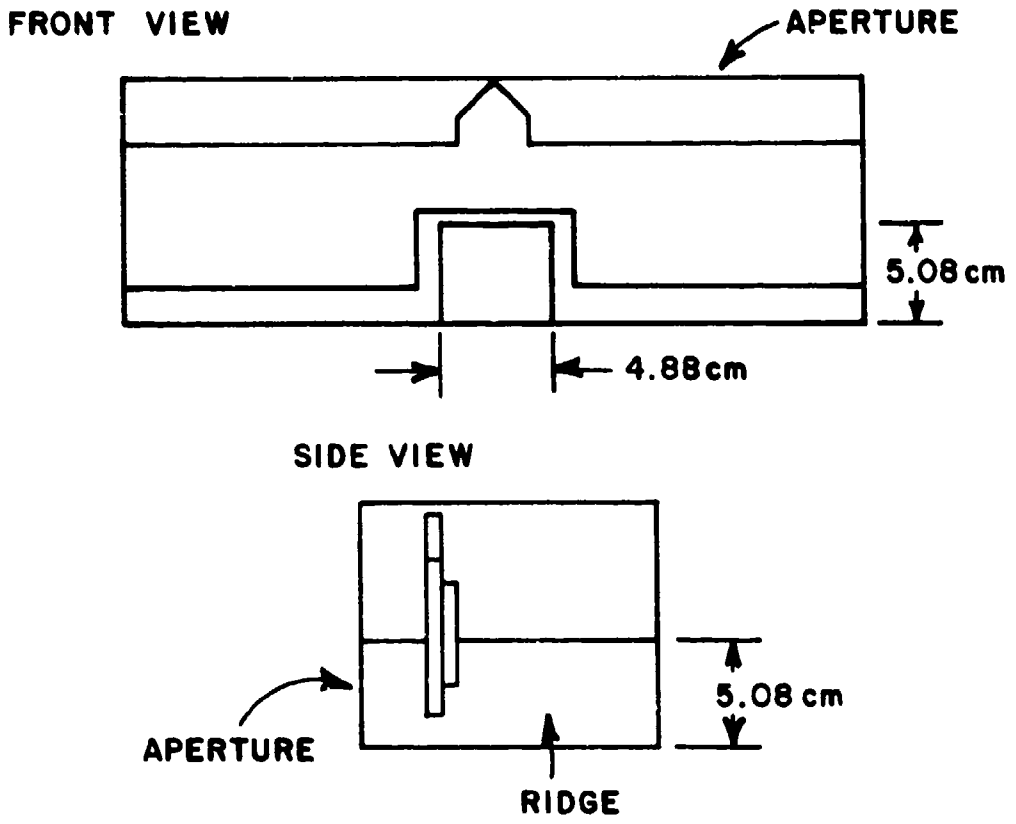

Fig. 2-2. b) The planar T-bar slot antenna with single ridge.

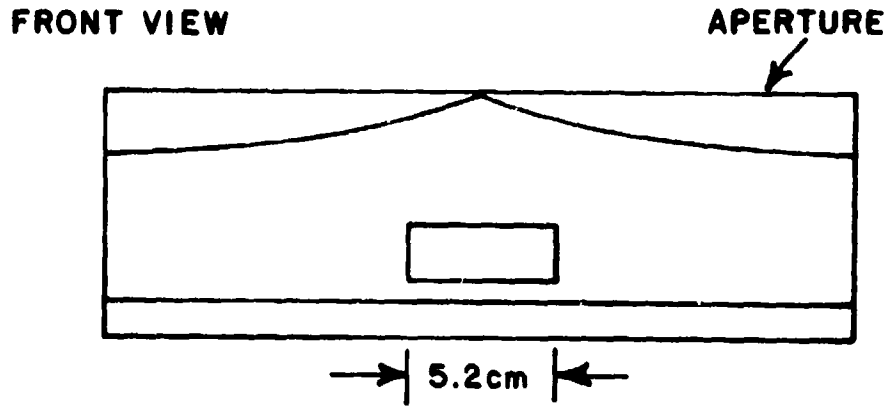

Fig. 2-3. The front view of the planar T-bar slot antenna showing the slotted T-bar which resulted from the ridge investigation.

Following the discovery of the slot within the T-bar as a useful tuning aid, the next investigation was to determine what effect the length, width, shape of such a slot, and its position in the T-bar has on the overall performance of the antenna. Investigation of the slot length initiated with a small circular hole in the center of the region where the slot was previously located in the T-bar. This hole was then lengthened symmetrically in incremental steps recording the insertion loss after each increase. Results of this experiment are shown in Fig. 2-4. The best performance is achieved when the slot length is 7.5 cm which corresponds to 0.5 wavelength at the highest frequency of the desired bandwidth and decreases when the length is increased above 7.5 cm. The slot affects only the bandwidth above 1500 MHz and the insertion loss shows greatest improvement (10 dB above the no slot case) at 2000 MHz.

After establishing the length of the slot within the T-bar, the next investigation was to determine the effects of the width of such a slot. Following the same procedure as before, the width of a 7.5 cm slot was increased incrementally with no substantial improvements in previous performance.

The position of the slot was investigated by constructing T-bars with the bottom of the slot incrementally moved from 1 cm above the bottom of the T-bar up to 5.0 cm. The insertion loss performance improved in each case to a distance of 4.0 cm. Above 4.0 cm the insertion loss remained essentially the same. Figure 2-5 shows this improvement to a distance of 4.0 cm. Note again that this

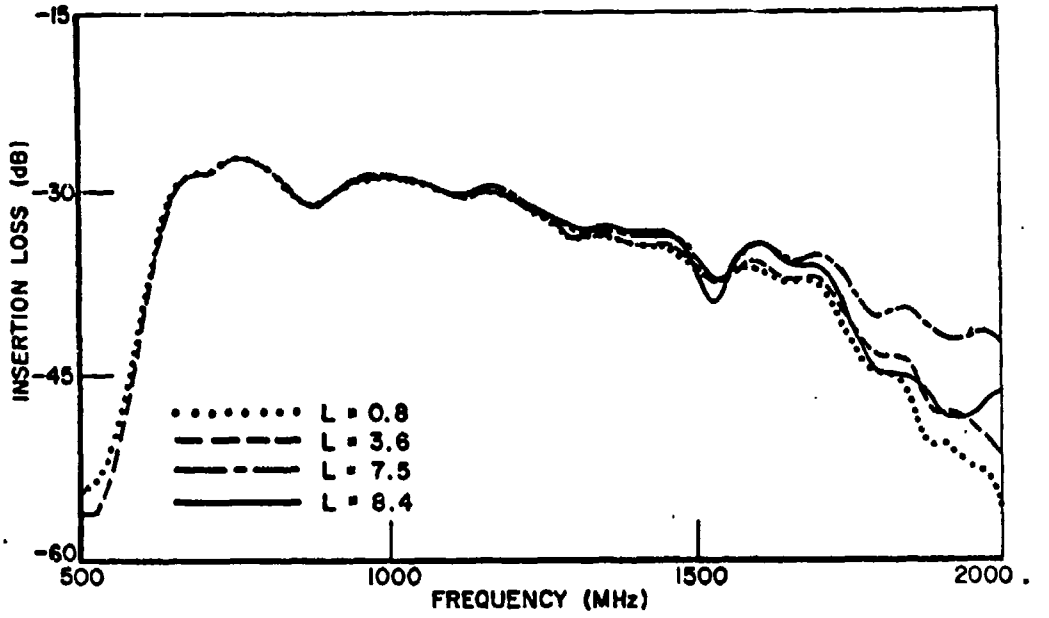

Fig. 2-4. Insertion loss investigation of the slot length within the T-bar (CD = 2.125, X = 2.2).

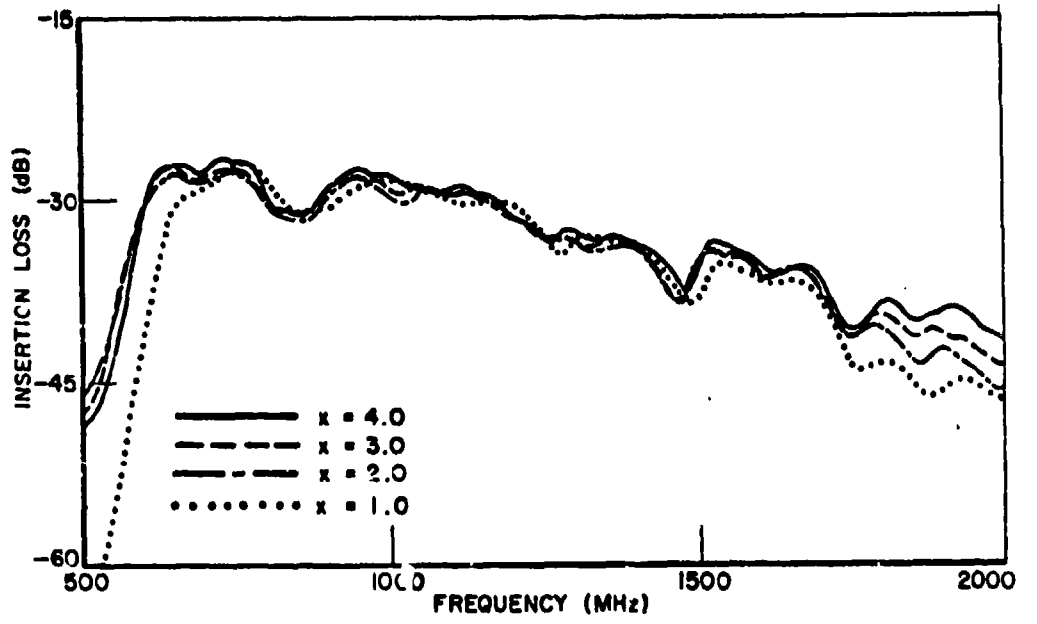

Fig. 2-5. Insertion loss investigation of the position of the slot within the T-bar (CD = 2.125).

improvement is confined to the higher end of the bandwidth (above 1500 MHz). This T-bar with slot length 7.5 cm, slot width 0.8 cm, and distance from slot to T-bar bottom 4.0 cm shall hereafter be termed T-bar D. This is the T-bar that is shown in Fig. 1-1.

The remaining questions about the T-bar geometry concern the shape of such a slot and the actual shape and size of the T-bar. After an experimental study of the triangular, square, and rectangular slot shapes, it was concluded that the original narrow rectangular slot with rounded corners was optimum. Various feed angles and T-bar widths were also investigated but did not give comparable performance to T-bar D.

C. Air-Filled Cavity Investigations

The next measurements were made to determine the effects of cavity depth on bandwidth performance. The best VSWR-impedance bandwidth should occur when the distance from the T-bar probe feed to the back wall of the cavity is a quarter wavelength at mid-frequency.[2] Therefore, it is desirable to determine what trade-offs exist between bandwidth and cavity depth in terms of insertion loss and VSWR. Using T-bar D, the air filled T-bar slot antenna was investigated while varying cavity depth from 2.25 inches to 1.25 inches in 0.125 inch steps. The experimental results (Fig. 2.6) show that from 500 to 1500 MHz the insertion loss increases as cavity depth is decreased, whereas above 1500 MHz it decreases. The limit of the insertion loss decrease occurs at a cavity depth of 1.5 inches, but at the lower end of the bandwidth the insertion loss continues to increase as cavity depth decreases. This result should be expected since the cavity depth approaches a quarter wavelength for the upper limit of the bandwidth and greatly decreases from a quarter wavelength at the lower frequency as it decreases to 1.5 inches ($\lambda/4$ for 2000 MHz = 1.47 inches).

The VSWR measurements for the same experiment (Fig. 2-7) indicate that as cavity depth decreases, the VSWR of the antenna increases from 500 to 1500 MHz but decreases from 1500 to 2000 MHz until a cavity depth of 1.5 inches is reached. This agrees with the insertion loss measurements because the ratio of power transfered should increase as the VSWR decreases and likewise decrease as the VSWR increases. This fact is also apparent in the results of the absolute gain measurements of the T-bar slot antenna shown in Fig. 2-8. An interesting note in Fig. 2-8 is the decrease in gain at 1500 MHz when the tuning stubs are removed from the aperture. Far field analysis shows that the H-plane pattern is reduced in magnitude but retains the same shape if the tuning stubs are removed.

Therefore, the tradeoffs involved due to cavity depth seem to balance out since the loss at the low end of the bandwidth is counterbalanced by an almost equal increase in performance on the high end.

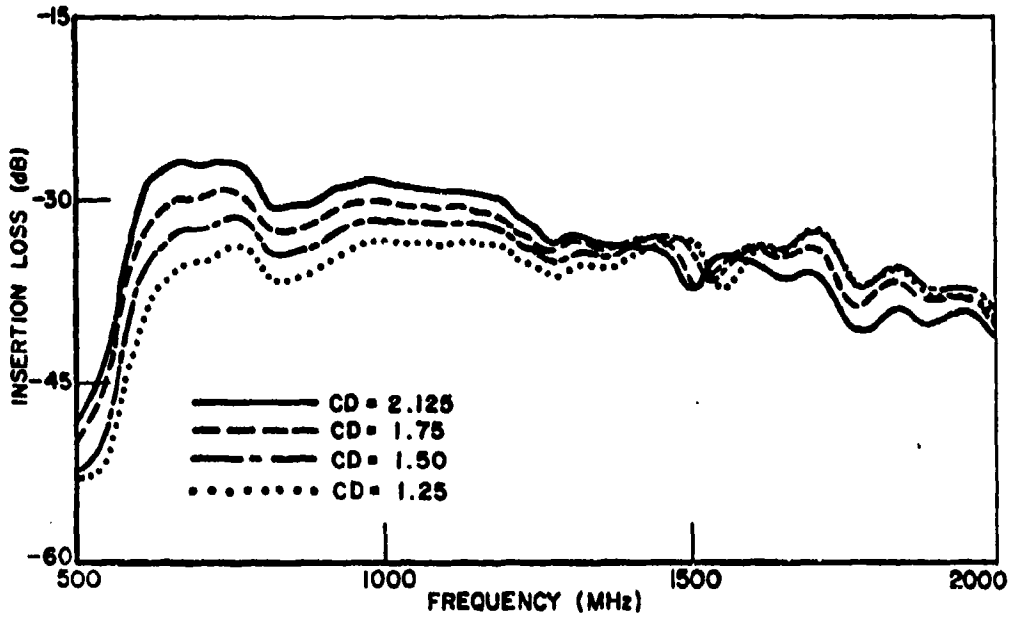

Fig. 2-6. Insertion loss results recorded as the cavity depth was varied.

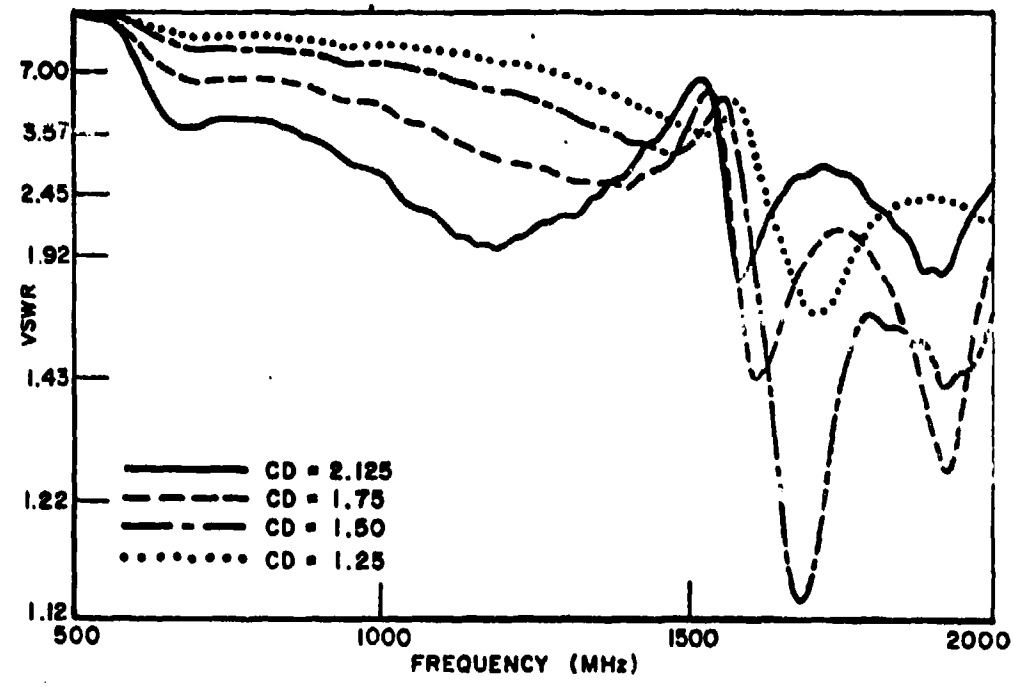

Fig. 2-7. VSWR measurements recorded as the cavity depth was varied.

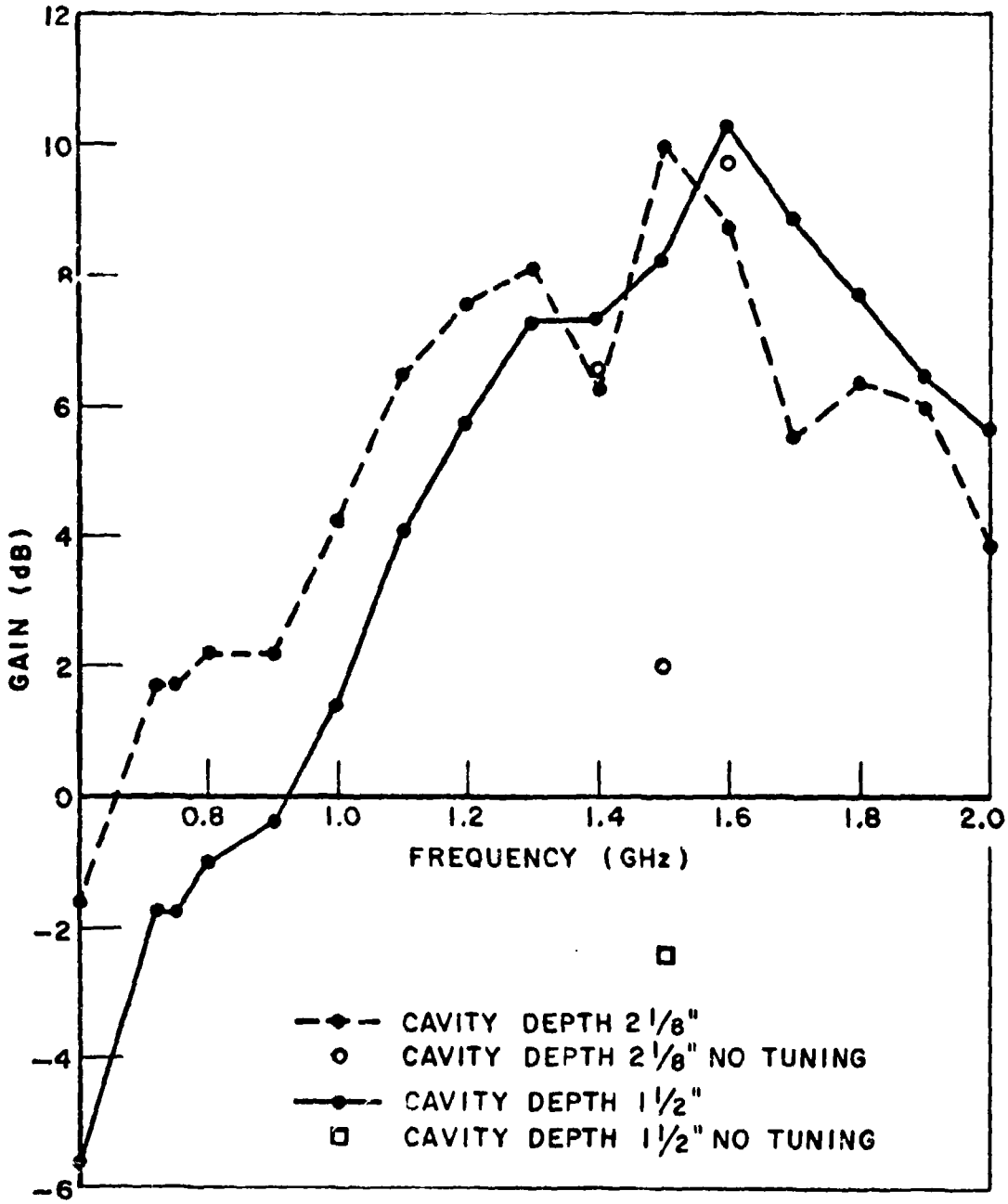

Fig. 2-9. Absolute gain of T-bar slot compared to isotropic.

Furthermore, these variations are caused by variations in the VSWR (which can be compensated with wide band matching)[2] rather than efficiency losses, since there are negligible losses in the antenna structure itself. It is concluded that the cavity depth of the air filled T-bar slot antenna may be decreased to 1.5 inches with only a slight decrease in overall performance. Note that while the antenna is $\lambda/2$ wide at 500 MHz, it does not assume a cavity depth of $\lambda/4$ until the frequency reaches 2000 MHz.

D. Dielectric Loaded Cavity Investigations

Dielectric loading of the T-bar slot antenna with a low loss dielectric material should produce similar results to the air case with the air-filled cavity size reduced by about $1/\sqrt{\varepsilon_r}$. Experiments were conducted to investigate this expectation by varying the cavity depth and filling the distance between the T-bar and back wall with 1/16 inch thick sheets of polystyrene. Then the experiments were repeated with the area in front of the T-bar filled with polystyrene. Theoretically, similar performance (compared to the air-filled 2.125 inch deep cavity) should be attained if the entire cavity is filled with polystyrene and the cavity depth decreased to 1.33 inches or if the area directly behind the T-bar is filled with dielectric and the cavity depth reduced to 1.6 inches. Figure 2-9 contains information obtained from this investigation for polystyrene material behind the T-bar. At a cavity depth of 1.25 inches, the insertion loss at the upper end of the bandwidth approximates that of the 2.125 inch air cavity; however performance is lost on the low end

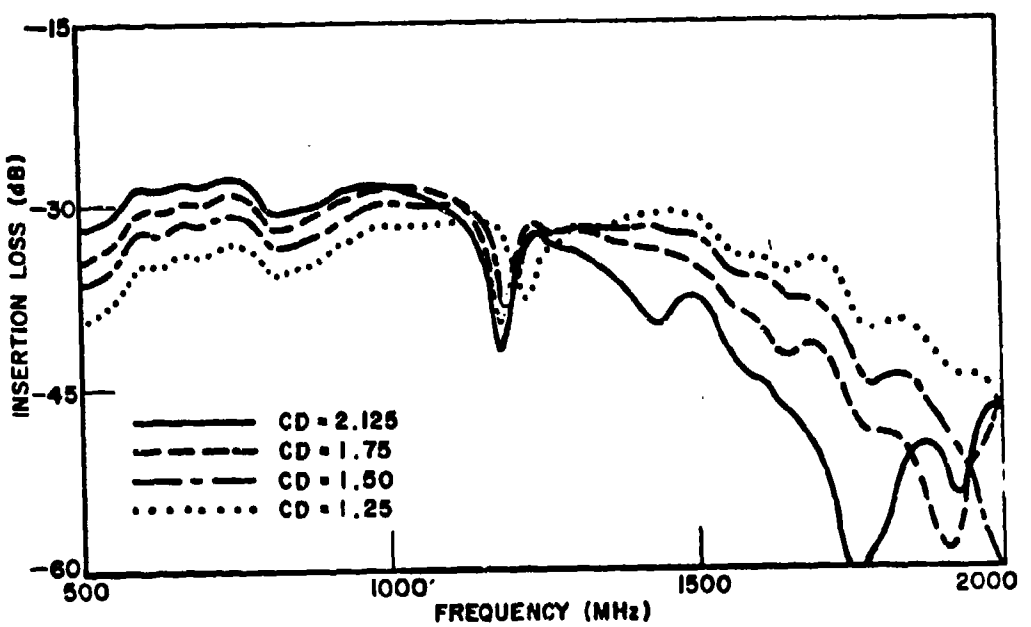

Fig. 2-9. Insertion loss measurements recorded as the cavity depth was varied with dielectric loading behind the T-bar.

of the bandwidth. The spike in insertion loss has moved from 1500 MHz to 1250 MHz, presumably due to the fact that the higher order modes are excited at a lower frequency in the dielectric. When the entire cavity was filled with dielectric, the insertion loss performance was again best at a cavity depth of 1.25 inches, however these results were not as good as the case where polystyrene was behind the T-bar only. Therefore, when dielectric loading is discussed elsewhere in this report, it should be assumed that all the dielectric is behind the T-bar unless stated otherwise.

Comparing the data obtained with dielectric material behind the T-bar with data obtained for equal air-filled cavity depths (Figs. 2-6 and 2-9), indicates that the air-filled cavity is superior until a cavity depth of 1.5 inches is reached. At a cavity depth of 1.5 inches and below the information obtained must be explained in terms of tradeoffs. Cavity depths 1.25, and 1.5 inches possess better insertion loss performance, when dielectric loaded behind the T-bar, up to a frequency of 1600 MHz with the exception of the spike occurring at 1250 MHz. It is assumed from previous experience that the spike may be tuned out by repositioning the tuning stubs. However, above 1600 MHz insertion loss performance decreases rapidly for the dielectric loaded antenna. Therefore, for a shorter bandwidth, the performance is improved with the addition of dielectric materials behind the T-bar. But, if a 4:1 bandwidth is required, the better of the two cases would be the air-filled cavity.

Recall that the effect of the slot within the T-bar is to improve the insertion loss at the high end of the band, then a logical question would be, is the slot within the T-bar the optimum length for a dielectric loaded antenna? The slot length within the T-bar for a cavity depth of 1.5 inches and 0.75 inches of polystyrene behind the T-bar was investigated with the same procedure as the air case. The results of this experiment indicate that the optimum length for the slot with a dielectrically loaded cavity is 7.6 cm which is approximately the same as before.

Continuing the dielectric experiments, only the region in front of the T-bar was filled with polystyrene and the cavity depth was reduced to 1.25 inches from 1.5 inches. Comparing these results (Fig. 2-10) to the previous dielectric experiments (Fig. 2-9), the case with tuning stubs is in agreement with the previous case of comparable cavity depth and slight improvements in the spike region and higher end of the bandwidth are noted. These responses are similar on the low end and improved on the high end and spike region (when compared to Fig. 2-9). Comparing these results to the air case of comparable cavity depth shown in Fig. 2-6 does not show an improvement over the air-filled case. Since most slot antennas are covered with radome material (low loss dielectric) the information obtained is of some value. The comparison shows that the insertion loss performance gained on the low end of the bandwidth ($\cong$ 2 to 3 dB) is approximately matched to that lost on the high end. So,

covering the T-bar slot with a dielectric radome should not greatly degrade the performance.

To complete the investigation of dielectric loading, the VSWR of the antenna with polystyrene behind the T-bar was investigated. The results of this experiment at cavity depths 2.0 and 1.5 inches compared to previous air-filled cases are shown in Fig. 2-11. The dielectric loading changes the VSWR bandwidth at a cavity depth of 2.0 inches, however at 1.5 and 1.25 inches the VSWR seems to be only shifted in frequency. The peak in VSWR also occurring at 1500 MHz for the air case is shifted to approximately 1250 MHz for the same reasons as stated before.

E. Far Field Analysis

At cavity depths of 1.5 and 1.25 inches the normalized far field patterns (H-plane) were recorded with and without dielectric loading behind the T-bar. The far field patterns are broadband until 1500 MHz where lobing occurs for the air-filled cavity. This result should be expected since the aperture is 1.5 wavelengths long at 1500 MHz, and thus the TE_{30} mode is excited. With dielectric loading behind the T-bar, the antenna exhibits a less broad pattern and lobing occurs at a lower frequency (1300 MHz). The TE_{30} mode is excited at a lower frequency with the addition of dielectric, thus causing the lobing to occur at 1300 MHz.

The general shape of the patterns was unchanged with various cavity depths for the air case. However measured power levels decreased with cavity depth as predicted by the insertion loss measurements. Normalized patterns are shown in Figs. 2-12 and 2-13.

F. Resistive Tuning Techniques

It is desirable that the T-bar slot antenna exhibit a broad beam pattern over the entire specified bandwidth. To accomplish this goal, the antenna's electrical length must remain less than three-halves wavelength over the entire bandwidth or else the higher order modes must be suppressed. Choosing the latter method to extend the pattern bandwidth, resistive tuning techniques were applied to the aperture. Resistive tuning stubs were constructed from narrow 20 ohm resistance cards to fit the width of the aperture. With a cavity depth of 1.5 inches and polystyrene dielectric behind the T-bar, the resistive tuning stub positions were varied in the aperture while measuring the insertion loss. Comparing the results to the dielectric case in Fig. 2-14 it is seen that the insertion loss was increased over most of the bandwidth by approximately 5 dB and that it slightly decreased above 1700 MHz, presumably, due to pattern improvement at the higher frequencies. Since resistance has been introduced into the aperture, the possibility of decreasing antenna efficiency exists.

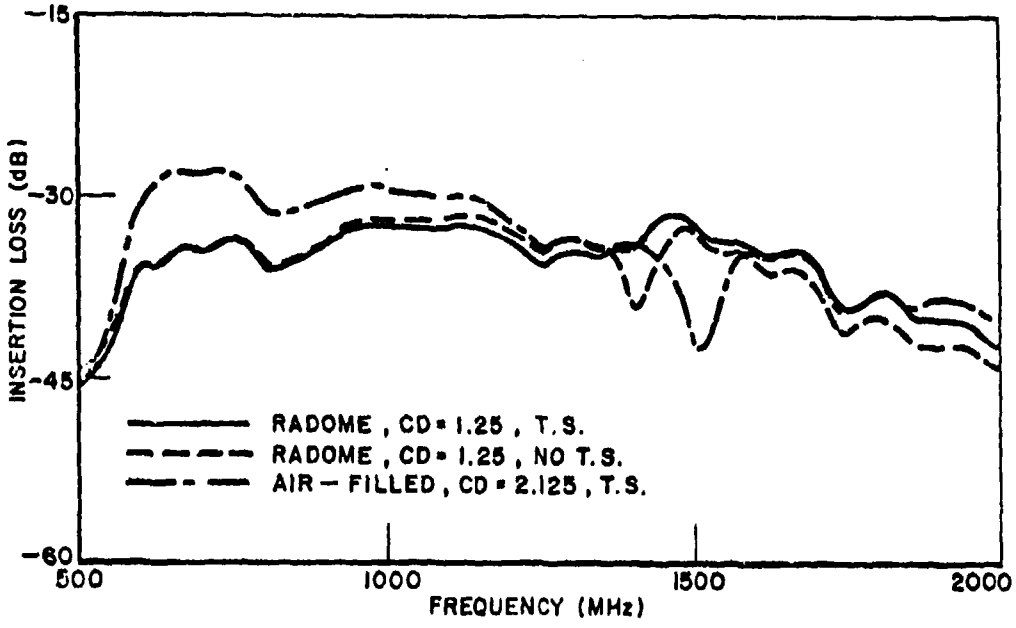

Fig. 2-10. Insertion loss comparisons of the air-filled case and radome covered case. In the radome case, polystyrene fills only the region in front of the T-bar.

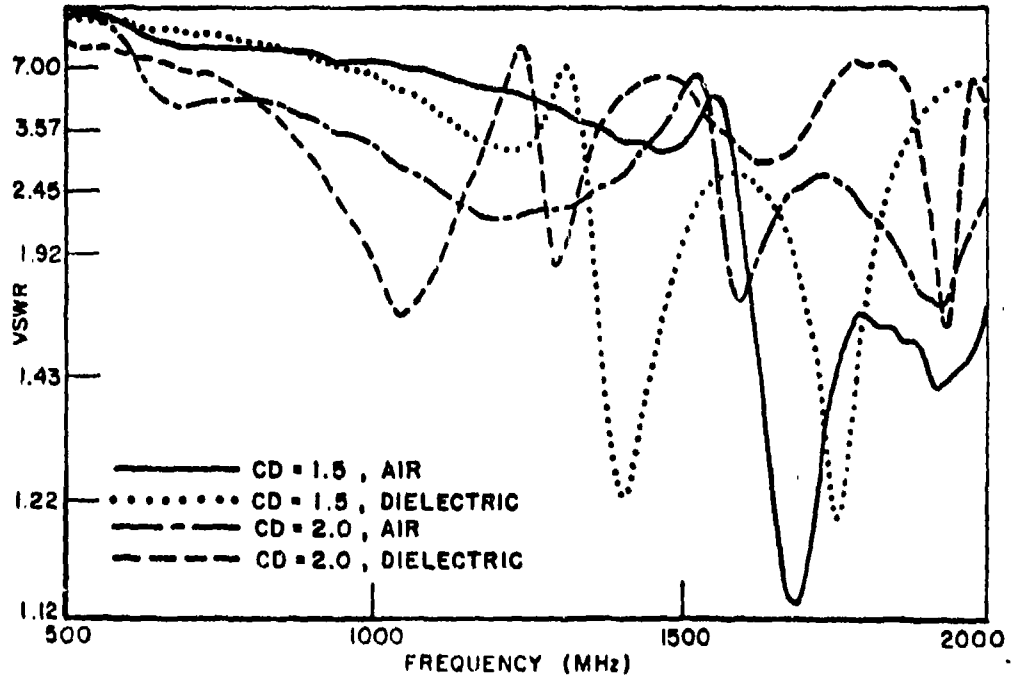

Fig. 2-11. Comparisons of the VSWR measured for the air-filled cavity and the dielectric loaded cavity.

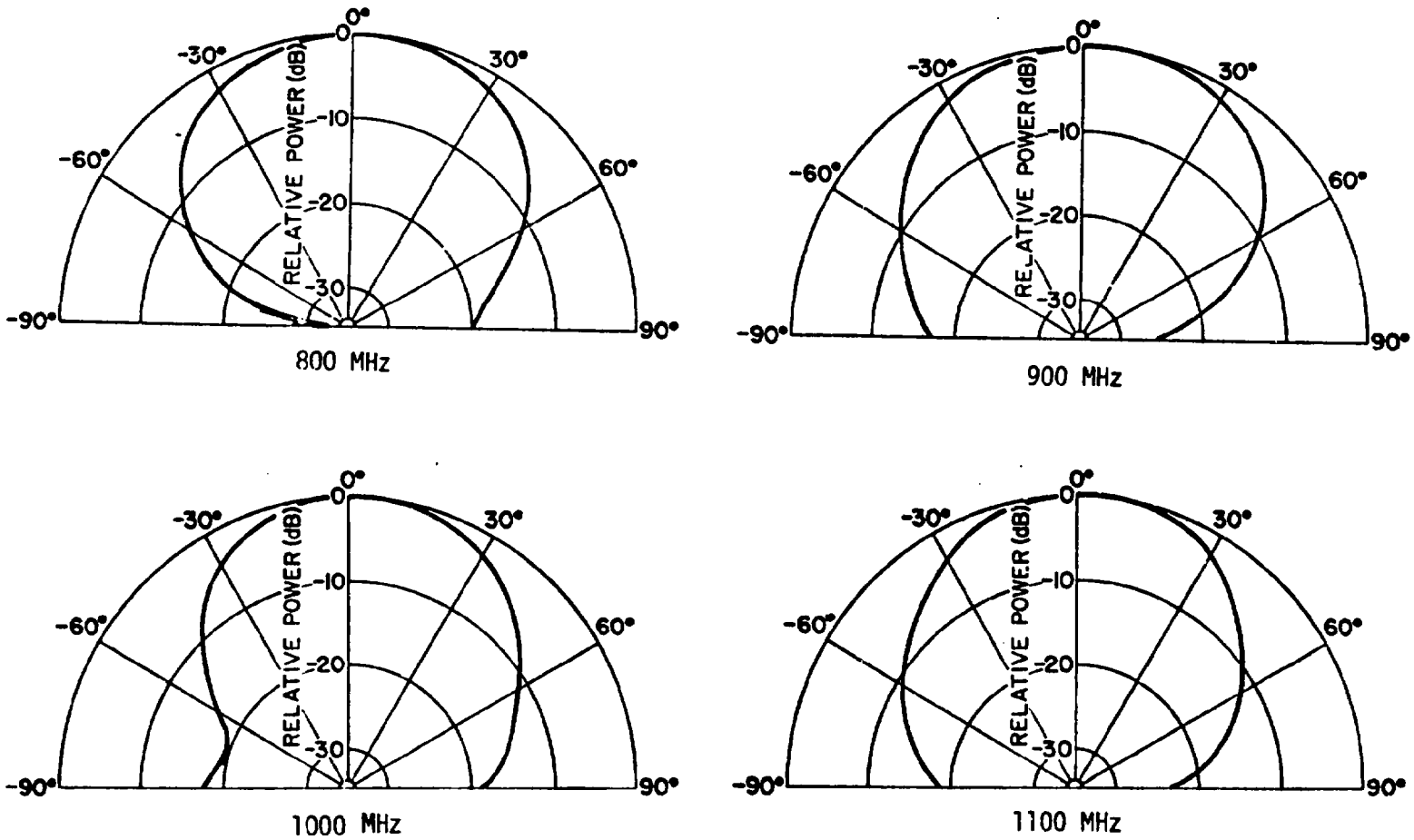

Fig. 2-12. Normalized far field patterns (H-plane) of the planar T-bar antenna. The air-filled cavity depth for these measured patterns is 1.5 inches.

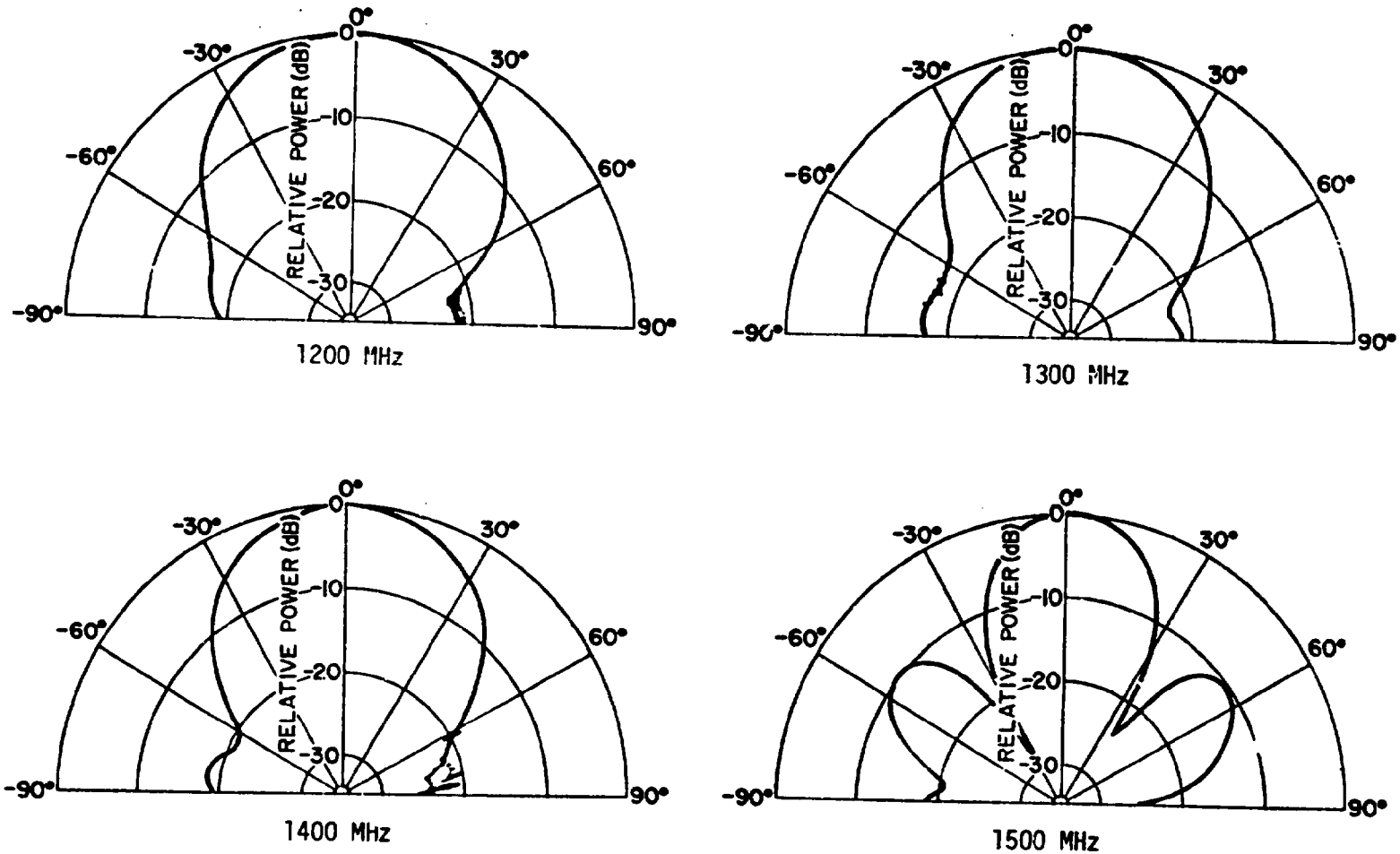

Fig. 2-12. (Continued).

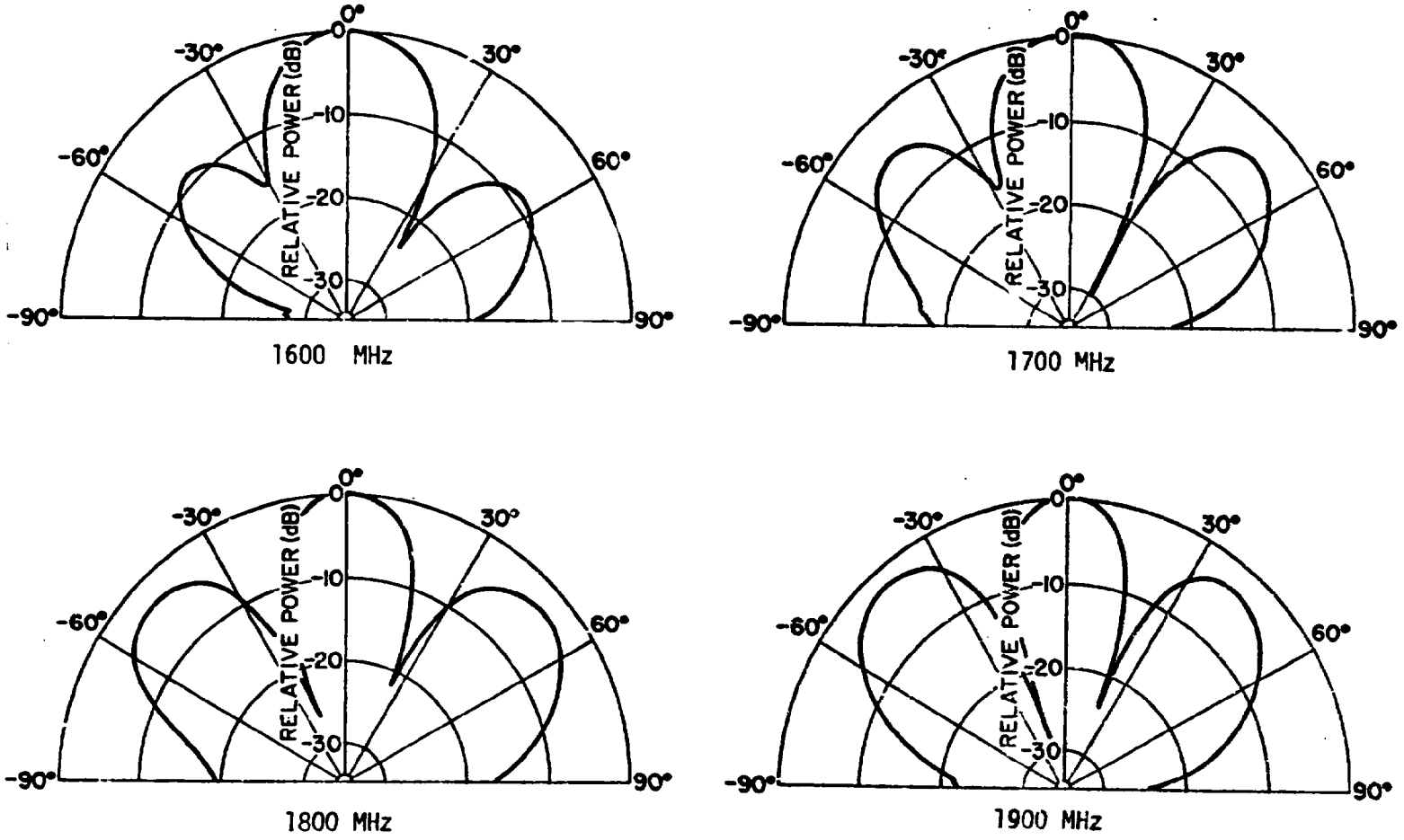

Fig. 2-12. (Continued).

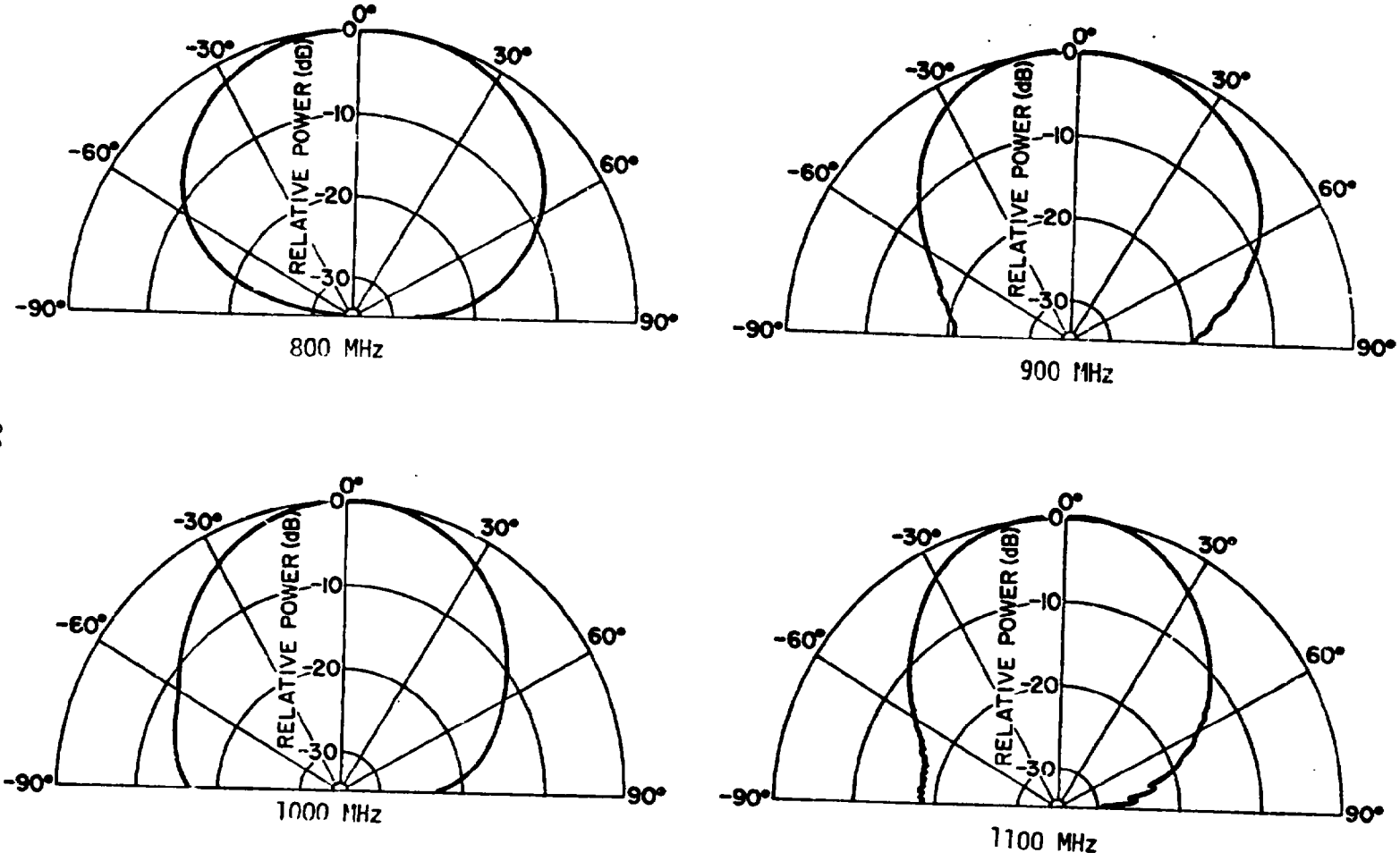

Fig. 2-13. Normalized far field patterns (H-plane) of the planar T-bar antenna with dielectric loading behind the T-bar. (CD = 1.5)

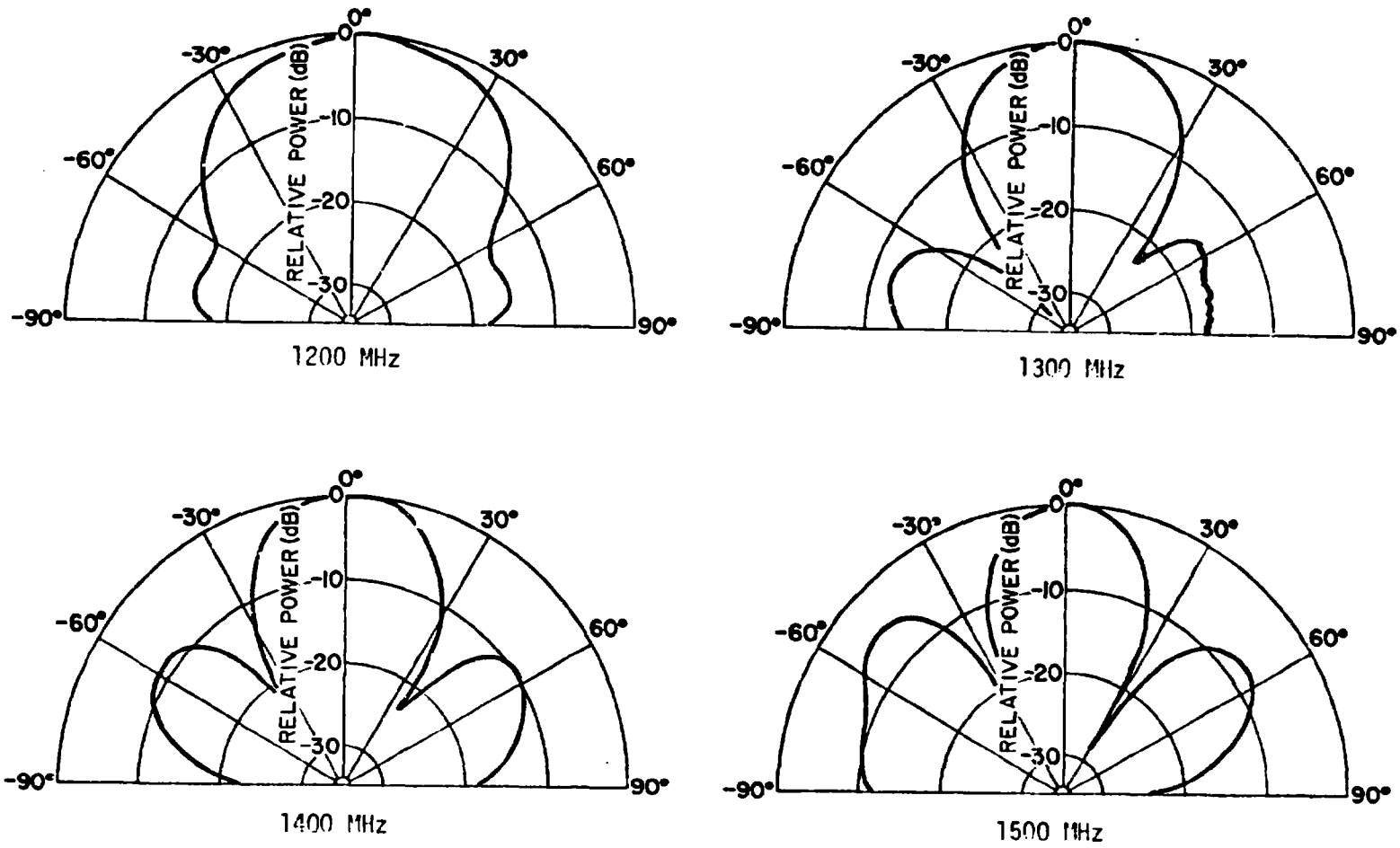

Fig. 2-13. (Continued).

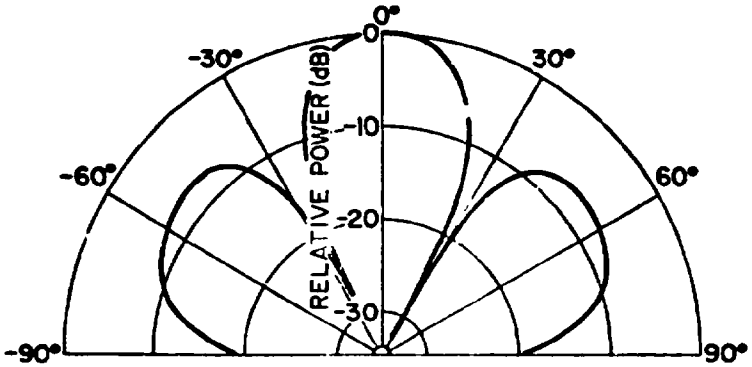

1600 MHz

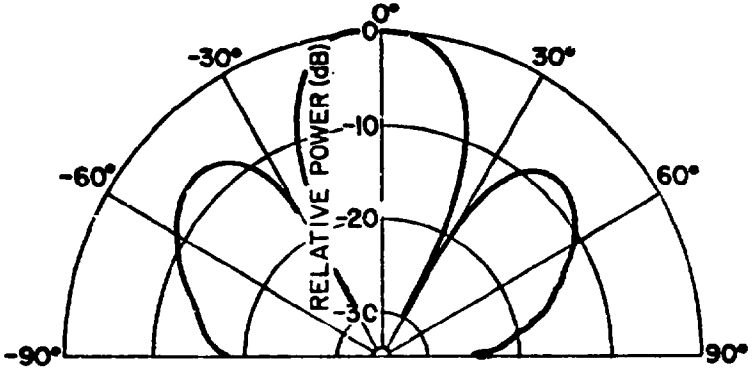

1700 MHz

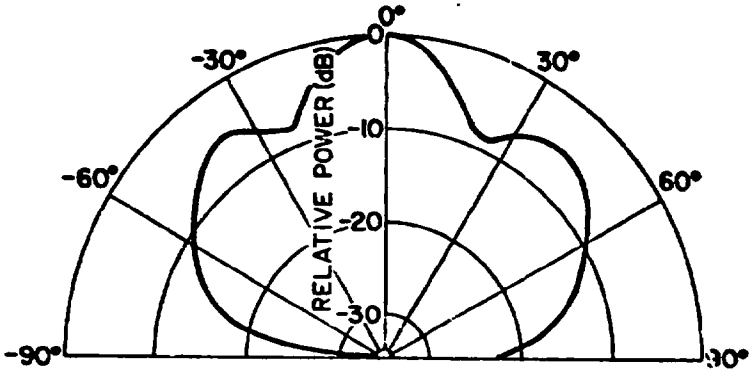

1800 MHz

Fig. 2-13. (Continued).

The insertion loss measurement did not verify that the TE_{30} mode had been suppressed, so the VSWR of the antenna was measured. The VSWR was better across the entire bandwidth than either the air or dielectric loaded case as shown in Fig. 2-15 and specifically the peak at 1500 MHz has been suppressed. Therefore, the higher order modes have been tuned out at the expense of efficiency in the antenna as indicated by the insertion loss measurement (Fig. 2-14). To further verify this conclusion, normalized far field patterns were recorded for the resistive tuned cavity with resistance cards located at 2.75 inches from each side wall of the cavity directly in front of the T-bar. These results are shown in Fig. 2-16. The patterns are sufficient proof that the TE_{30} mode is suppressed since the T-bar slot antenna now has a 4:1 pattern bandwidth.

G. Investigation of Effects Due to T-bar Depth from the Aperture

Since it was desired to reduce the cavity depth from 1.5 inches, the tradeoffs between T-bar depth from the aperture and bandwidth performance were investigated. The T-bar depth from the aperture was reduced by a factor of 4 to only a depth of 3/16 inches, but the spacing between the T-bar and back wall remained the same so as to obtain similar performance to the previous 2.125 and 1.50 inch cavity depths. This results in cavity depths of 1.56 and 0.94 inches to replace each previous cavity depth respectively. Insertion loss studies were conducted to determine which cavity depths did produce similar results to previous measurements. The insertion loss measurements which compare most evenly with those of cavity depths 2.125 and 1.5 inches are 1.625 and 1.125 inches respectively. Allowing for experimental errors, the comparisons are considered quite close as shown in Figs. 2-17 and 2-18. Therefore, the cavity depth of the T-bar slot antenna can be reduced by decreasing the T-bar depth from the aperture plane while maintaining the same distance between the back wall and T-bar.

Dielectric loading and VSWR studies were made to complete the study of this new configuration, which will be called the 316 T-bar slot antenna. The conclusions derived from the dielectric study were the same as before. The VSWR (Fig. 2-19) as well as insertion loss results show an improvement in the region of 1500 MHz. Experimental studies reveal that if the tuning stubs, which are now positioned directly under the T-bar, are removed, the singularities previously observed in insertion loss and VSWR return. However, comparing these results to the VSWR of the resistive tuned case. the improvement is not enough to suppress the TE_{30} mode. Therefore, similar far field patterns and gain measurements compared to the previous 1.5 inch air filled cavity should be expected. Since both the insertion loss and VSWR measurements of the 316 T-bar slot antenna (CD = 1.125) are in good agreement with the previous 1.5 inch case, it is concluded the 316 T-bar can replace the previous case.

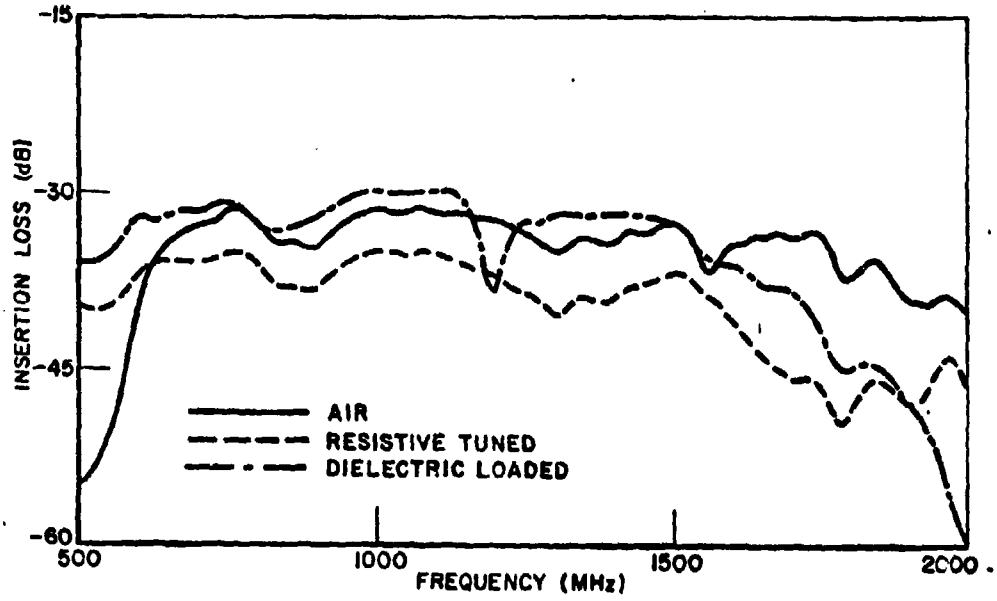

Fig. 2-14. Insertion loss measurement comparison of the air-filled, dielectric loaded, and resistive tuned T-bar slot antennas. Cavity depth in each case is 1.5 inches.

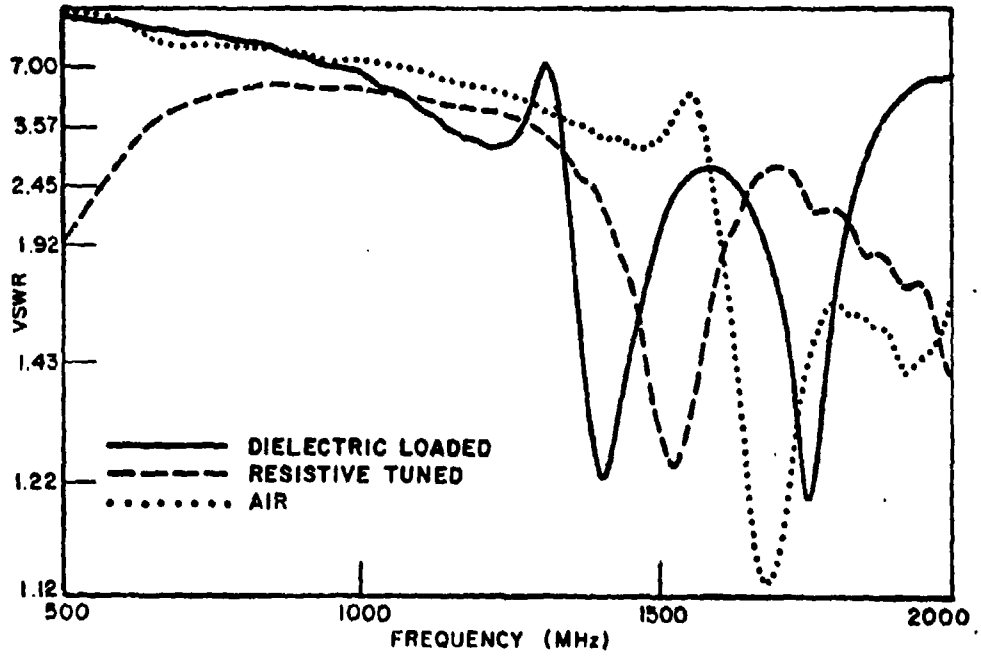

Fig. 2-15. VSWR comparison of the air-filled, dielectric loaded, and resistive tuned T-bar slot antennas. Cavity depth in each case is 1.5 inches.

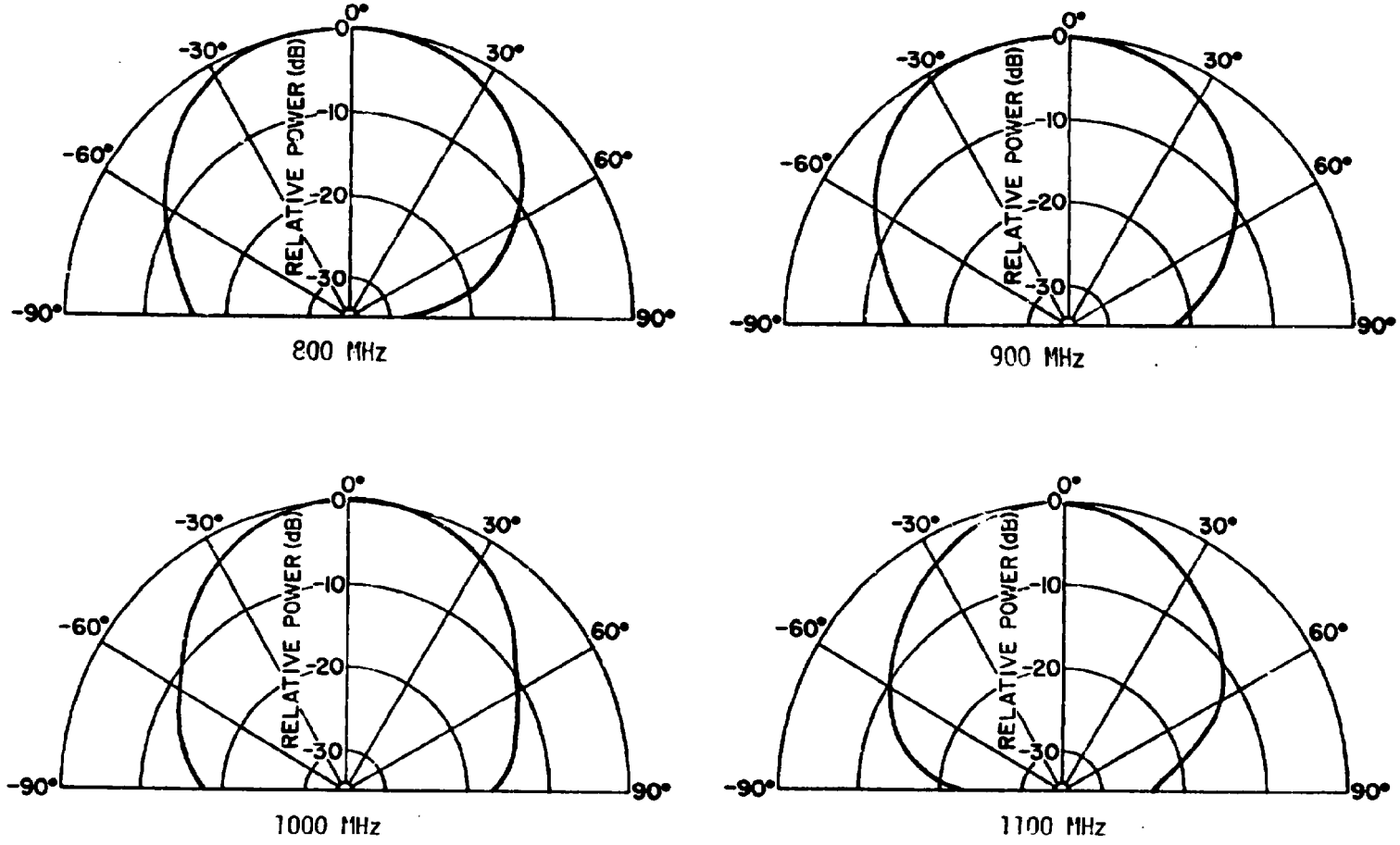

Fig. 2-16. Normalized far field (H-plane) patterns of a resistive tuned T-bar slot antenna. The cavity depth is 1.5 inches with dielectric loading behind the T-bar.

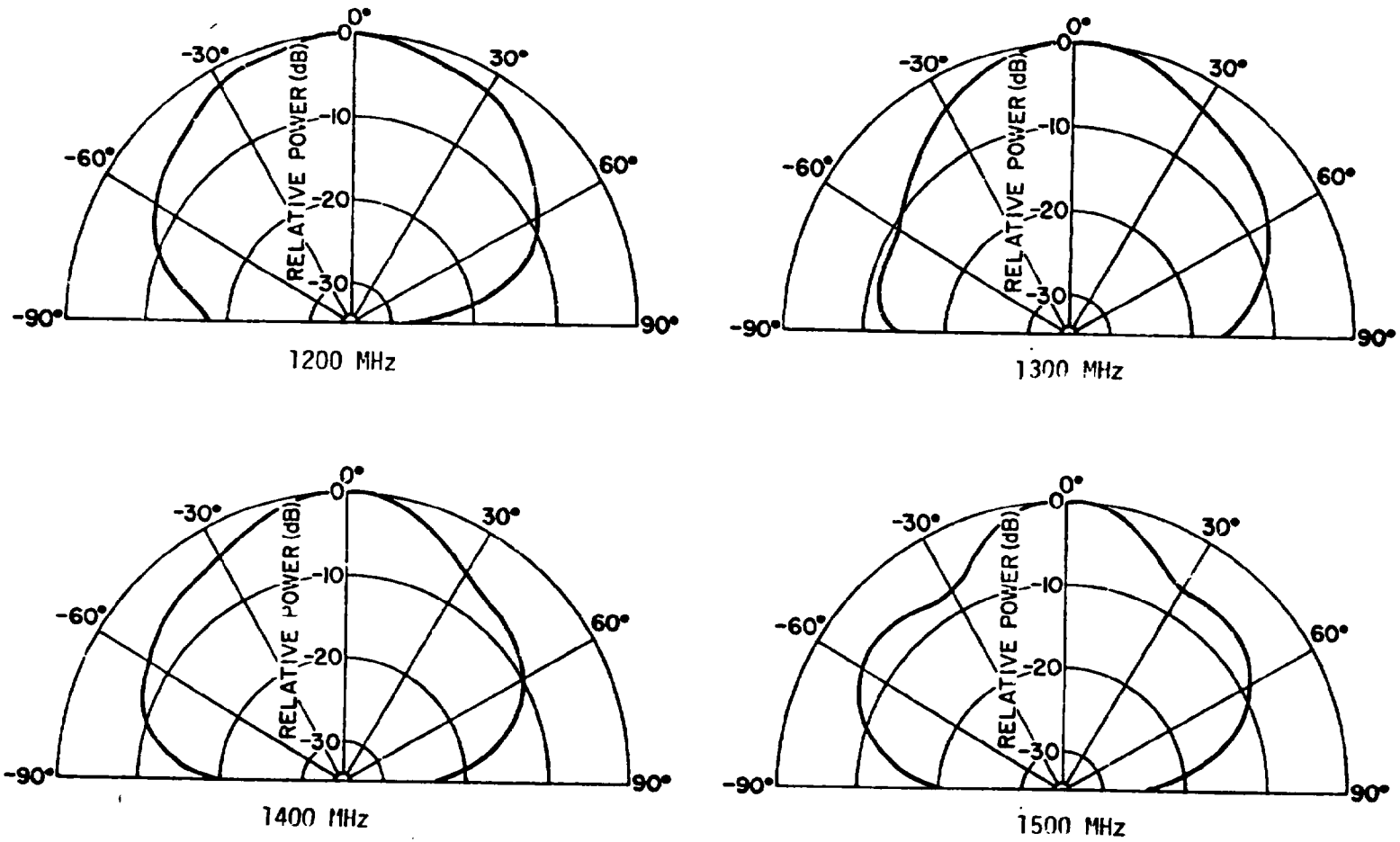

Fig. 2-16. (Continued).

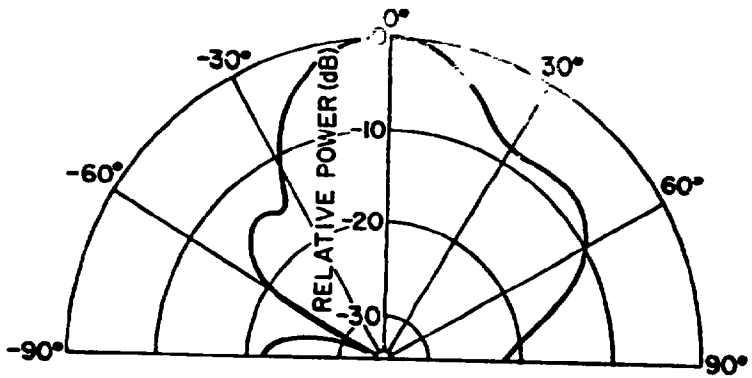

1600 MHz

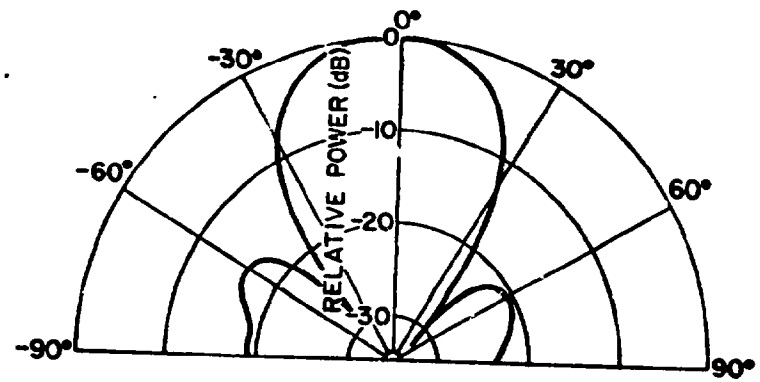

1700 MHz

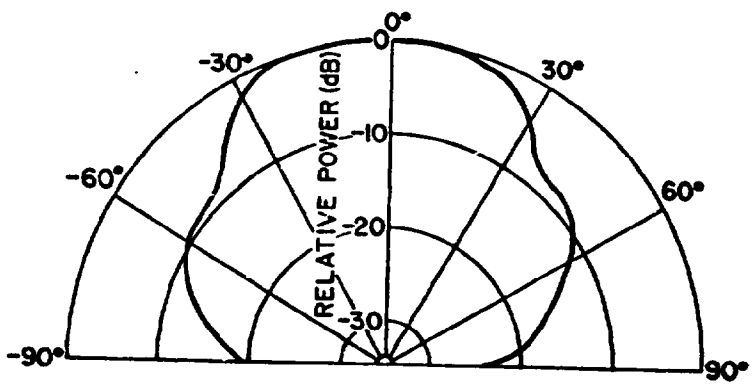

1800 MHz

Fig. 2-16. (Continued).

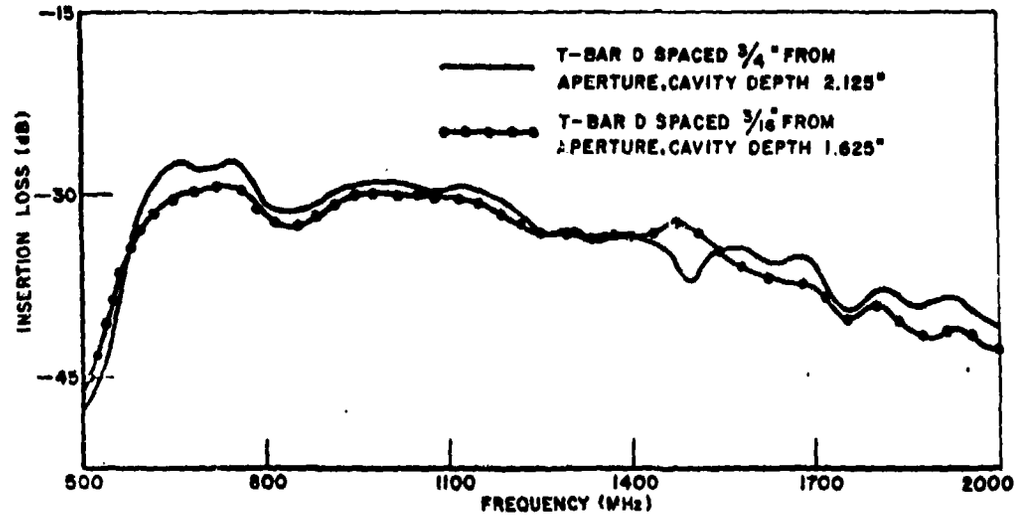

Fig. 2-17. Insertion loss comparison between previous 2.125 inch T-bar antenna and its 316 T-bar antenna replacement.

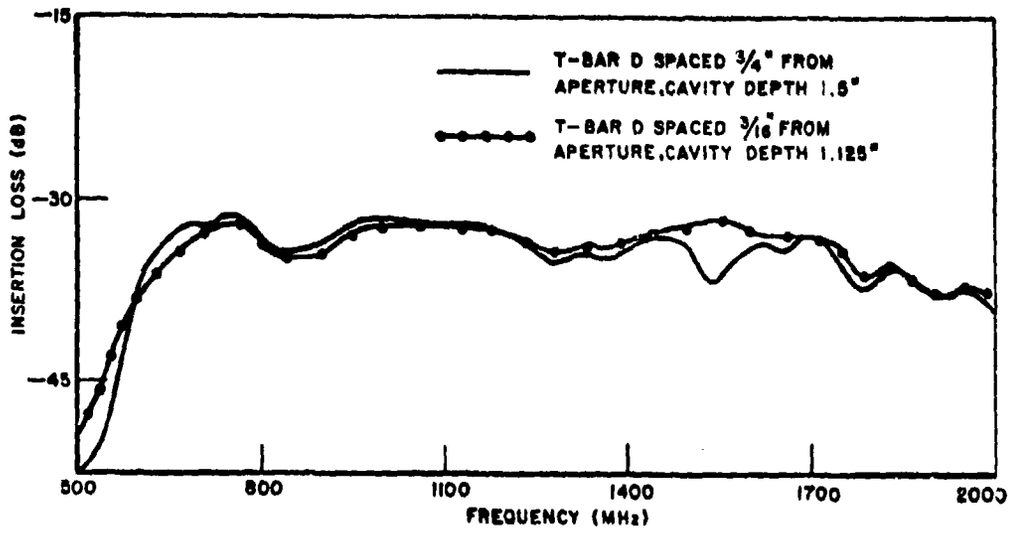

Fig. 2-18. Insertion loss comparison between previous 1.5 inch T-bar antenna and its 316 T-bar antenna replacement.

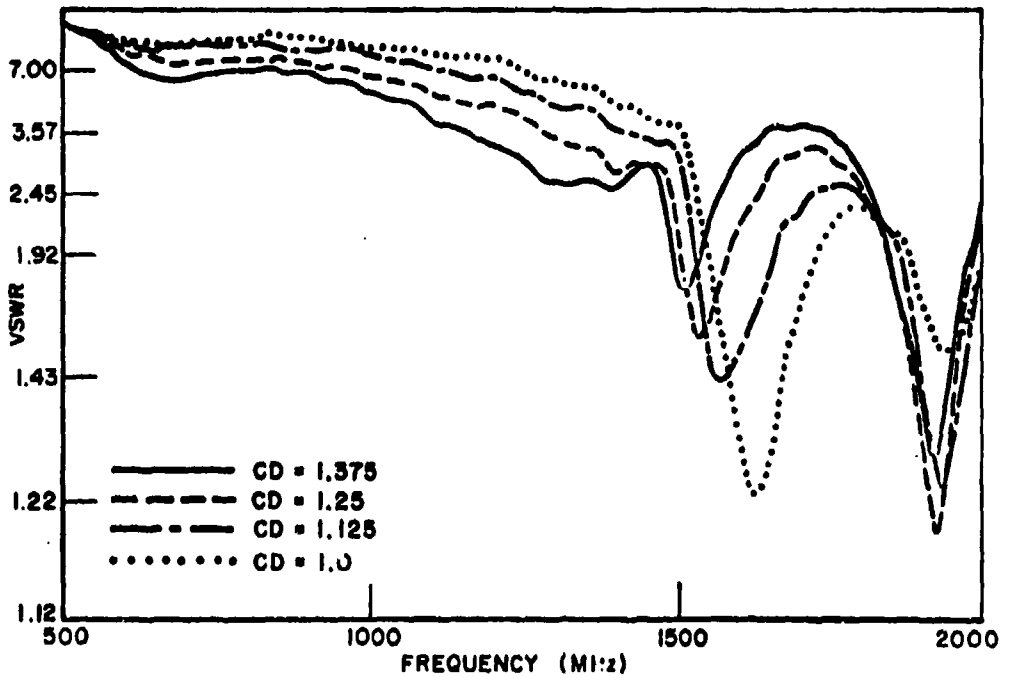

Fig. 2-19. VSWR of the 316 T-bar antenna as the cavity depth is varied.

H. Summary

The results of the experimental investigation have shown two important improvements in T-bar fed slot antennas. The first improvement is that the bandwidth of the T-bar slot antenna can be increased by a factor of two over the conventional T-bar slot antenna design. The second improvement is that the depth of the antenna may be significantly reduced from that required of previous designs.

The bandwidth improvement of the antenna was accomplished by replacing the T-bar of circular cross section with a T-bar of thin rectangular cross section and then optimizing the geometry of the T-bar as described in section B of this chapter.

The size reduction of the antenna was accomplished by decreasing the total cavity depth from $\lambda/4$ at mid-band to $\lambda/4$ at the highest frequency (shortest wavelength) of interest and by moving the T-bar as close as practical to the aperture. This causes some decrease in gain at the low frequency end of the bandwidth but also results in improved performance at the high frequency end. These results were discussed in sections C and G.

Section D showed that dielectric loading was not effective in improving the electrical performance or in reducing the size over that obtainable for the air-filled case above.

The following evaluation of the T-bar antenna performance serves to illustrate the characteristics described above. This evaluation is done by comparing the T-bar slot antenna to another antenna of comparable bandwidth using the insertion loss measurement technique discussed in section A. The insertion loss comparison was made with a pair of 500 to 2000 MHz log periodic antennas and the results are shown in Fig. 2-20. These results show several things. First, the T-bar antenna of cavity depth 2.125 inches compares well with the log periodic. Secondly, as the cavity depth is decreased, the low frequency performance declines but the high frequency performance increases as noted above. Even for the smaller cavity depths, the overall performance is remarkably good when compared to the highly efficient log periodic antenna.

Thus, the T-bar slot antenna evolving from this investigation offers a viable solution to receiving situations requiring a wide band slot antenna of shallow cavity depth.

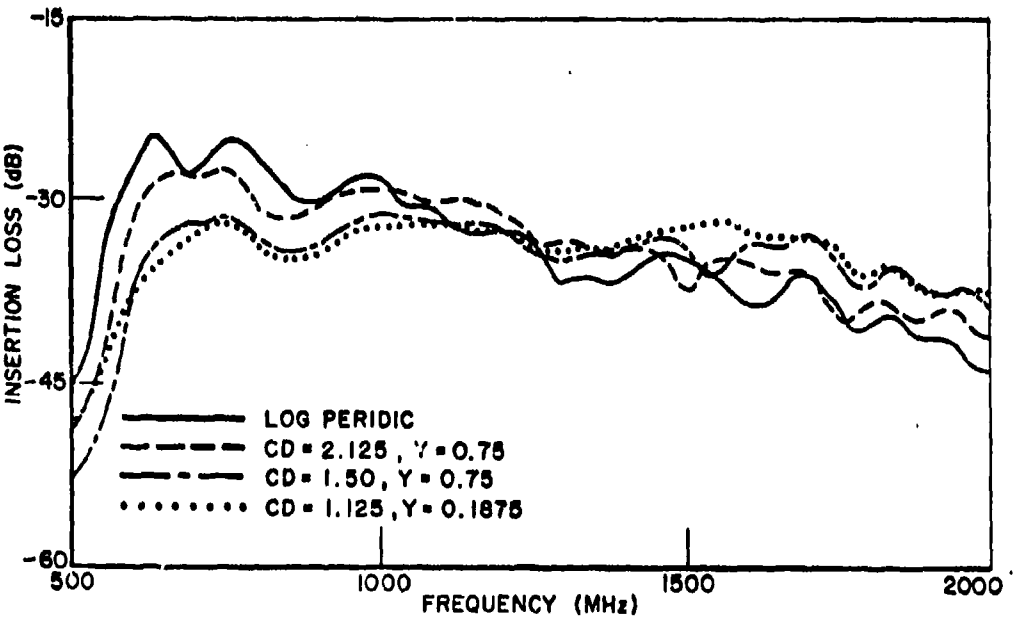

Fig. 2-20. Insertion loss measurements comparing 3 different planar T-bar slot antenna configurations with a log periodic antenna. The cavity depth (CD) and T-bar depth (Y) are denoted on graph.

CHAPTER III

DESIGN AND EXPERIMENTAL INVESTIGATION OF A T-BAR FED SLOT ANTENNA MOUNTED TRANSVERSELY ON A CYLINDER

A. Introduction

Recall from Chapter I that the ultimate gool of this investigation is to design a transverse T-bar fed slot antenna on a seven inch diameter cylindrical surface. Designing a cylindrical slot of the exact dimensions as the planar version resulted in a slot which spanned more than half the circumference of a seven inch diameter cylinder. The final design shown in Fig. 3-1, was arrived at by making the aperture dimensions (width and arc length) and T-bar shape identical to the planar model. The back walls of the cavity and T-bars were constructed from sections of circular cylinders which could be easily interchanged to provide variable cavity depth, T-bar depth, and interchangeable T-bars. To simplify construction, the side walls of the cavity were radial arms extending from the center of the seven inch diameter cylinder. Therefore the interior arc length (back wall) was slightly less than the aperture length. The cylindrical design possessed the same variable parameters as the planar model, and therefore the same testing procedures could be used to determine the bandwidth performance as were used for the planar model.

B. Air-Filled Cavity

Initially, the VSWR of the cylindrical T-bar slot antenna was investigated as the cavity depth was varied. The results of this experiment, shown in Fig. 3-2, indicate that the higher order mode may not be excited in the cylindrical aperture for an air-filled cavity. As the cavity depth is decreased from 1.5 inches the VSWR increases, and in each case the aperture appears to be cut off from 500 to 700 MHz. This cutoff is probably due to the cavity construction. That is, the shorting plate of the cavity is not the same length as the aperture opening (pie slice shaped - see Fig. 3-1) thereby causing a higher cutoff frequency for the antenna.

Continuing the VSWR investigation, the slot within the T-bar was removed by replacing T-bar D with a T-bar of the same dimensions except there was no slot. The presence of the slot is responsible for the improvement in VSWR in the 1500-1800 MHz region as shown in Fig. 3-3. This was the same conclusion derived from the planar T-bar slot antenna, except in the planar study, improvement in VSWR continued above 1800 MHz. In the cylindrical case, no difference is noted between the two cases above 1800 MHz.

a) b) c)

Fig. 3-1. A T-bar slot antenna mounted transversely on a seven inch diameter circular cylinder.
a) front view
b) side view
c) top view with top cylinder removed.

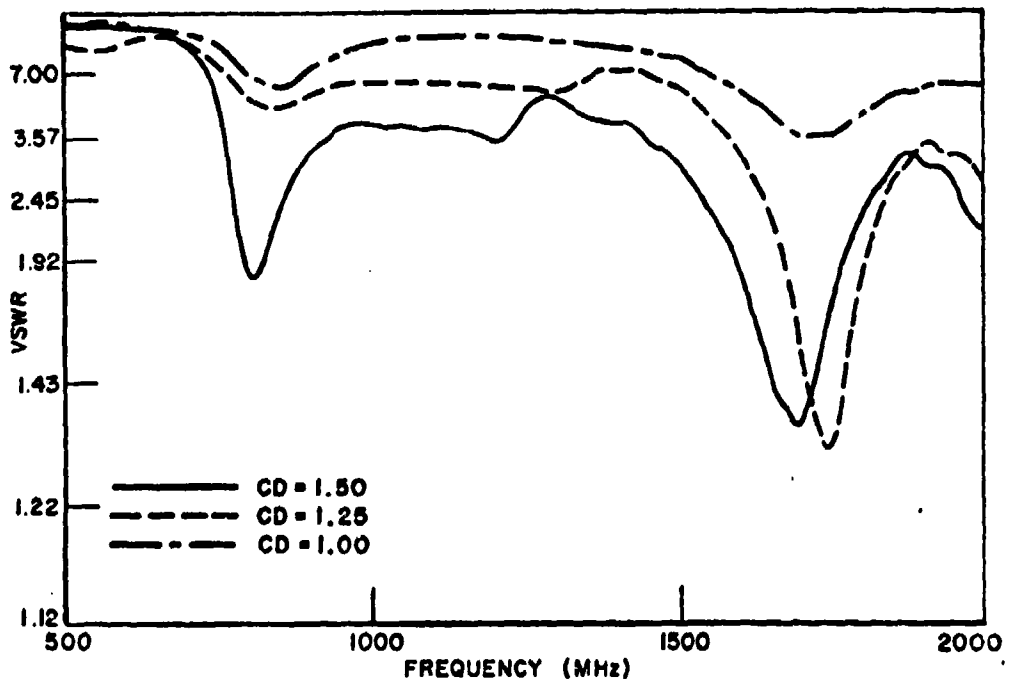

Fig. 3-2. VSWR of cylindrical T-bar slot antenna as the cavity depth is varied.

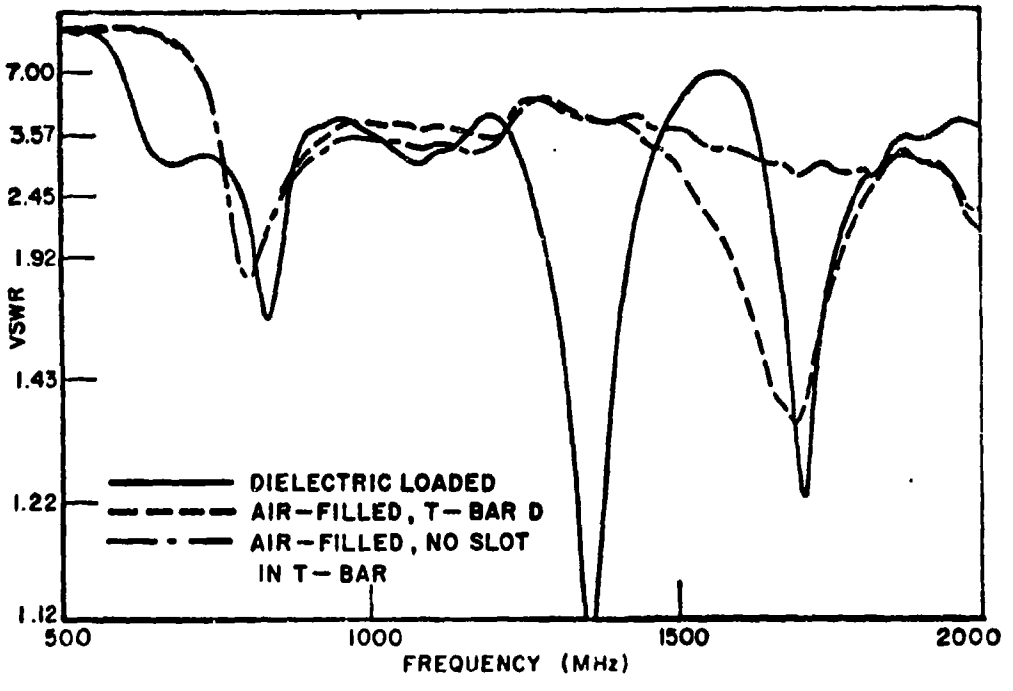

Fig. 3-3. VSWR comparison of three different cylindrical T-bar antenna configurations. (CD = 1.5)

The normalized far field patterns (H-plane) of the air-filled cavity shown in Fig. 3-4 exhibit a much broader pattern than the planar model with no lobing until 1800 MHz where the pattern completely splits into two lobes. The broader patterns were expected since the effects of the planar ground plane (a sin θ element pattern) were not present with the cylindrical surface. The lobing pattern at 1800 MHz introduces the idea that the TE_{30} mode is established at a higher frequency than observed for the planar model. Further investigation showed that as the cavity depth was varied, there was no distinct change in pattern shape; however relative power levels did change as predicted by VSWR results.

To further investigate the cylindrical T-bar slot antenna, insertion loss studies were conducted. As the air-filled cavity depth was decreased, the insertion loss increases in agreement with VSWR measurements with a slight decrease noted above 1700 MHz. Further investigation shows that this decrease is caused by the grating lobes becoming more broad beam, not an increase in the small broadside lobe.

The impressive trade-offs in bandwidth performance characterized by the planar T-bar slot antenna are not apparent in the results of the cylindrical T-bar slot antenna since the investigations began at the shallow cavity depth of 1.5 inches. The size of the slot on the cylinder is prohibitively large to allow for a deeper cavity depth.

It is apparent from this study that the air-filled cavity (1.5 inch deep) has a bandwidth of nearly 800 to 1700 MHz (2.1:1) in terms of reasonable VSWR, insertion loss, and nonlobing patterns. This could possibly be extended to a lower frequency (500 MHz) if the corners of the back wall are corrected as shown in Fig. 3-5.

C. Dielectric Loaded Cavity

Attempting to improve the T-bar slot antenna, polystyrene dielectric loading behind the T-bar was investigated. Results (Fig. 3-3) indicate that there is an improvement in the regions 600 to 750 MHz and 1250 to 1450 MH· with slight degradation between 1500 and 1600 MHz. This degradation resembles the peak in VSWR which the TE_{30} mode caused in the planar model. It appears that the cutoff frequency of the aperture has been extended on the lower end of the bandwidth at the expense of exciting the TE_{30} mode at a lower frequency. These results are identical to the conclusions derived in the planar study, and thus filling the entire cavity with dielectric material was not investigated after considering the negative results of the planar model experiments.

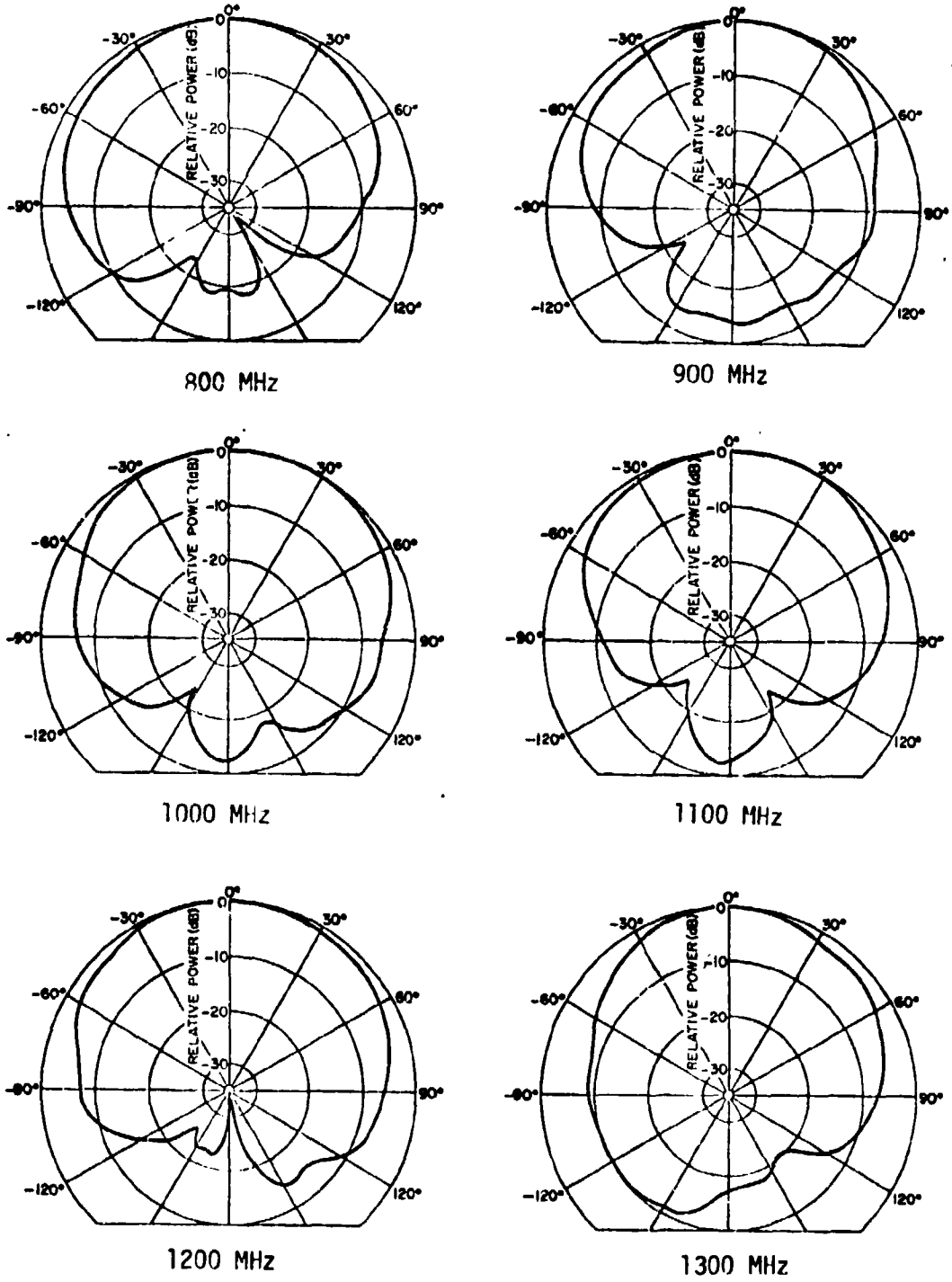

Fig. 3-4. Normalized far field (H-plane) patterns of the cylindrical T-bar slot antenna. The air-filled cavity depth is 1.5 inches.

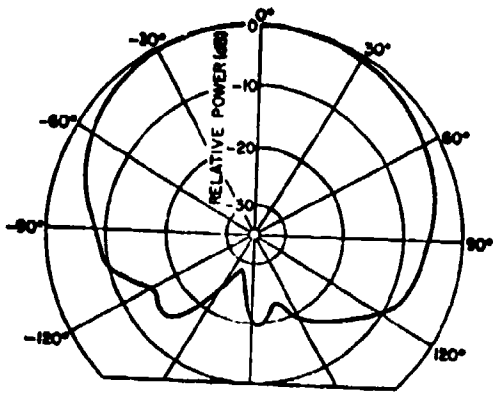

1400 MHz

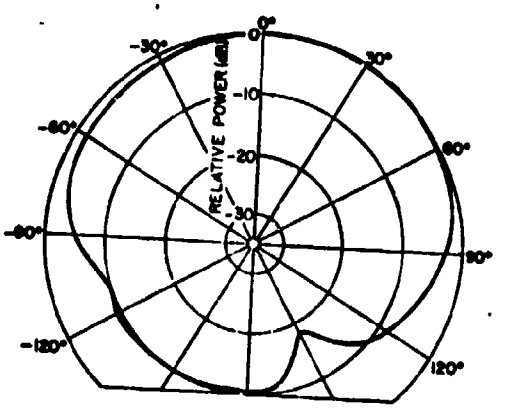

1500 MHz

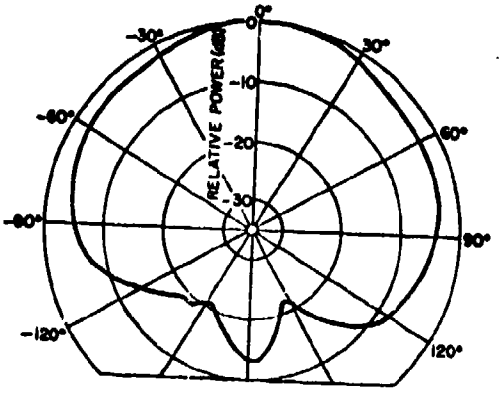

1600 MHz

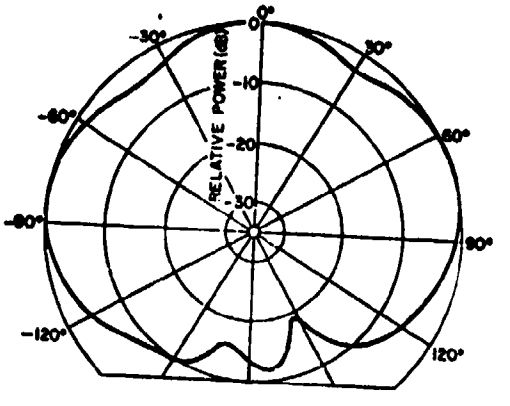

1700 MHz

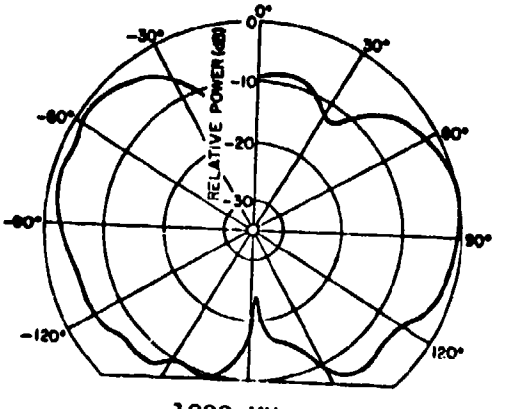

1800 MHz

Fig. 3-4. (Continued).

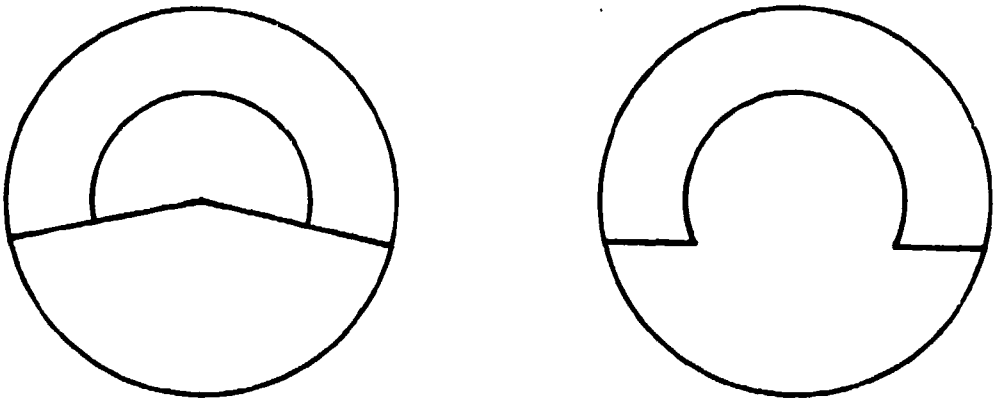

a) b)

Fig. 3-5. a) Top view of present cylindrical T-bar antenna.
b) Top view of proposed improved cylindrical T-bar antenna.

Figure 3-6 compares the insertion loss of the air cavity to a cavity with dielectric loading behind the T-bar. As expected, the performance on the low end of the bandwidth is improved with the addition of dielectric but there appears to be a trade-off in performances from 1500 to 2000 MHz. This result follows the predictions of the VSWR investigation in that the VSWR showed improvements and impairments in those regions respectively except above 1800 MHz where the VSWR increased with the addition of dielectric. If the VSWR of an antenna increases with the addition of dielectric or a tuning device, then likewise the insertion loss measurement should increase unless the far field pattern has been altered. Rotating the cylinder and repeating the insertion loss experiments showed that the pattern lobes at 1600 MHz but the main lobe is broadside which accounts for the decrease in insertion loss. Concluding, the dielectric loading suppresses the grating lobes occurring at 1800 MHz in the air case at the expense of establishing the TE_{30} mode at a lower frequency thus producing a lobed pattern at a lower frequency.

Summarizing the results of this section, the bandwidth of the dielectric loaded cylindrical T-bar slot antenna is 2.4:1 (650 to 1600 MHz) in terms of reasonable VSWR, insertion loss, and nonlobing patterns. Further, the grating lobes experienced in the air-filled case have been replaced with a lobed pattern with its maximum broadside to the slot antenna.

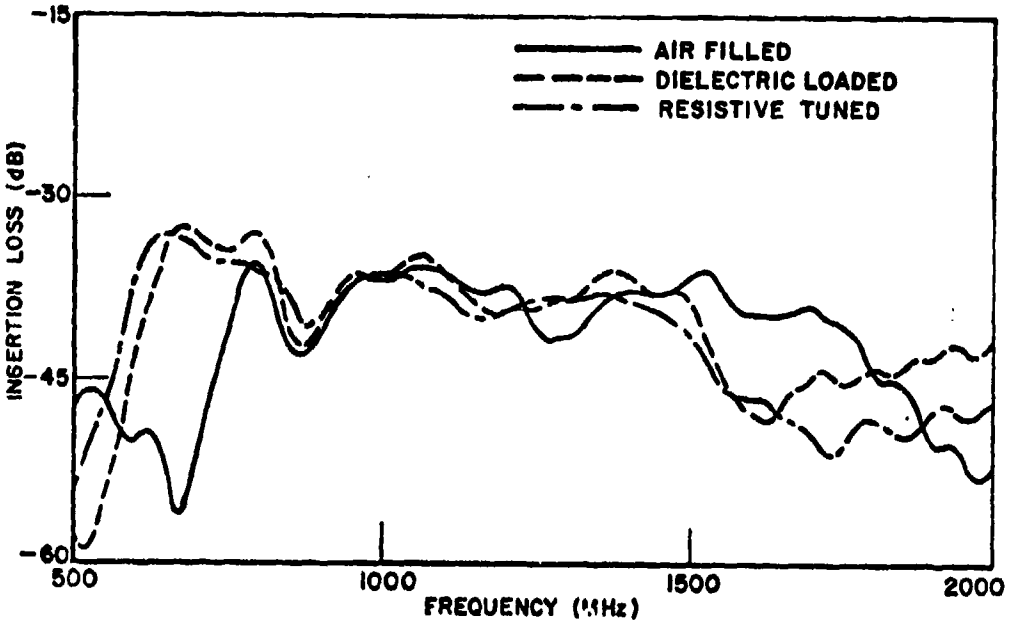

Fig. 3-6. Insertion loss comparison of the air-filled, dielectric loaded, and resistive tuned cylindrical T-bar slot antenna. (CD = 1.5)

D. Resistive Tuning

Recall from the planar study that the resistive tuning was effective in suppressing the TE_{30} mode and thereby reducing the VSWR and expanding pattern bandwidth. This procedure was unsuccessful with an air filled cavity on the cylinder but when applied to the dielectric loaded case, a broadside far field pattern is exhibited up to a frequency of 2200 MHz. Unfortunately the patterns above 1800 MHz have a lobed shape but they have no zero nulls except on the back of the cylinder and they have no grating lobes. The side lobe levels range from 3 to 5 dB down from the main beam with nulls approximately 10 dB down. Although this is not the desired pattern, it is an improvement over the air filled cavity with it grating lobes. The far field patterns for the resistive tuned case shown in Fig. 3-7 at frequencies below 1600 MHz were recorded on an outdoor range, while above 1600 MHz they were recorded in an anechoic chamber. The patterns recorded in the anechoic chamber proved to be more symmetrical than those recorded outside.

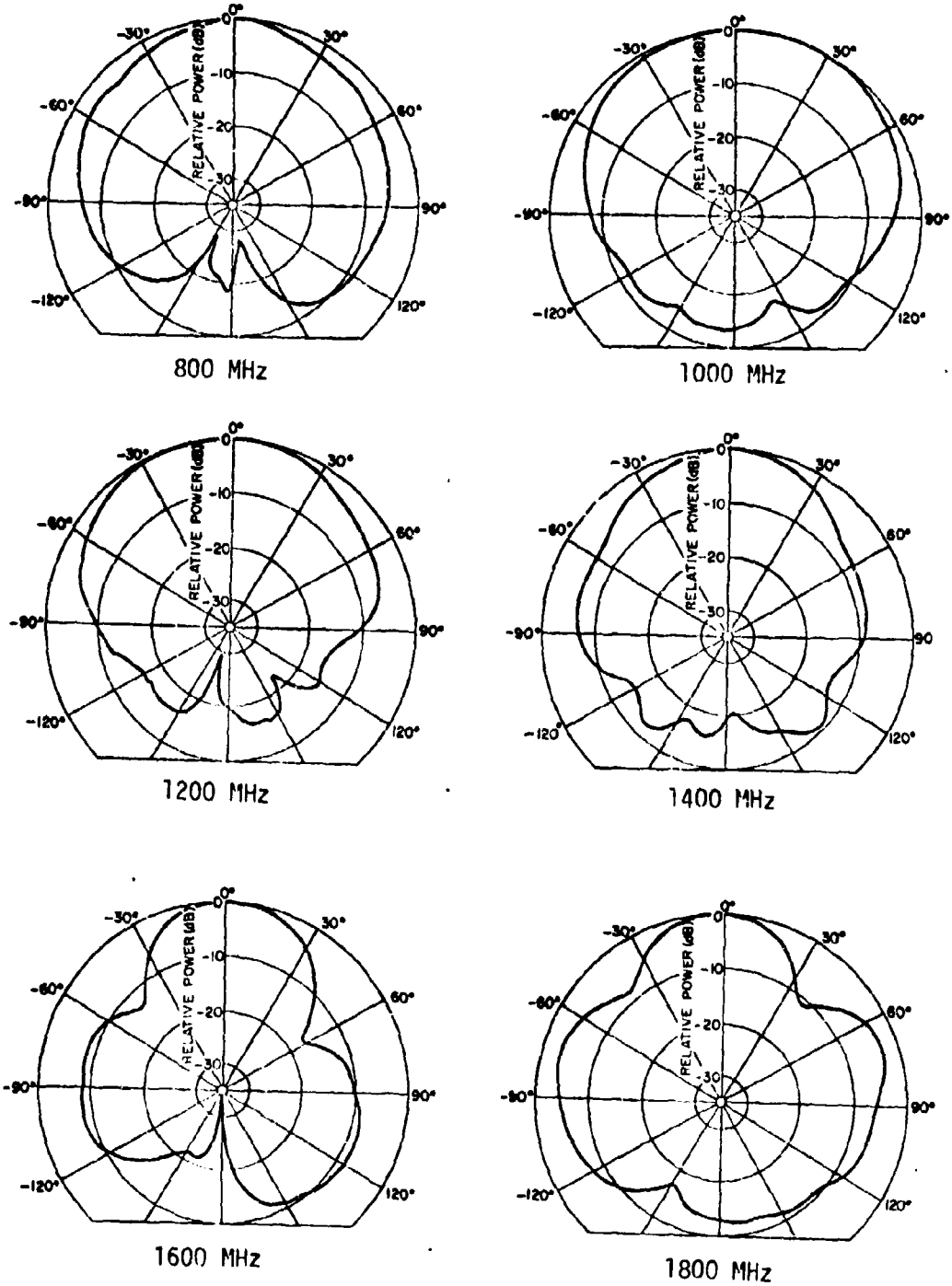

Fig. 3-7. Normalized far field patterns (H-plane) of a resistive tuned cylindrical T-bar slot antenna. (CD = 1.5).

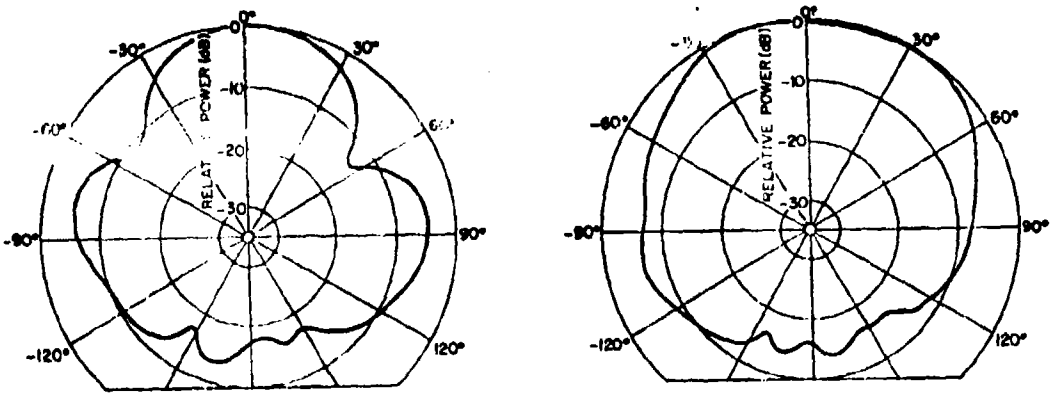

2000 MHz 2200 MHz

Fig. 3-7. (Continued).

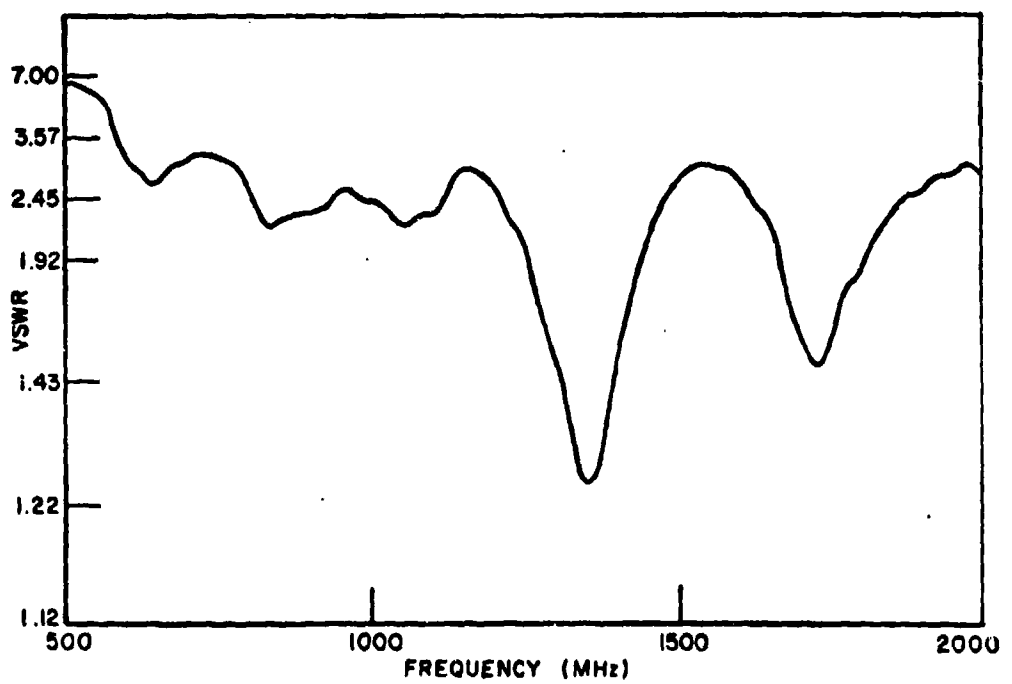

Fig. 3-8. VSWR of a resitive tuned cylindrical T-bar slot antenna.

VSWR measurements shown in Fig. 3-8 indicate that the TE_{30} mode has not been completely suppressed but the VSWR has shown an overall improvement. The corresponding insertion loss study of the resistive tuned case verified the VSWR prediction, showing that lobing occurs above 1800 MHz. The broadside case of this study is shown in Fig. 3-6. The insertion loss measurements also showed a slight drop in efficiency but not as much loss as experienced in the planar resistive case.

Concluding, the resistive tuning is not as effective for the cylindrical T-bar as for the planar T-bar. However it does produce an acceptable pattern (no zero nulls, no grating lobes, and a broadside pattern) over an increased bandwidth (3.38:1) with a slight decrease in efficiency.

E. Conclusions

The results of this chapter have shown that the T-bar fed slot antenna examined in Chapter II has been successfully adapted to a circular cylinder. Further, it has been suggested that an improvement in the cavity construction of the cylindrical T-bar antenna would probably enhance the performance of the antenna.

It would be difficult to compare the two antennas (planar and cylindrical) by simply comparing the data sets recorded, however a few general comments of that nature are in order. When comparing the cylindrical insertion loss studies to the planar studies, the planar model appears to have superior performance. This decrease in performance is not due to efficiency losses (there are no lossy structures in the antenna) but is due to a decrease in directivity for the cylindrical model. This is apparent by simply comparing the far field patterns recorded of each case. The VSWR exhibited by cylindrical T-bar antenna is equally as good as the planar version if not better in some cases. Thus from the two observations above, the efficiency of the cylindrical T-bar slot antenna should be quite similar to that exhibited by the planar antenna.

CHAPTER IV

APERTURE INVESTIGATIONS AND FAR-FIELD ANALYSIS OF THE PLANAR AND CYLINDRICAL T-BAR ANTENNAS

A. Foreword

This investigation was conducted in an effort to learn more about the electromagnetic characteristics of a T-bar feed for a cavity backed slot antenna. The procedures employed for measuring aperture fields or calculating far fields from aperture distributions are not new. They are merely applied here to aid in investigating the characteristics of the T-bar fed slot antenna. The results of this investigation tend to confirm the conclusions previously discussed.

B. Experimental Procedures

Insight into the behavior of the T-bar may be gained if the modal characteristics* of the T-bar fed cavities are determined. To achieve this information, the aperture distributions of the planar and cylindrical models were probed and analyzed with the following procedures.

In the planar study, a vertical sampling probe was incrementally moved across the aperture using a series of bulkhead connectors mounted in the ground plane as shown in Fig. 4-1. The spacing between data points (0.127λ at the highest frequency) was much less than the maximum allowable spacing for far field evaluation. The tip of the probe was positioned 2 cms from the bottom of the aperture and spaced a horizontal distance of 2 cms from the groundplane as also shown in Fig. 4-1.

The procedure for measuring the E-field in the cylindrical slot study involved rotating the cylinder while the probe position remained fixed relative to the cylinder. In this procedure the vertical probe was positioned directly in front of the aperture as shown in Fig. 4-2. The E-field was sampled at spacings of one degree across the aperture and recorded by a computer. In the procedures thus defined, the probe (a center conductor of coaxial cable) was 2.3 cm in length which corresponds to 0.038λ and 0.15λ at each end point of the bandwidth considered. The probe satisfied the probe criteria as set forth by Richmond and Tice.[6] That is, the probe was small enough such that the aperture fields

---

*By modal characteristics we mean the various types of waveguide modes established in the cavity and the frequencies at which they are established.

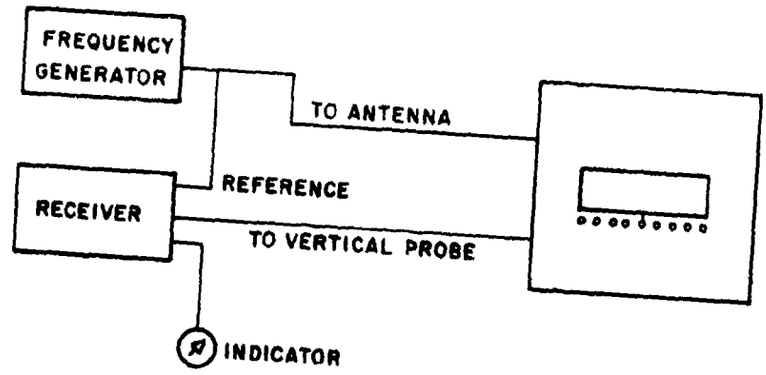

a)

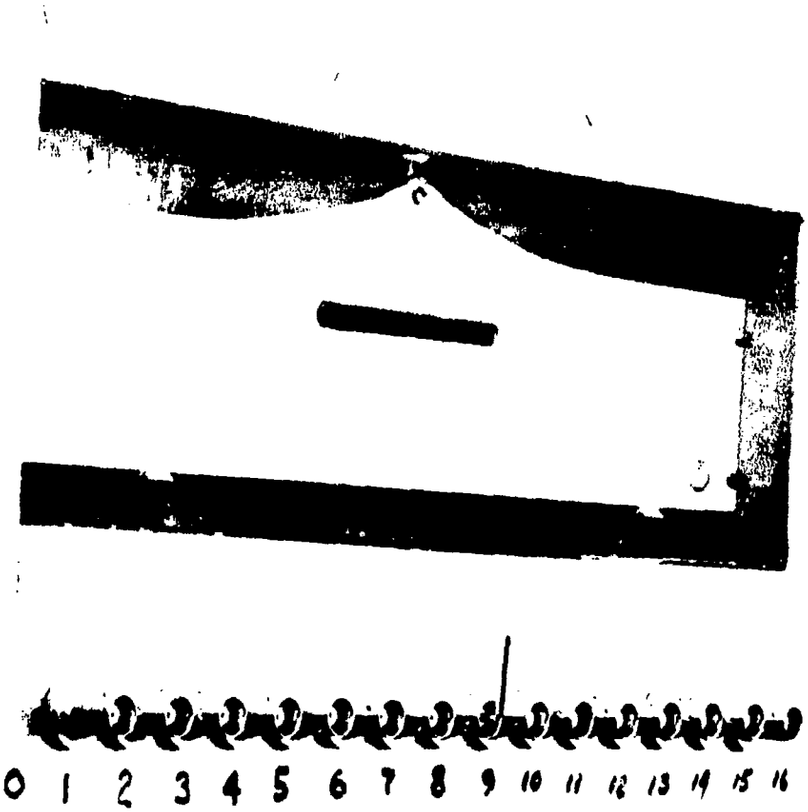

b)

Fig. 4-1. a) Block diagram of the experimental procedure used to measure the E-field in the aperture of the planar T-bar slot antenna.
b) Photograph of the planar T-bar slot antenna showing bulkhead connectors.

were not significantly disturbed, it was oriented with the correct polarization, and it delivered enough signal voltage to permit accurate measurements. The effects of being in a plane outside of the aperture versus just inside the aperture plane was not dedetermined in either study.

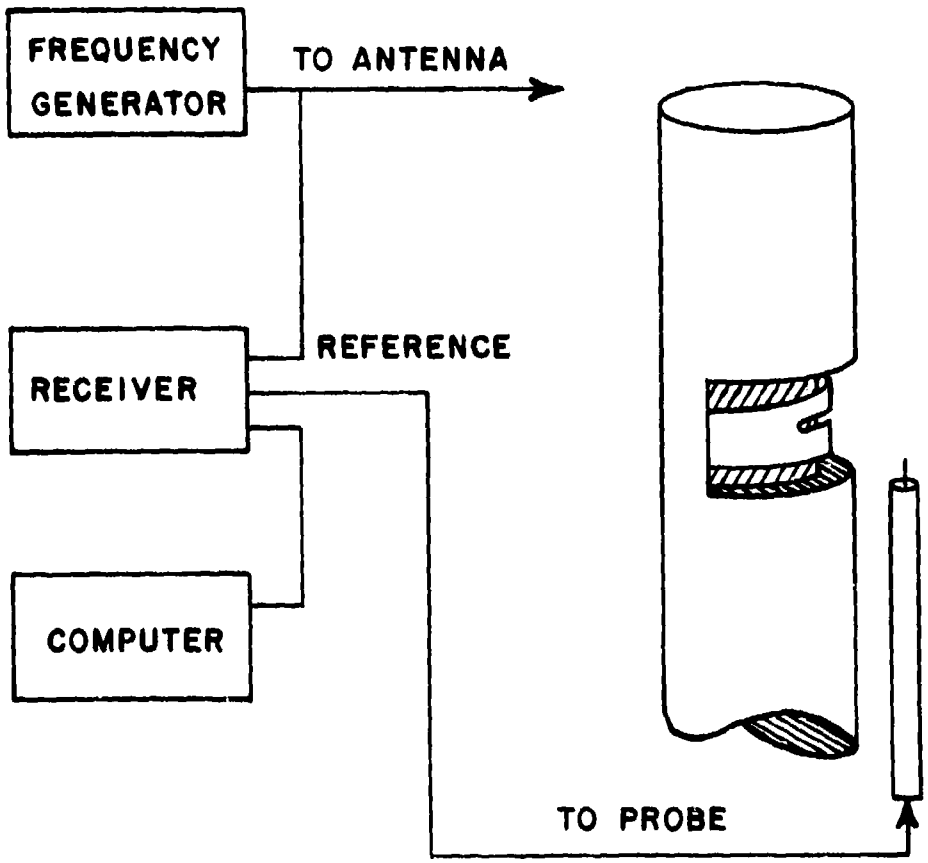

Fig. 4-2. Block diagram of the experimental procedure used to measure the E-field in the aperture of the cylindrical T-bar slot antenna.

C. Planar Antenna Results

The planar, air-filled 1.5 inch cavity depth, aperture distributions are shown in Fig. 4-3. In some instances the measured E-field amplitudes do not go to zero at the endpoints of the aperture, probably due to measuring the E-field in a plane slightly in front of the aperture. In the analytic analysis this error can be corrected by forcing the E-field to zero in a Fourier series representation of the distribution. However, the amplitude errors at the aperture endpoints may also suggest errors in the phase data which are not as simple to compensate.

With the aperture distributions of the planar T-bar fed slot antenna known, the application of the equivalence theorem [7] yields an equivalent current distribution which can be used to calculate the far field patterns. Due to the uniqueness theorem [7], an analytic evaluation of the far field from the equivalent currents, which would agree with the measured patterns, would verify the accuracy of the aperture distributions. Assuming that the planar T-bar fed slot is mounted in a perfectly conducting, infinitely large groundplane, the far field E-field component in the H-plane ($\theta,\phi = 90°$) is given by:

$$E_\phi = \frac{-jke^{-jkr}}{2\pi r} \sin\theta \int_{-a/2}^{a/2} A(z')e^{j\psi(z')}\, e^{-jkz'\cos\theta} dz'$$

where $A(z')e^{j\psi(z')}$ is the aperture E-field amplitude and phase expressed in source coordinates. The geometry and coordinate system are shown in Fig. 4-4. The results of this analytic investigation are shown in Fig. 4-5. Comparing the patterns shown in Fig. 4-5 to the measured patterns of Fig. 2-12, good agreement exists except at 1500, 1600 and 1800 MHz. At 1800 MHz the calculated main beam and side lobe locations are correct, however the side lobe levels differ by approximately 3 dB. The same conclusion can be reached for 1600 MHz except the calculated pattern does not predict the nulls. This conclusion is not valid for 1500 MHz where the calculated results do not accurately predict either the side lobes or their location.

Since the calculated and measured far field patterns did not agree at each frequency, there is some doubt as to the accuracy of the measured aperture distributions, particularly the phase. To make certain that there were no calculation errors, different computer evaluation techniques were used in the questionable cases, but each produced almost identical patterns.

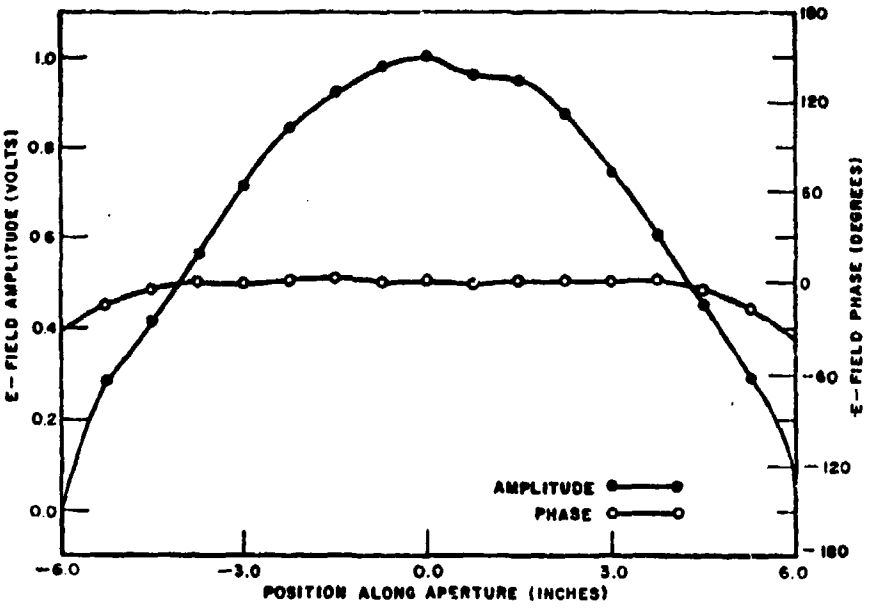

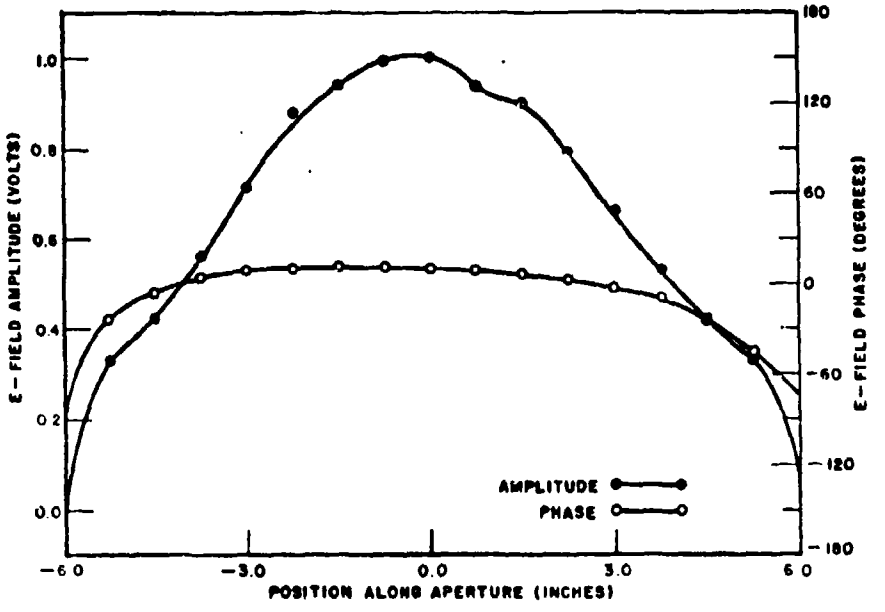

Fig. 4-3. Aperture distributions of the planar T-bar slot antenna. Air-filled cavity depth is 1.5 inches.

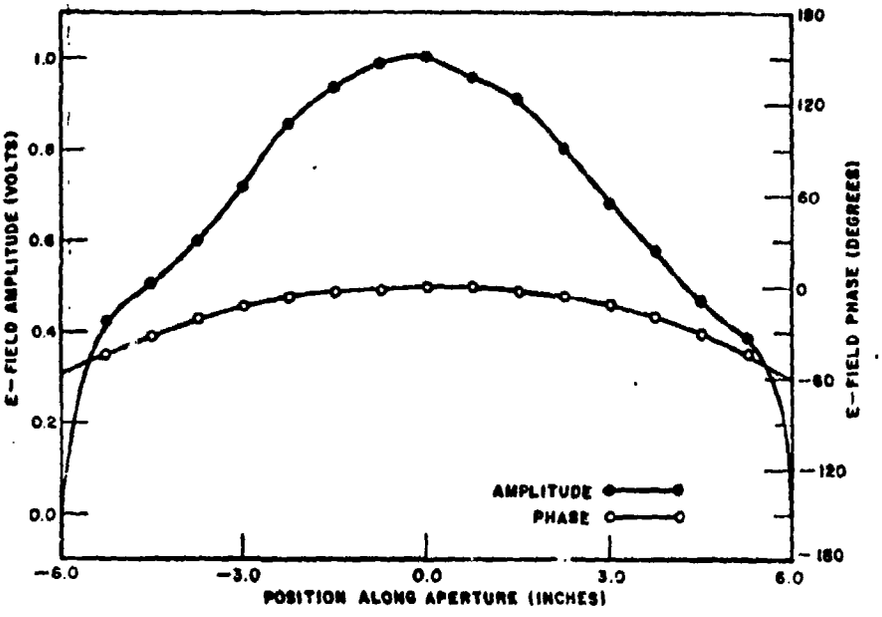

1200 MHz

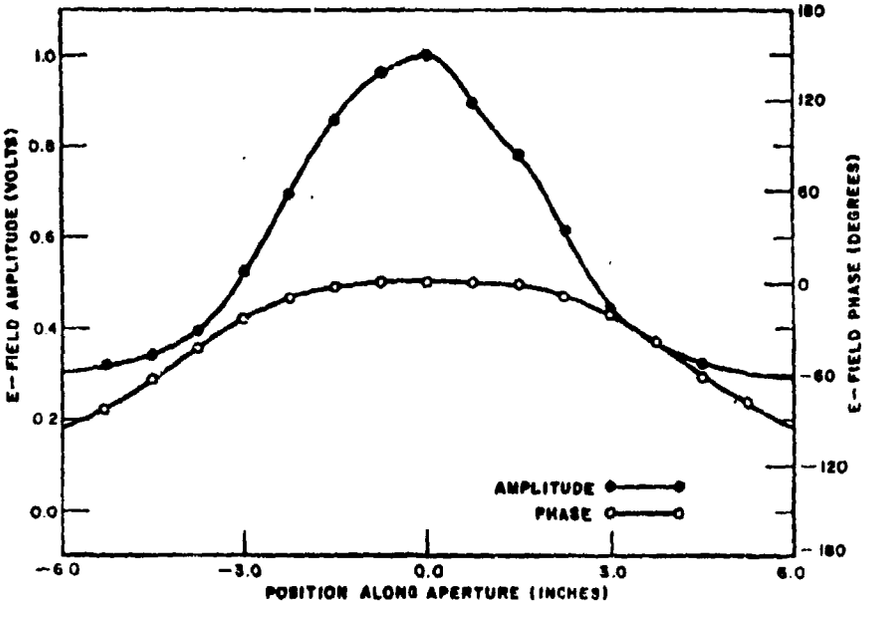

1400 MHz

Fig. 4-3. (Continued).

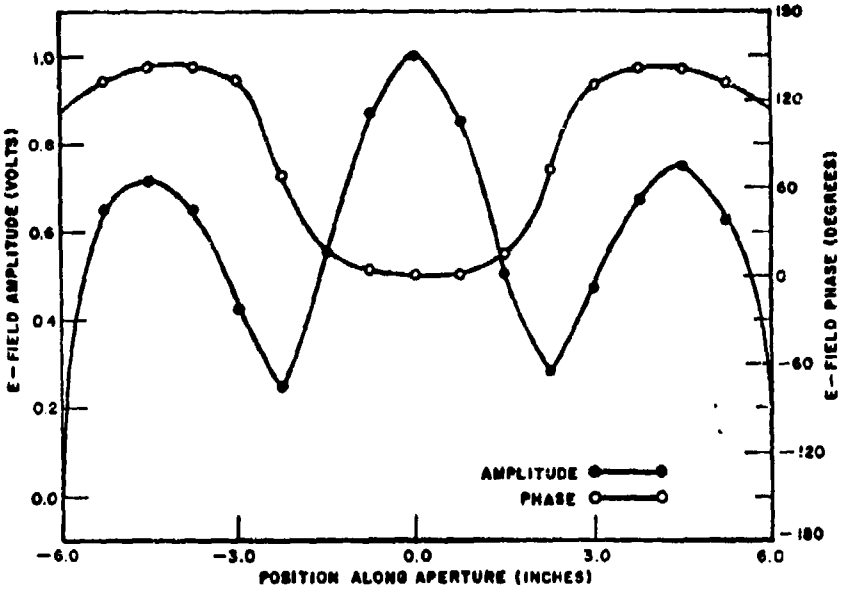

1500 MHz

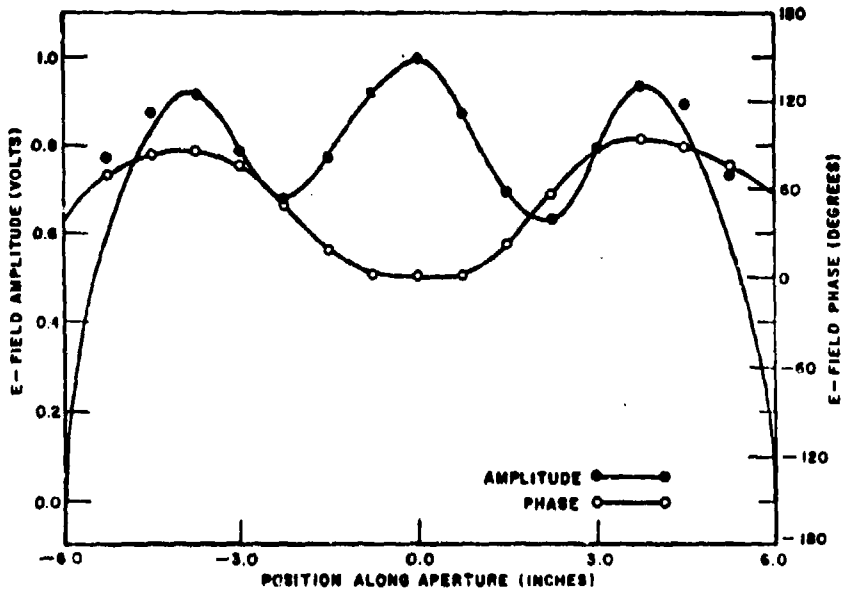

1600 MHz

Fig. 4-3. (Continued).

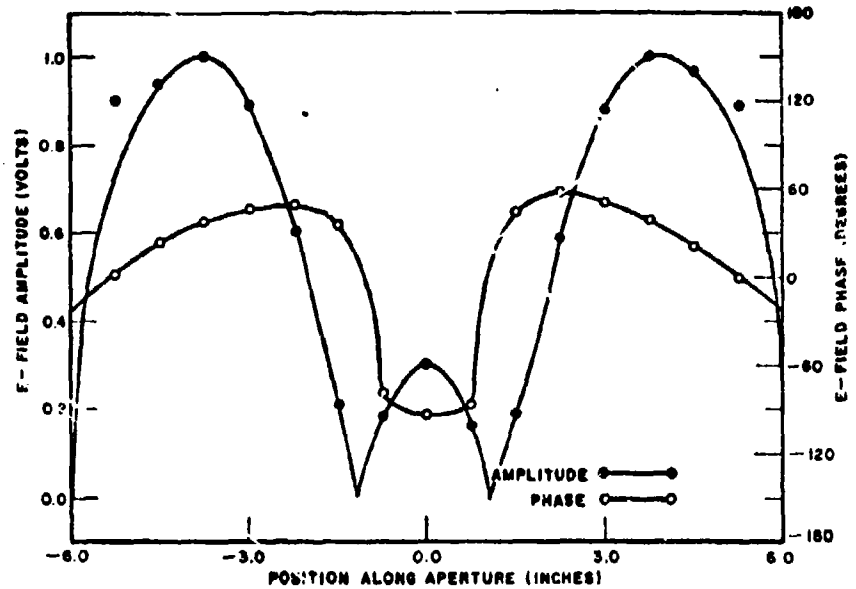

1800 MHz

Fig. 4-3. (Continued).

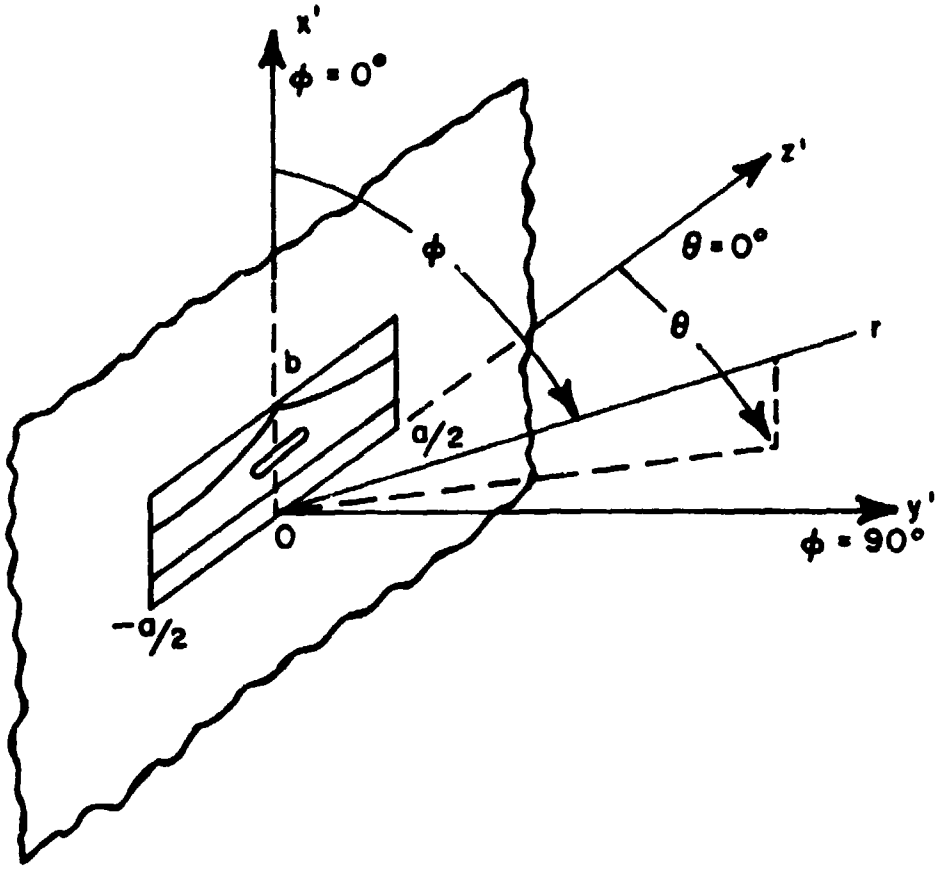

Fig. 4-4. The coordinate system used in the analytic investigation of the planar T-bar antenna.

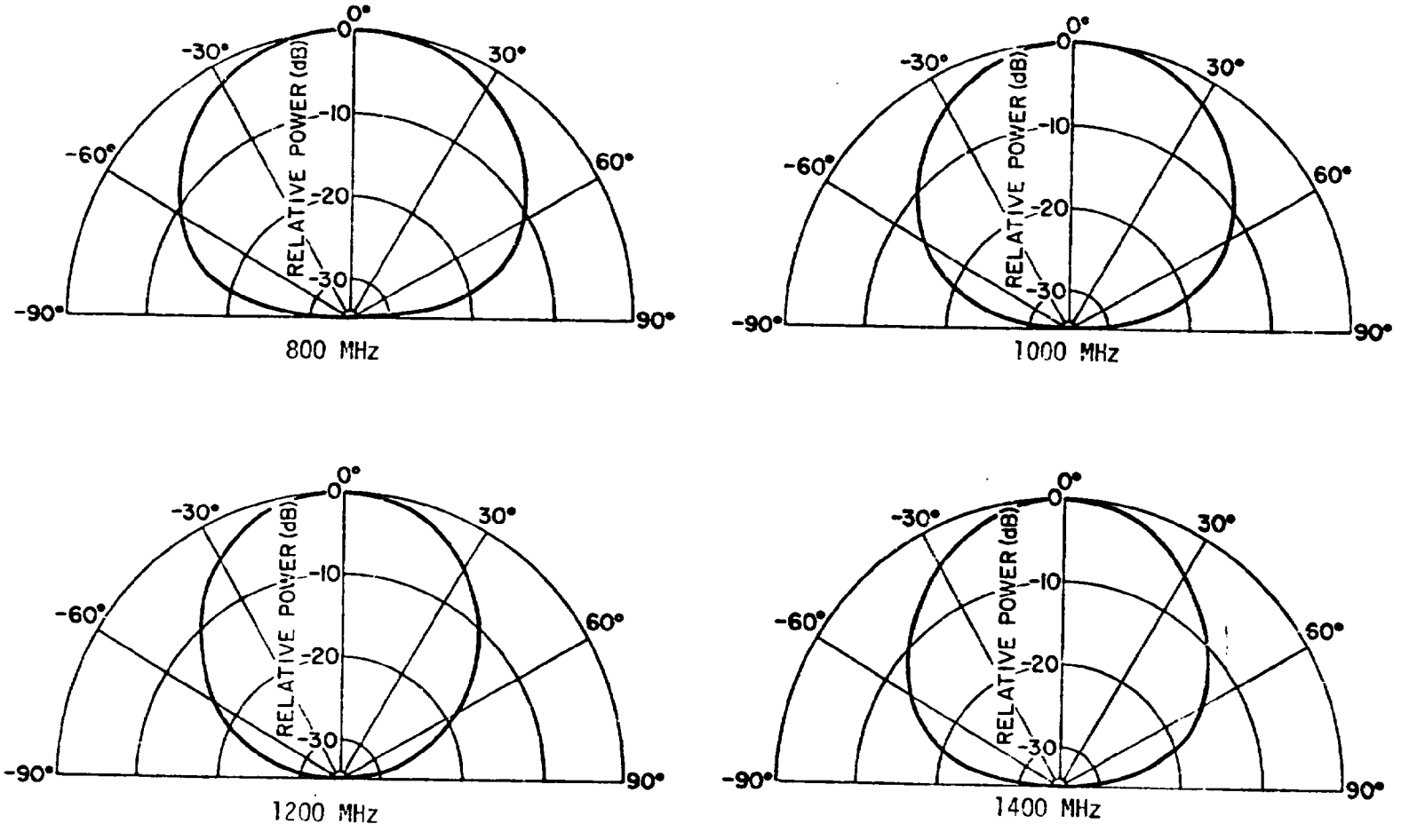

Fig. 4-5. Calculated H-plane patterns of the planar T-bar slot antenna.

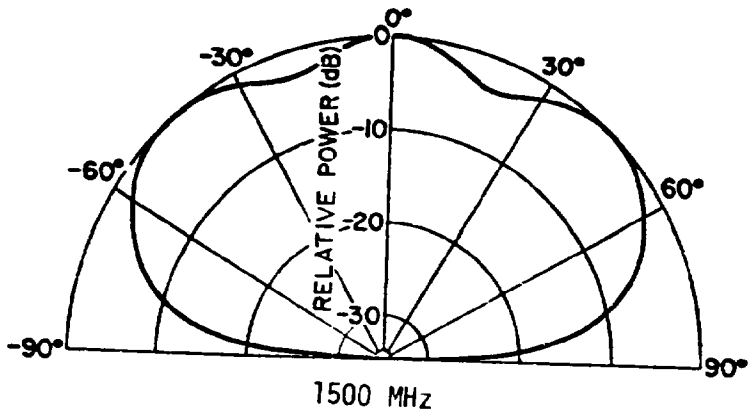

1500 MHz

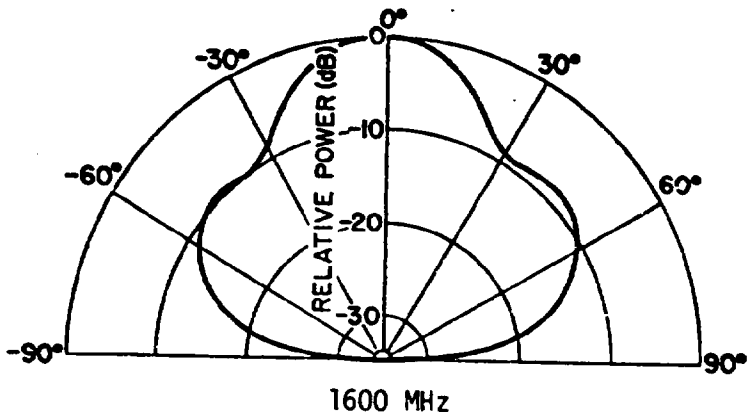

1600 MHz

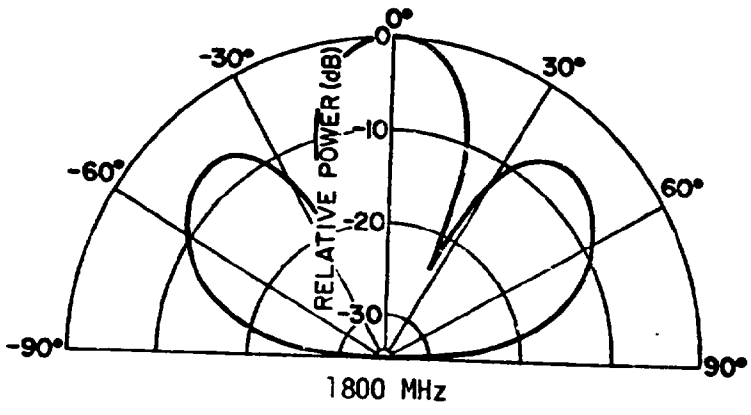

1800 MHz

Fig. 4-5. (Continued).

In the far field evaluation it was assumed that there was no E-field variation along the x-axis. However, due to the fact that the length to width ratio of the aperture is 3:1, it is theoretically possible that the TE_{01} mode could be excited in the cavity. Probing the width of the aperture in the same manner as before but measuring only the amplitude of the horizontal E-field verifies this hypothesis. The results of the air filled cavity investigation (Fig. 4-6) shows that a higher order mode (TE_{01}) is established at 1500 MHz. Observing the TE_{01} mode in the cavity, the far field was examined to determine if there was a horizontal component of the E-field. Negative results of that investigation indicated that the TE_{01} mode is an evanescent mode existing only in the near field of the antenna. Therefore, since the TE_{01} mode was non-propagating, the far field analysis was correct in assuming no x-variation in the E-field. However, the question of accuracy concerning the aperture distributions was still unsolved.

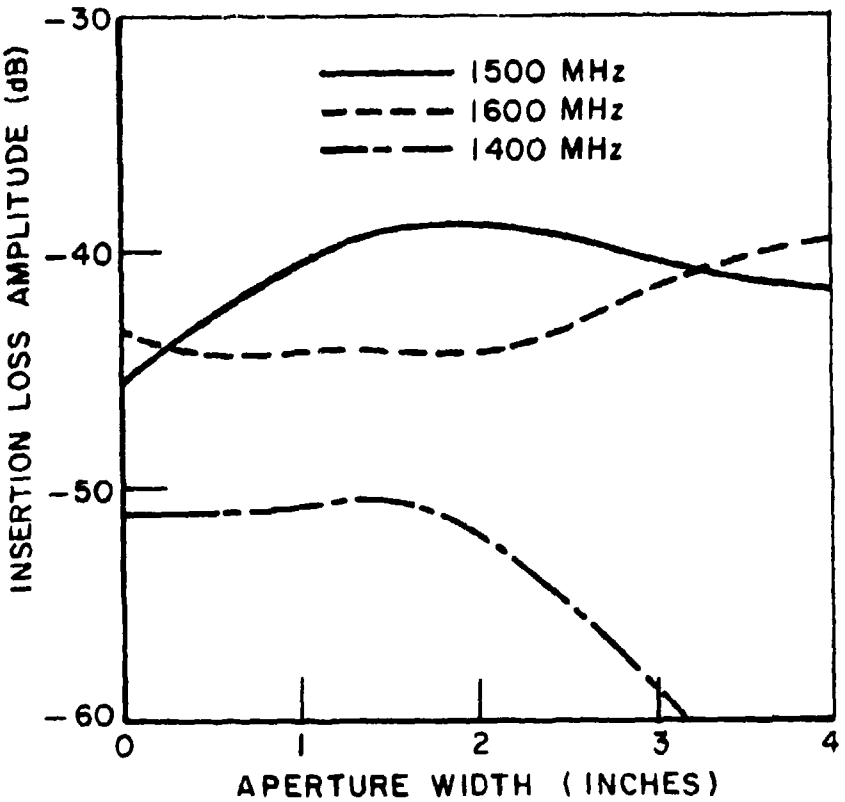

Fig. 4-6. Amplitude distribution of the horizontally polarized E-field of the planar T-bar slot antenna.

Recall that the measured and calculated patterns begin to disagree at 1500 MHz particularly in the side lobe regions. Since the aperture was probed with a vertical probe, it is unlikely that the TE_{01} horizontal E-field affected the data in the mid section of the aperture. This is verified by the main lobe agreement above 1500 MHz. However, it is possible that a diffracted component of the horizontal or vertical E-field was measured in addition to the desired vertical component at the endpoints of the aperture. This measurement would distort the experimentally determined aperture distribution at the aperture endpoints and thus cause inaccurate side lobe predictions in the analytically determined far field. Figure 4-7 illustrates the diffracted fields of a vertically polarized E-field at a waveguide opening.[8] The horizontal component would contribute diffracted rays on the opposite edges due to the orthogonality of the waveguide modes. Thus, it is assumed that the distorted measured aperture distribution above 1500 MHz is caused by the excitation of the TE_{01} mode in the cavity. Therefore, a more sophisticated probing technique should be investigated for the higher frequencies to obtain more accurate results. One suggestion is to measure the E-field right at the aperture plane of the cavity or measure the near field at such a distance that the evanescent mode has decayed to an insignificant factor.

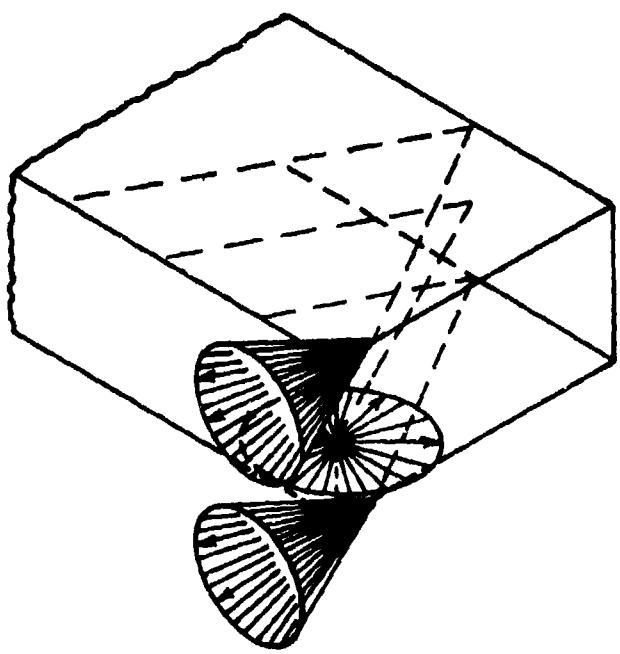

Fig. 4-7. The diffracted rays of a vertically polarized E-field propagating in a rectangular waveguide.

The data contained in this section, although not accurate at all frequencies, does give some insight to the behavior of the T-bar fed slot antenna at frequencies where the higher order modes are not excited.

The Fourier series representation of the aperture distributions of Fig. 4-3 was expanded into a TE_{mo} modal series as described in Appendix I. The magnitude of each mode established is tabulated in Table 4-1.

TABLE 4-1

	Air Filled 1.5" CD			
Freq	TE_{10}	TE_{20}	TE_{30}	TE_{40}
800	1.02	0.017	0.04	0.006
1000	0.98	0.076	0.114	0.013
1200	1.00	0.024	0.171	0.005
1400	0.824	0.033	0.277	0.023
1500	0.395	0.168	0.786	0.009
1600	0.836	0.068	0.710	0.006
1800	0.516	0.014	0.75	0.021

As is apparent from the graphs, the TE_{10} mode is dominant to 1400 MHz and at 1500 MHz the TE_{30} mode is dominant. However above 1500 MHz there does not appear to be a dominant mode, because the amplitudes of the TE_{10} and TE_{30} are approximately the same. These results should be expected below 1500 MHz since the TE_{30} mode is not excited until the aperture electrical length is $3/2\lambda$. As discussed previously the accuracy of the data above 1500 MHz where the cavity width is $1/2\lambda$ is obviously questionable. One interesting note is the magnitude of the TE_{20} and TE_{40} modes. These modes should not be established due to the symmetry of the T-bar feed, and as is apparent from the modal analysis, they are insignificant. The amplitudes which are shown are probably due to measurement errors causing the recorded data to be slightly asymmetrical.

The procedures previously defined were applied to various other cases of the planar T-bar antenna with almost the same results. In the dielectric case, the TE_{01} mode was established at a lower frequency causing analytic inaccuracies to go below 1500 MHz, but accurate far field patterns were predicted below 1400 MHz. This was also the case when the resistive tuned T-bar was investigated. Results for the resistive-tuned case did differ by the fact that they did predict a broadside nonlobing pattern over the entire bandwidth. However the inaccuracies experienced at the aperture endpoints caused the predicted patterns to be more narrow beam than those actually measured.

D. Cylindrical Antenna Results

For the far field investigation of the cylindrical case, the far field component of the $\theta = 90°$, ϕ plane for the transverse cylindrical T-bar fed slot antenna (Fig. 4-8) is given by:

$$H_\phi = \frac{-jke^{-jkr}}{r} \int_{\phi'} A_z(\phi') e^{jka \cos(\phi-\phi')} \, d\phi'$$

where $A_z(\phi')$ is the amplitude and phase of the aperture distribution. The cylinder was assumed to be of infinite length and constructed of a perfect conductor. Since this is a cylindrical surface, the image theory used in the planar model must be replaced with geometrical optics where the integration is performed only over that region of the aperture seen in the far field. Slight errors were anticipated in the side and back lobe regions using this procedure because it does not account for the creeping waves established on the surface of the cylinder. This error would be greater if the slot were axially mounted, since the E-field in the aperture would be perpendicular to the cylindrical surface.

The far field patterns for the air-filled case were calculated using the aperture distributions shown in Fig. 4-9. The results shown in Fig. 4-10, agree very well with the measured results of Fig. 3-4 except at 1800 MHz. This disagreement was anticipated from the results of Chapter III and the conclusions previously derived for the planar aperture investigations. When the higher order modes, particularly the TE_{01}, are established the probing system used here becomes inadequate.

The dielectric loaded and resistive tuned cases were also studied and again good agreement was achieved until the higher order modes were established. The results are not shown because the dielectric loading and resistive tuning affect only the patterns above the frequency where the higher order modes are established.

The TE_{m0} modal expansion of the Fourier series representation for the air-filled case is tabulated in Table 4-2. As predicted in Chapter III, the TE_{10} mode is dominant until 1800 MHz, where the TE_{30} mode becomes dominant. Although the aperture distribution has been shown to be inaccurate at 1800 MHz, one can be assured of the TE_{30} dominancy at 1800 MHz by reviewing the results of Chapter III.

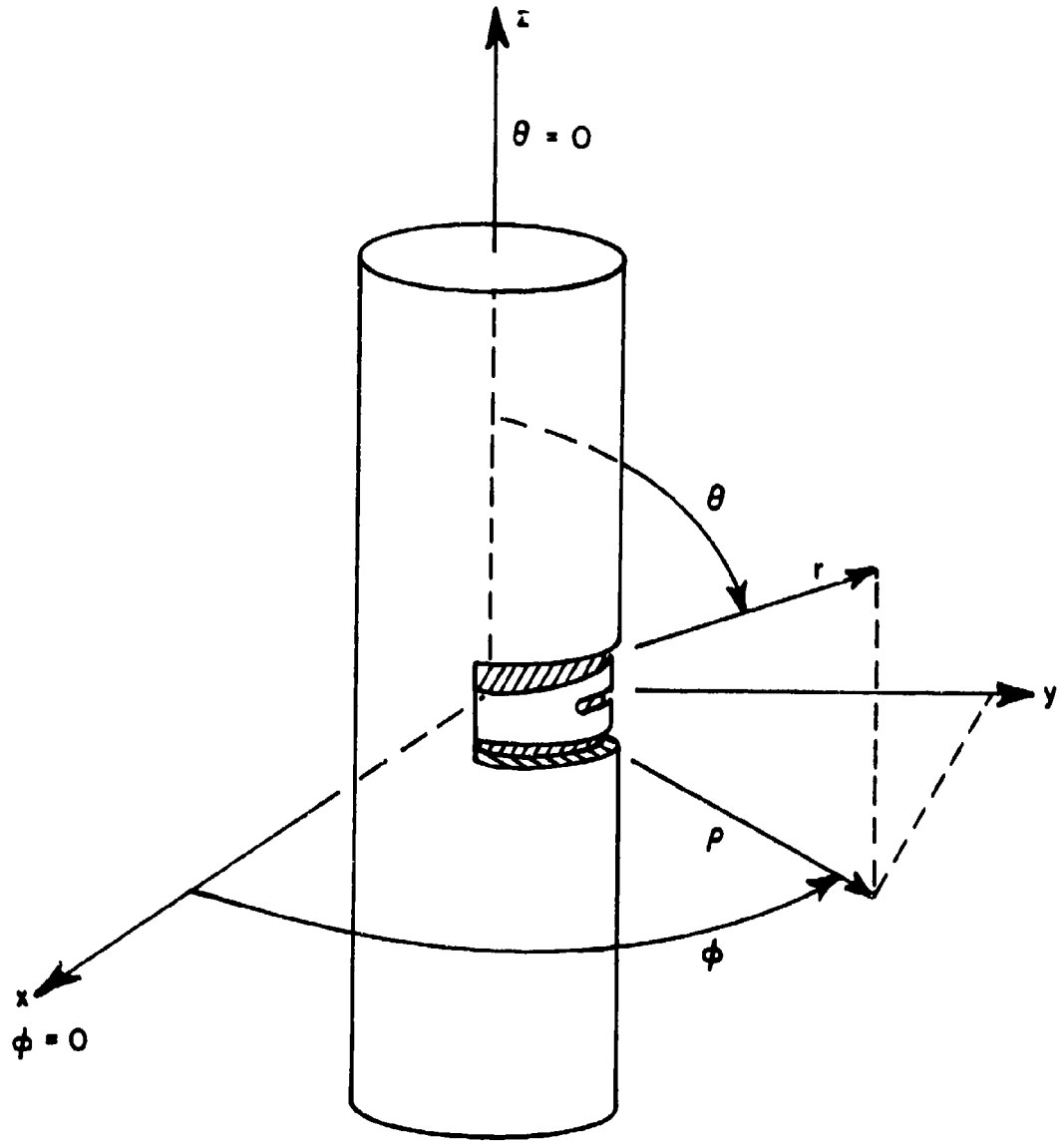

Fig. 4-8. The coordinate system used in the analytic investigation of the cylindrical T-bar slot antenna.

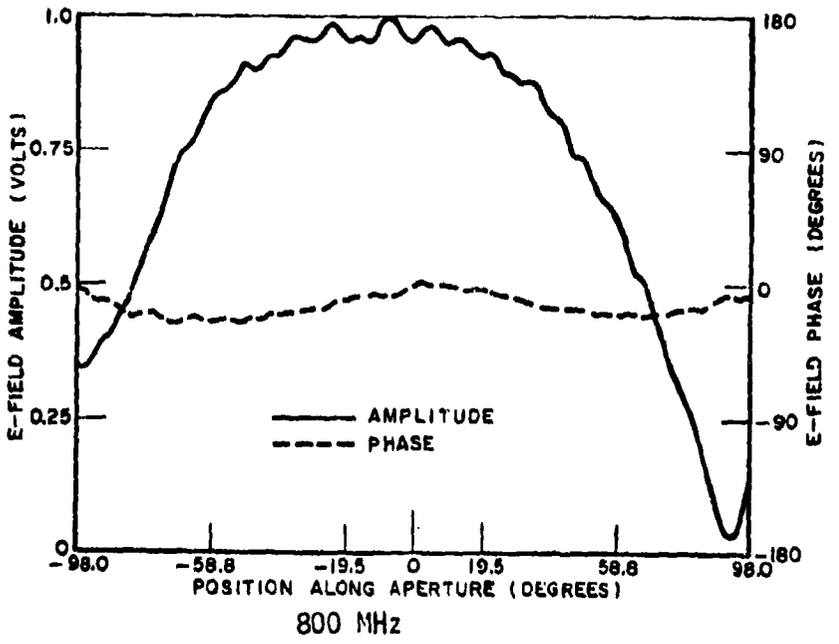

800 MHz

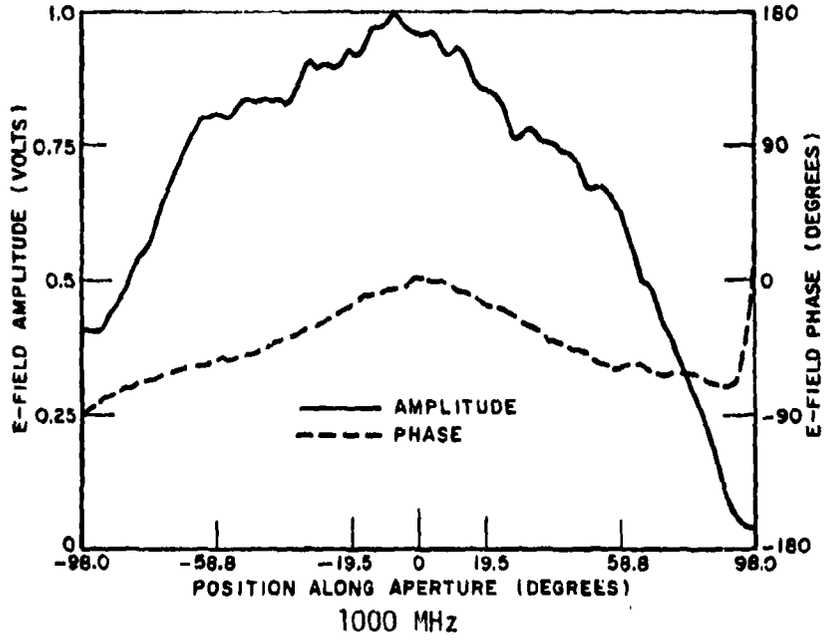

1000 MHz

Fig. 4-9. Aperture distributions of the cylindrical T-bar slot antenna. Air-filled cavity depth is 1.5 inches.

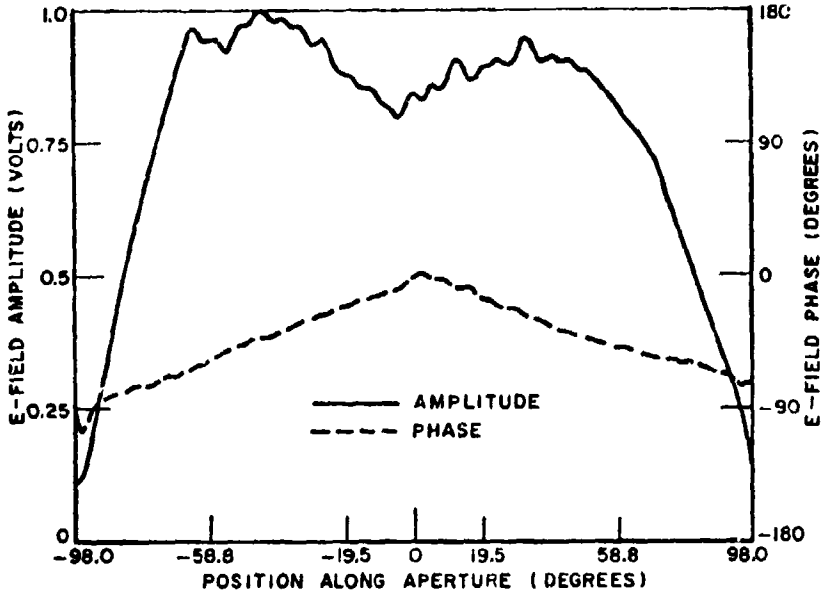

1400 MHz

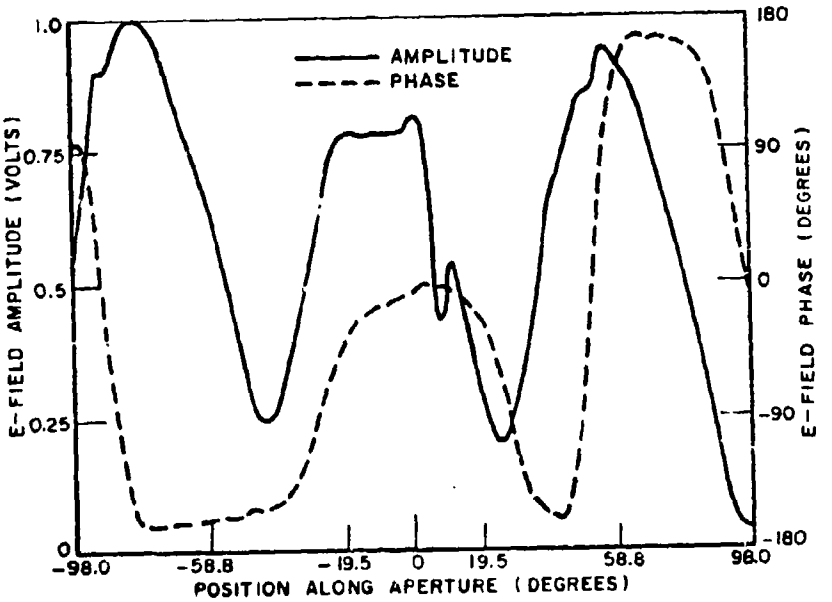

1800 MHz

Fig. 4-9. (Continued).

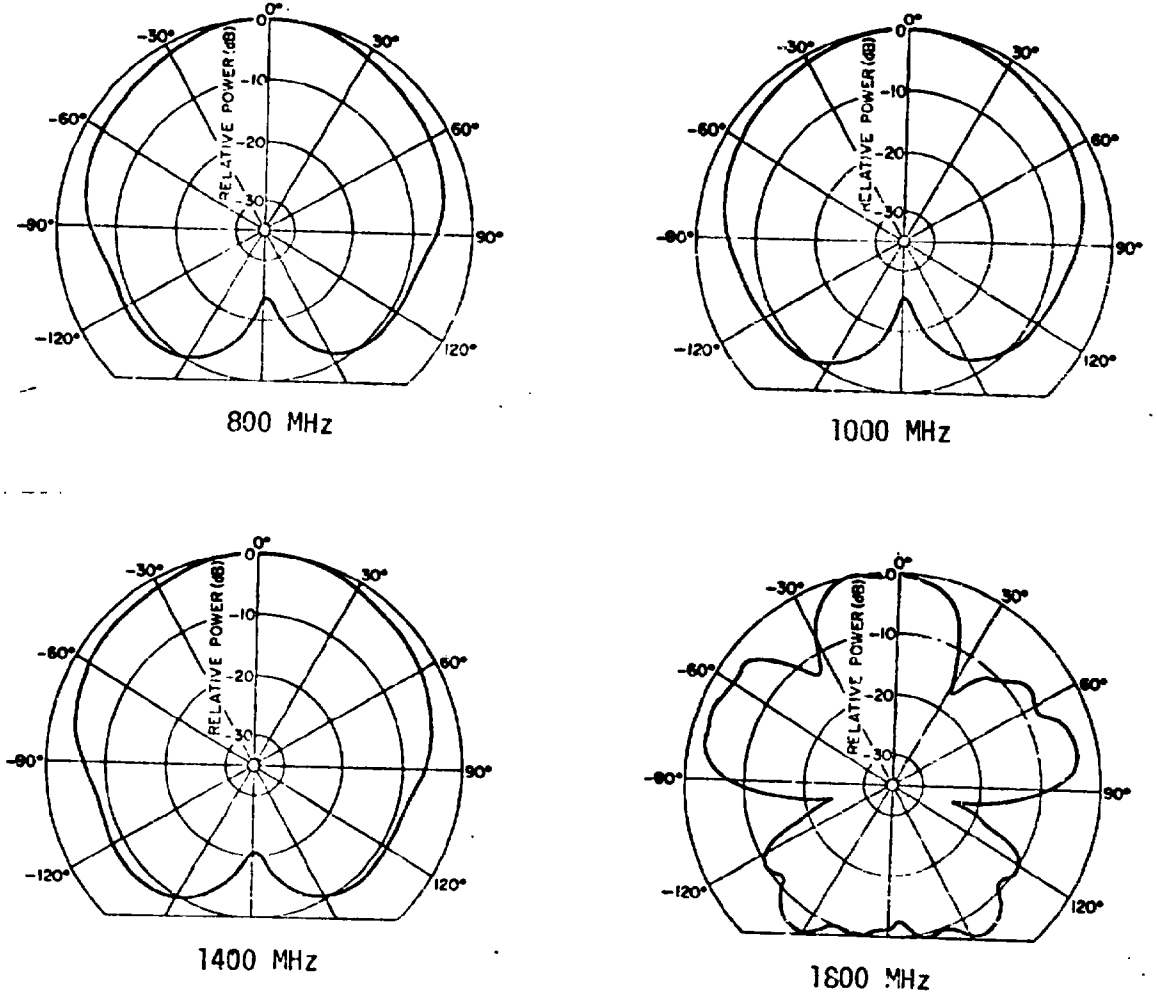

Fig. 4-10. Calculated H-plane patterns of the cylindrical T-bar slot antenna.

TABLE 4-2

Freq	TE_{10}	TE_{20}	TE_{30}	TE_{40}
800	0.264	.029	0.042	.016
1000	0.237	.025	0.095	.016
1400	0.258	.022	0.114	.005
1800	0.056	.045	0.162	.032

E. Conclusions

While it is unfortunate that the aperture investigations did not reveal accurate information about the T-bar antenna operation above the cutoff frequency of the TE_{01} mode, the investigations did lend insight into the general characteristics of the antenna over a wide frequency range. Further, the probing procedures employed here, while adequate below the TE_{01} cutoff frequency, appear to have significant short comings above that frequency. Thus, any future aperture probing should be done in such a manner so as to overcome this difficulty, possibly by measuring the field in the actual aperture plane.

CHAPTER V

SUMMARY AND CONCLUSIONS

Jasik [1] has shown that the T-bar fed slot antenna can be designed to exhibit a VSWR less than 2.0 over a frequency range of nearly 2:1 when the length to width ratio is approximately 3, and the T-bar to cavity shorting plate spacing is about $\lambda/4$ where λ is the wavelength at midfrequency of the 2:1 range. The results of Chapter II of this study indicate that if an increase in VSWR can be tolerated over the original 2:1 bandwidth then the bandwidth can be extended to a 4:1 range. To achieve this extension the conventional T-bar design should be altered with the following procedure: (1) replace the circular cross section T-bar with a thin rectangular cross section T-bar whose width at the ends is approximately 1/5 the length of the aperture, (2) the coax to T-bar connection must be a gradual transition, (3) cut a narrow slot centered within the T-bar whose length is $\lambda_{HF}/2$ (λ_{HF} is the wavelength of the upper endpoint of the bandwidth), and (4) reduce the mismatch effects of the TE_{30} mode with tuning stubs located $\pm \lambda_{30}/2$ from the center of the aperture directly under the T-bar (λ_{30} is the wavelength where the TE_{30} mode is excited). Furthermore, reducing the cavity depth to $\lambda_{HF}/4$ results in a loss of performance on the low end but a nearly equal increase occurs on the high end of the bandwidth. Results also indicate that the cavity depth may be decreased by decreasing the T-bar depth while maintaining the same distance from T-bar to cavity shorting plate.

The T-bar fed slot antenna altered as described above offers a viable solution to some of the unusual design requirements experienced by antenna engineers. The T-bar antenna is small in size, may be flush mounted with little cavity depth required, and possesses favorable electromagnetic characteristics over a 4:1 frequency bandwidth.

The results of Chapter III show that the planar T-bar antenna can be successfully adapted to a cylindrical surface. Furthermore, considering the size of the T-bar fed slot compared to the cylindrical surface on which it was mounted, the T-bar fed slot antenna shows promise of being adaptable to a wide range of surface geometries while retaining most of the characteristics of a planar model.

In Chapter IV, the aperture distributions and analytic investigations show that the T-bar transition causes the cavity backed slot antenna to exhibit electromagnetic properties similar to those experienced in a rectangular waveguide. That is, the excitation of the TE_{mn} modes in the cavity backed T-bar fed slot antenna (air filled or dielectric loaded) may be predicted by the familiar equations governing the cutoff frequencies of a rectangular waveguide of the same dimensions. The tuning techniques (tuning stubs,

resistive tuning, ridge devices) used to increase the bandwidth of a waveguide have been successfully employed in the T-bar antenna to improve its bandwidth. Considering the cavity depth involved, these are important conclusions and factors to consider when designing T-bar antennas for various surfaces and when scaling for different frequency ranges.

Although the T-bar antenna has been discussed previously by various authors, little information is available concerning its characteristics. This investigation has addressed this problem and established a useful design process for broadband T-bar slot antennas.

REFERENCES

1. Jasik, Henry, Antenna Engineering Handbook, McGraww Hill, 1961, pp. 8-13 to 8-14.

2. Newman, E.H., "A Note on the Important Parameters in the Design of T-bar Fed Slot Antennas," prepared for Contract N00014-67-A-0232-0018, 9 April 1973.

3. Kraus, John D., Antennas, McGraw Hill, 1950, pp. 54, 55.

4. Ragan, George L., Microwave Transmission Circuits, McGraw Hill, 1948, pp. 358-361.

5. The Microwave Engineers' Handbook and Buyer's Guide, Horizon House, 1965, p. 59.

6. Richmond, J. H. and Tice, T. E., "Probes for Microwave Near-Field Measurements," IRE Transactions Microwave Theory Tech., vol. MTT-3, pp. 32-34, April 1955.

7. Harrington, Roger F., Time Harmonic Electromagnetic Fields, McGraw Hill, 1961, Chapter 3.

8. Rudduck, Roger C., "Application of Wedge Diffraction and Wave Interaction Methods to Antenna Theory," GTD and Numerical Techniques Short Course Notes, Ohio State University, pp. 43-45, and 100.

9. Popović, Branko D., Introductory Engineering Electromagnetics, Addison and Wesley, 1971, pp. 559-562.

10. Kreyszig, Erwin, Advanced Engineering Mathematics, John Wiley and Sons, 1962, pp. 510-513.

11. Sincalir, George, Jordan, E.C., and Vaughn, E. W., "Reference Measurements of Aircraft Antenna Patterns Using Models," Proceedings of I.R.E., Vol. 35, pp. 1451-1462 (December 1947).

APPENDIX

Assume that the waveguide whose cross section as shown in Fig. A-1 is infinitely long, filled with perfect dielectric, and its walls are of perfect conducting materials. The transverse electric waves (E_y=0) traveling through the guide in the positive y direction may be derived from Maxwell's equations:

$$\text{(A1)} \qquad \bar{E}_z = \frac{-j\omega\mu}{k^2} \frac{\partial}{\partial x} H_y \hat{\mu}_z$$

$$\text{(A2)} \qquad \bar{E}_x = \frac{+j\omega\mu}{k^2} \frac{\partial}{\partial z} H_y \hat{\mu}_x$$

and

$$\text{(A3)} \qquad \bar{H}_y = X(x)\, Z(z)\, \hat{\mu}_y$$

where $e^{-\gamma y}$ dependence is assumed in each equation. The solution of H_y for the coordinate system shown as a function of x and z assuming no y dependence is derived from the telegrapher's equation [9] using separation of variables.

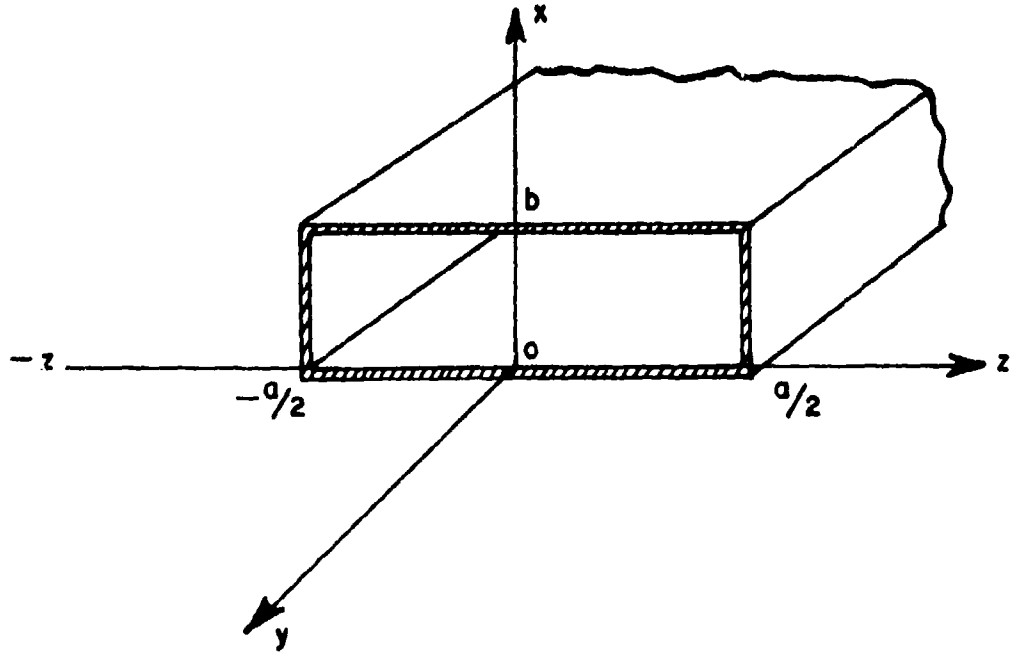

Fig. A1. Rectangular waveguide and coordinate system used in the modal analysis procedure.

(A4) $$\bar{H}_y = (A_x \sin k_x x + B_x \cos k_x x)\left(A_z \sin k_z\left(z - \frac{a}{2}\right) + B_z \cos k_z\left(z - \frac{a}{2}\right)\right)\hat{\mu}_y .$$

To form a complete solution of the transverse electric fields the boundary conditions must be matched, i.e., $E_z = 0$ at $(x,z) = (0,z)$ and $(x,z) = (b,z)$, and $E_x = 0$ at $(x,z) = (x,-a/2)$ and $(x,z) = (x,a/2)$. Therefore the TE_{mn} fields in the guide must be the following.

(A5) $$\bar{E}_z = \frac{j\omega\mu}{k^2}\left(\frac{n\pi}{b}\right) H_o \sin\left(\frac{n\pi x}{b}\right) \cos\left[\frac{m\pi}{a}\left(z - \frac{a}{2}\right)\right]\hat{\mu}_z$$

(A6) $$\bar{E}_x = \frac{-j\omega\mu}{k^2}\left(\frac{m\pi}{a}\right) H_o \cos\left(\frac{n\pi x}{b}\right) \sin\left[\frac{m\pi}{a}\left(z - \frac{a}{2}\right)\right]\hat{\mu}_x$$

and

(A7) $$\bar{H}_y = H_o \cos\left(\frac{n\pi x}{b}\right) \cos\left[\frac{m\pi}{a}\left(z - \frac{a}{2}\right)\right]\hat{\mu}_y$$

$$H_o = B_x B_z \qquad n = 1,2,3 \cdots \quad m = 1,2,3 \cdots .$$

Assume that the rectangular waveguide thus described has the same cross sectional dimensions as the cavity of the planar T-bar fed slot described in Chapter II. The TE_{mn} modes which may be established in this waveguide dependent upon probe location are listed with their respective cutoff frequency and field expressions in Table A-1.

TABLE A-1

Mode	f_c	$\bar{E}$
TE_{10}	492.0 MHz	$E_x = C_1\cos(\pi z/a)$, $E_z = 0$
TE_{20}	984.25 MHz	$E_x = C_2\sin(2\pi z/a)$, $E_z = 0$
TE_{30}	1476.37 MHz	$E_x = -C_3\cos(3\pi z/a)$, $E_z = 0$
TE_{40}	1968.50 MHz	$E_x = -C_4\sin(4\pi z/a)$, $E_z = 0$
TE_{01}	1476.37 MHz	$E_x = 0$, $E_z = B_1 \sin(\pi x/b)$

where $C_n = \frac{j\omega\mu\, m\pi}{k^2 a} H_o$ and $B_n = \frac{j\omega\mu\, n\pi}{k^2 b} H_o$

The amplitude and phase of the vertically polarized E-field measured in the aperture of the T-bar fed slot antenna (described in Chapter IV) may be expressed as a Fourier series over the aperture length. Assuming that the cavity backed slot exhibits some waveguide characteristics the Fourier series may be represented by a TE_{mo} modal expansion series. To solve for the modal coefficients the orthogonality of the trigonometric functions may be used [10] as follows:

$$(A8) \quad F(z) = a_o + \sum_{n=1}^{6} a_n \cos\left(\frac{2n\pi}{a} z\right) + \sum_{n=1}^{6} b_n \sin\left(\frac{2n\pi}{a} z\right)$$

is a Fourier series representation of the aperture distribution with a_o, b_n, a_n complex coefficients. The TE_{mo} expansion series through the fourth term may be expressed as follows:

$$(A9) \quad TE(z) = C_1 \cos\frac{\pi z}{a} + C_2 \sin\frac{2\pi z}{a} - C_3 \cos\frac{3\pi z}{a} - C_4 \sin\frac{4\pi z}{a}$$

Substitute $a/2 = \pi$ into each equation so that the orthogonality expressions may be recognized with ease. Then, to solve for C_1 set $F(z) = TE(z)$, multiply each side of the equation by $\cos z/2$ and integrate from $-\pi$ to π yielding Eq. (A10).

$$(A10) \quad \int_{-\pi}^{\pi} a_o \cos\frac{z}{2}\, dz + \sum_{n=1}^{b} \int_{-\pi}^{\pi} \left[a_n \cos(nz)\cos\left(\frac{z}{2}\right) + b_n \sin(nz)\cos\left(\frac{z}{2}\right)\right] dz$$

$$= \int_{-\pi}^{\pi} \left(C_1 \cos^2\frac{z}{2} + C_2 \sin z \cos\frac{z}{2} - C_3 \cos\frac{3}{2} z \cos\frac{z}{2} - C_4 \sin 2z \cos\frac{z}{2}\right) dz$$

Recall the following orthogonal definitions:

$$(A11) \quad \int_{-\pi}^{\pi} \cos mx \sin nx = 0 \quad \text{for all m and n}$$

$$\int_{-\pi}^{\pi} \sin mx \sin nx\, dx$$

$$= \int_{-\pi}^{\pi} \cos mx \cos nx = \begin{cases} 0 & \text{for } m \neq n \text{ m,n integers} \\ 2\pi & \text{if } m=n=0 \\ \pi & \text{if } m=n=1,2,3 \cdots \end{cases}$$

Therefore, Eq. (A10) can be reduced to Eq. (A12). The second summation of the Fourier series does not equal zero because m and n are not integers over the sum.

$$(A12) \qquad \int_{-\pi}^{\pi} a_o \cos\frac{z}{2}\,dz + \sum_{n=1}^{6}\int_{-\pi}^{\pi} a_n \cos nz \cos\frac{z}{2} = \int_{-\pi}^{\pi} C_1 \cos^2\frac{1}{2}\,z\,dz$$

solving the above equation for C_1

$$(A13) \qquad C_1 = \frac{4a_o}{\pi} + \frac{2}{\pi}[0.6667\,a_1 - 0.1333\,a_2 + 0.0572\,a_3 - 0.0317\,a_4 + 0.0202\,a_5 - 0.014\,a_6]$$

To solve for C_2 each side of the equation $F(z) = TE(z)$ must be multiplied by $\sin z$ and integrated from $-\pi$ to π.

$$(A14) \qquad \int_{-\pi}^{\pi} a_o \sin z\,dz + \int_{-\pi}^{\pi}\sum_{n=1}^{6} a_n \cos nz \sin z\,dz + \sum_{n=1}^{6} b_n \sin nz \sin z\,dz = \int_{-\pi}^{\pi} C_2 \sin^2 z\,dz\,.$$

The above equation reduces to a simple expression after orthogonality is applied because all m and n values are integers. Equation (A15) results which should be expected since for C_2 the arguments of the modal sine function agreed with that associated with b_1 of the Fourier series.

$$(A15) \qquad C_2 = b_1$$

The same techniques may be applied to the remaining unknowns C_3 and C_4. These expressions are given in Eqs. (A16) and (A17).

$$(A16) \qquad C_3 = \frac{4a_o}{3\pi} - \frac{2}{\pi}[1.2a_1 + 0.8752a_2 - 0.2222a_3 + 0.1091a_4 - 0.0659a_5 + 0.0445a_6]$$

$$(A17) \qquad C_4 = -b_2\,.$$

Consider the transverse slot on a cylindrical surface as shown in Fig. A2. Assume that the vertically polarized aperture E-field may be described by Eq. (A18) where ϕ_0 is the aperture length in degrees and m = 1,2,3,4. For m=1 this expression becomes the TE_{10} mode which is widely used in literature as the assumed distribution in the transverse slots on cylindrical surfaces.[11]

$$(A18) \qquad E_z = -C_m \sin\left[\frac{m}{\phi_0}\left(\phi - \frac{\phi_0}{2}\right)\right]\hat{u}_z \ .$$

This equation satisfies the tangential E-field boundary conditions and furthermore it is very similar to the TE_{m0} modal expansion discussed earlier for the planar case. The planar rectangular aperture has been curved so that the long length now corresponds to the ϕ coordinate of the cylinder coordinate system. Therefore, the coordinate used to describe the boundary conditions is chosen to be ϕ which represents the only difference between this expression and that derived earlier for the rectangular study. Thus the Fourier series analysis of the experimentally determined aperture data may be expressed as a TE_{m0} modal expansion in the same manner as before. Furthermore the equations for determining the modal coefficients are identical to those earlier derived.

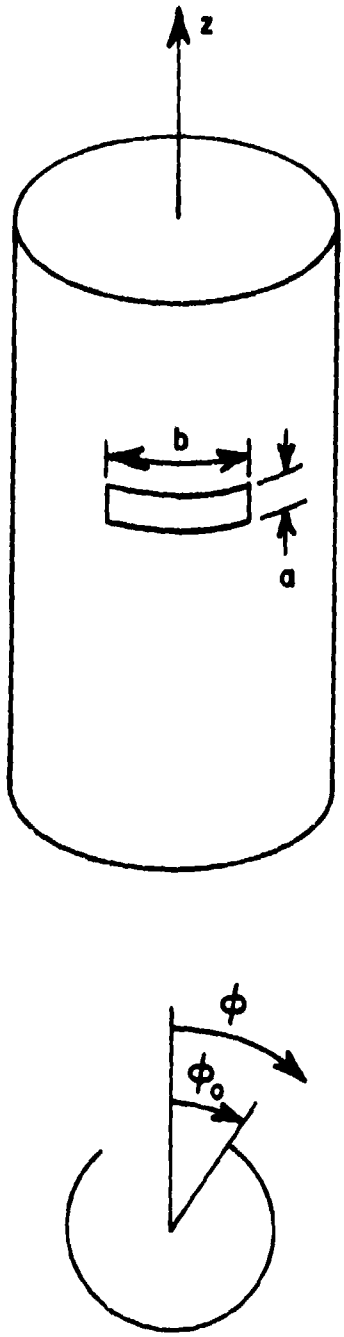

Fig. A2. A transverse slot antenna on a circular cylinder.